

# Climate Change Impacts on Precipitation for a Deep Geological Repository (Ignace Study Area)

**NWMO-TR-2020-04**

**June 2020**

**Andre Schardong, Janya Kelly, Sean Capstick**

Golder Associates Ltd

**nwmo**

NUCLEAR WASTE  
MANAGEMENT  
ORGANIZATION

SOCIÉTÉ DE GESTION  
DES DÉCHETS  
NUCLÉAIRES

**Nuclear Waste Management Organization**

22 St. Clair Avenue East, 6<sup>th</sup> Floor

Toronto, Ontario

M4T 2S3

Canada

Tel: 416-934-9814

Web: [www.nwmo.ca](http://www.nwmo.ca)

# **Climate Change Impacts on Precipitation for a Deep Geological Repository (Ignace Study Area)**

**NWMO-TR-2020-04**

June 2020

**Andre Schardong, Janya Kelly, Sean Capstick**  
Golder Associates Ltd

This report has been prepared under contract to NWMO. The report has been reviewed by NWMO, but the views and conclusions are those of the authors and do not necessarily represent those of the NWMO.

All copyright and intellectual property rights belong to NWMO.

### Document History

Title:	Climate Change Impacts on Precipitation for a Deep Geological Repository (Ignace Study Area)		
Report Number:	NWMO-TR-2020-04		
Revision:	R000	Date:	June 2020
Golder Associates Ltd			
Authored by:	Andre Schardong, Golder Associates Ltd		
Verified by:	Janya Kelly, Golder Associates Ltd		
Approved by:	Sean Capstick, Golder Associates Ltd		
Nuclear Waste Management Organization			
Reviewed by:	Helen Leung, Jeremy Chen and Melissa Mayhew		
Accepted by:	Paul Gierszewski		

Revision Summary		
Revision Number	Date	Description of Changes/Improvements
R000	2020-06-15	Initial issue

**ABSTRACT**

**Title:** Climate Change Impacts on Precipitation for a Deep Geological Repository (Ignace Study Area)  
**Report No.:** NWMO-TR-2020-04  
**Author(s):** Andre Schardong, Janya Kelly, Sean Capstick  
**Company:** Golder Associates Ltd  
**Date:** June 2020

The Nuclear Waste Management Organization (NWMO) completed a literature review on climate change impacts and developed a preferred method to assess the climate change impacts on probable maximum precipitation (PMP). The objective of this study is to apply the preferred method to assess the climate change impacts on the PMP and Intensity-Duration-Frequency (IDF) amounts for a case study (Ignace study area) during currently planned Deep Geological Repository (DGR) implementation periods for used fuel. The results have been presented for a range of global climate models within the ensemble and are expressed in terms of percentiles so that the level of acceptable risk can be selected by using the desired percentile. Climate extreme projections for the 2050s and 2080s are indicating a future that is likely to be wetter, which is consistent with the current and future climate projections. Both the 1-day PMP values and the 1-day rainfall events are projected to increase during the 2050s and 2080s at the 50<sup>th</sup> percentile level. The increase in rainfall depth at the sub-daily temporal scale is less significant than increases in those estimated for daily and multi-daily IDF curves and PMP values.

There is a level of inherent uncertainty when projecting future climate; however, the approach taken in this study aims to address this uncertainty by relying on a multi-model ensemble and providing percentiles. The estimated percent changes to precipitation through the PMP and IDF curves has been described in terms of percentiles, allowing for different levels of acceptable risk. The selection of future projections for a climate change risk assessment should be based on the balance between the extra investment and consequential risks. Based on Golder's experience in climate change projections, the proposed approaches are considered best guidance for the industry.

# TABLE OF CONTENTS

	Page
<b>ABSTRACT</b>	<b>iii</b>
<b>LIST OF TABLES</b>	<b>v</b>
<b>LIST OF FIGURES</b>	<b>v</b>
<b>GLOSSARY OF TERMINOLOGY AND ABBREVIATIONS</b>	<b>vi</b>
<b>1. INTRODUCTION</b>	<b>1</b>
<b>2. APPROACH AND METHODOLOGY ON PMP AND IDF ANALYSES</b>	<b>2</b>
<b>2.1 Current Climate Methodology on PMP and IDF Analyses</b>	<b>2</b>
<b>2.2 Future Climate Methodology on PMP and IDF Analyses</b>	<b>4</b>
<b>3. ANALYSES OF CURRENT CLIMATE ON PMP AND IDF</b>	<b>6</b>
<b>3.1 Climate Baseline Development</b>	<b>6</b>
3.1.1 Daily climate dataset	6
3.1.2 Daily infilled dataset series for the Ignace study area	8
3.1.3 IDF engineering dataset	10
<b>3.2 Baseline IDF Curves</b>	<b>11</b>
3.2.1 Sub-daily IDF curves for the selected stations	11
3.2.2 Spatial interpolation to the Ignace study area	15
3.2.3 Comparison with other sources	16
3.2.4 Daily and multi-day IDF curve for the Ignace study area	16
<b>3.3 Baseline PMP Calculations</b>	<b>18</b>
3.3.1 Historical storms for the Transposition Method	18
3.3.2 Estimates of PMP with the Hershfield method	19
3.3.3 Development of DAD Curves in Estimate of PMP with the Transposition Method	19
3.3.4 PMP comparison	21
3.3.5 Sub-daily PMP estimates	22
<b>3.4 Rainfall on Snow</b>	<b>23</b>
<b>4. ANALYSES OF FUTURE CLIMATE ON PMP AND IDF ESTIMATES</b>	<b>25</b>
<b>4.1 Future Climate Projections</b>	<b>25</b>
<b>4.2 Climate Change Impacts on IDF Curves</b>	<b>27</b>
4.2.1 Percent changes in sub-daily IDF curves	29
4.2.2 Percent changes in daily and multi-daily IDF curves	30
<b>4.3 Climate Change Impacts on PMP Estimates</b>	<b>32</b>
<b>4.4 Climate Change Impacts on Rainfall on Snow</b>	<b>34</b>
<b>5. QUALITATIVE CLIMATE ASSESSMENT BEYOND THE YEAR 2100</b>	<b>37</b>
<b>6. UNCERTAINTY OF CLIMATE CHANGE PROJECTIONS FOR PMP AND IDF</b>	<b>39</b>
<b>7. USING THE RESULTS OF THIS ASSESSMENT IN DECISION MAKING</b>	<b>40</b>
<b>8. CONCLUSIONS AND RECOMMENDATIONS</b>	<b>41</b>

REFERENCES .....	43
APPENDIX A: DETAILED METHODOLOGY .....	45
APPENDIX B: FUTURE RAINFALL STATISTICS .....	70
REFERENCES .....	71

## LIST OF TABLES

	Page
Table 1: Climate Station Properties.....	7
Table 2: Correlation between Ignace TCPL 58 Station and MERRA-2 Data during 1981-1992 ...	9
Table 3: Annual Maximum of the Daily Total Precipitation Series for Ignace and Ignace TCPL 58 .....	10
Table 4: Stations from the Engineering Data Set for Sub-daily IDF Curves .....	10
Table 5: Best Distribution for Each Climate Station (Number of Times Selected for the Sub-Daily Durations) .....	11
Table 6: IDF Curves Summary – Rainfall Accumulation (mm).....	12
Table 7: IDF Curves for 6020LPQ ATIKOKAN (AUT) – Gumbel Distribution (mm).....	13
Table 8: IDF Curves for 6037775_SIOUX_LOOKOUT_A - Gumbel Distribution (mm) .....	13
Table 9: IDF Curves for 6119500 WIARTON A – Gumbel Distribution (mm) .....	14
Table 10: IDF Curves for 6048268_THUNDER BAY CS – GEV Distribution (mm).....	14
Table 11: IDF Curves for 6034073 KENORA RCS – PE3 Distribution (mm) .....	14
Table 12: IDF Curves for 6042716 GERALDTON A – GEV Distribution (mm).....	15
Table 13: Spatially Interpolated IDF Curves for the Ignace Study Area (mm) .....	15
Table 14: IDF Curves Comparison with Other Sources – 100-Year Return Period for 24-Hour Duration .....	16
Table 15: Daily and Multi-day IDF Curves for the Ignace Study Area (mm).....	17
Table 16: Comparison of the IDF Curves at Ignace Study Area .....	17
Table 17: PMP Summary for Statistical Method for the Ignace Study Area .....	19
Table 18: Data Points Used to Obtain the DAD Curves.....	20
Table 19: Original DAD Curves for the 49 <sup>th</sup> Parallel Storm .....	21
Table 20: Adjusted DAD Curves for the Ignace Study Area .....	21
Table 21: Conversion Ratios from 24-hour to Sub-daily PMP.....	22
Table 22: Estimated Sub-Daily PMP Values for the Ignace Study Area – Hershfield Method ....	22
Table 23: Estimated Sub-Daily PMP Values for the Ignace Study Area – Transposition Method .....	23
Table 24: Rainfall on Snow Projections for the Ignace Study Area (mm).....	24
Table 25: 1-Day Snowpack Accumulation for the Ignace Study Area (mm).....	24
Table 26: Summary of the Projected Changes (%) in 1-day Rainfall in 2050s for Ignace Study Area .....	29
Table 27: Summary of the Projected Changes (%) in 1-day Rainfall in 2080s for Ignace Study Area .....	30
Table 28: Summary of the 50 <sup>th</sup> Percentile of Projected Percent Changes in Rainfall in the 2050s for Ignace Study Area.....	31
Table 29: Summary of the 50 <sup>th</sup> Percentile of Projected Percent Changes in Rainfall in the 2080s for Ignace Study Area (%) .....	31
Table 30: Summary of Selected Percentiles of Projected Percent Changes in PMP Estimates in the 2050s for Ignace Study Area .....	33
Table 31: Summary of Selected Exceedance Probabilities of Projected Percent Changes in PMP Estimates in the 2080s for Ignace Study Area .....	33
Table 32: Summary of the 50 <sup>th</sup> Percentile of Projected Percent Changes in Rain on Snow Events in the 2050s for Ignace Study Area.....	35
Table 33: Summary of the 50 <sup>th</sup> Percentile of Projected Percent Changes in Rain on Snow Events in the 2080s for Ignace Study Area (%) .....	35
Table 34: Percent Change in Peak Snowpack Accumulation for the Ignace Study Area (50 <sup>th</sup> Percentile).....	36

## LIST OF FIGURES

	<b>Page</b>
Figure 1: High Level Step-Wise Approach.....	2
Figure 2: High-Level Summary of Evaluation of Current Climate on PMP and IDF Analyses .....	3
Figure 3: High-Level Summary of Evaluation of Future Climate on PMP and IDF Estimates.....	5
Figure 4: Annual Maximum of the Daily Total Precipitation Series for Ignace and Ignace TCPL 58.....	9
Figure 5: DAD Curves for 49 <sup>th</sup> Parallel Storm, 1-, 2- and 3-Day Duration (Non-Maximized Storm) .....	20
Figure 6: Overview of Project Phases and Selected Future Climate Periods.....	28
Figure 7: Illustration of RCP and ECP Scenario Radiative Forcing from 2000 to 2300 .....	37

## GLOSSARY OF TERMINOLOGY AND ABBREVIATIONS

Term/Acronym	Definition
AD	Anderson-Darling
AHCCD	Adjusted and Homogenized Canadian Climate Data
AMS	Annual Maximum Series
AR5	Fifth Assessment Report
BCCAQ	Bias Correction/Constructed Analogues with Quantile mapping reordering
CC	Climate Change
CCCR	Canada's Changing Climate Report
CDF	Cumulative Density Function
CMIP	Climate Model Intercomparison Project
CS	Climate Station
CSA	Canadian Standards Association
DAD	Duration-Area Depth
DGR	Deep Geologic Repository
ECCC	Environment and Climate Change Canada
ECMWF	European Centre for Medium-Range Weather Forecasts
ECP	Extended Concentration Pathways
EQM	Equidistant Quantile Matching
EV1	Extreme-Value Type 1 Distribution (Gumbel)
EV2	Extreme-Value Type 1 Distribution (Fréchet)
EV3	Extreme-Value Type 1 Distribution (Weibull)
GCM	Global Climate Model
GEV	Generalized Extreme Value
IDF	Intensity-Duration-Frequency

Term/Acronym	Definition
IPCC	Intergovernmental Panel on Climate Change
KS	Kolmogorov-Smirnov
LOCA	Localized Constructed Analogues
LP3	Log-Pearson Type 3
MERRA	Modern-Era Retrospective analysis for Research and Applications
MNRF	Ministry of Natural Resources and Forestry
MTO	Ministry of Transportation Ontario
NASA	National Aeronautics and Space Administration
NWMO	Nuclear Waste Management Organization
OFAT	Ontario Flow Assessment Tool
OMNR	Ontario Ministry of Natural Resources
PDF	Probability Density Function
PE3	Pearson Type 3
PMP	Probable Maximum Precipitation
PPT	Precipitation
PWC	Precipitable Water Content
PWM	Probability Weighted Moment
QDM	Quantile Delta Mapping
RCP	Representative Concentration Pathway
RCS	Regional Climate Station
RM	Ratio Method
SRES	Special Report on Emissions Scenarios
UNEP	United Nations Environment Program
WCRP	World Climate Research Program
WMO	World Meteorological Organization

## 1. INTRODUCTION

A changing climate within Ontario's watersheds may present physical risks to infrastructure if designs do not consider the impacts of these changes. Golder Associates Ltd. (Golder) was retained to apply the developed methodology by the Nuclear Waste Management Organization (NWMO) in Wood (2019) to assess the impacts of climate change on probable maximum precipitation (PMP) events for two study areas for a Deep Geologic Repository (DGR) for used fuel. In addition to the assessment of future PMP events, future Intensity-Duration-Frequency (IDF) values are estimated for 100-year and 500-year return periods.

Previous studies undertaken within the Ontario Power Generation's DGR Project for low and intermediate level radioactive waste at the Bruce nuclear site have identified the potential for flooding to impact the operations of the DGR based on the current climate (AMEC 2011). In the future, projected higher temperatures may change the capacity of the atmosphere to hold water, potentially resulting in more frequent and intense storms. This projected change in climate may increase vulnerabilities to potential climate extremes at the two DGR study areas (i.e., Ignace and South Bruce) for used fuel. Siting the potential placement of the DGR within these two study areas must consider the range of credible storms within the watershed to appropriately design the associated storm water management system. Therefore, the first step towards potential placement of the DGR is to understand how the projected changes in climate may impact PMP and IDF values at the study areas using the method developed in Wood (2019).

This report documents the climate change impacts on IDF and PMP values in the Ignace study area. The approach and methodology are summarized first to characterize the current and future climate conditions in the Ignace study area (Section 2). Detailed descriptions of the data sources and approaches used for both the climate baseline and future climate projections are provided in Appendix A. Next, for the baseline and future climate conditions, IDF and PMP values are estimated respectively in Section 3 and Section 4. Details of future rainfall statistics are given in Appendix B. Uncertainty of climate change projections and recommendations on how to use the data are discussed in Section 6 and Section 7 respectively. Finally, conclusions and recommendations are provided in Section 8.

## 2. APPROACH AND METHODOLOGY ON PMP AND IDF ANALYSES

Understanding what the current climate conditions of the study area are and understanding how they are projected to change under future climate change is fundamental to the following approach. The discussion of climate vulnerability is focused around rainfall events, namely PMP and IDF values with different return periods and durations. The approach follows the key steps in Figure 1. The following sections provide high level overviews of the methodologies used to develop the current climate and future projected climate datasets used in this assessment. More detailed information on each methodology is provided in Appendix A.

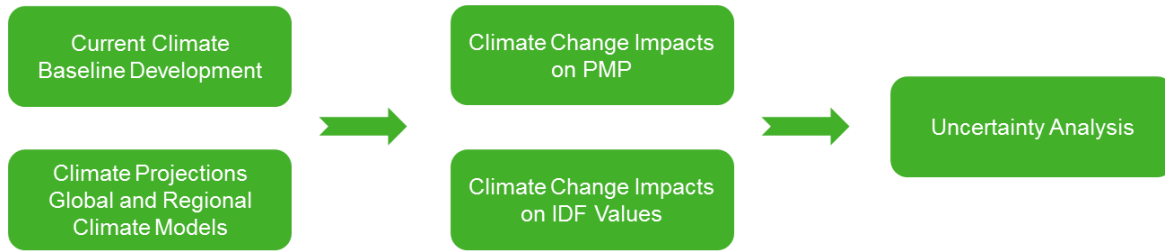


**Figure 1: High Level Step-Wise Approach**

### 2.1 Current Climate Methodology on PMP and IDF Analyses

Understanding the current climate and current climate trends is important when evaluating current design parameters. Where available, the climate baseline is grounded in observations from local climate observation stations. The baseline is established using available local climate stations and/or publicly available nearby regional climate stations infilled with reanalysis data whenever possible (to meet data completeness requirements, such as only considering observations where at least 90% observations are available in any given year or month). Before infilling, the reanalysis data are compared and correlated to available regional climate stations.

Reanalysis data from Version 2 of the National Aeronautics and Space Administration's (NASA's) Modern-Era Retrospective analysis for Research and Applications (MERRA-2) and the European Centre for Medium-Range Weather Forecasts (ECMWF) Re-Analysis (ERA5) data are used to represent current climate or to infill the missing data from observations. R-squared ( $R^2$ ) statistics is calculated between MERRA-2 and ERA5 and is used to complete missing historical observed dataset. The  $R^2$ , also known as coefficient of determination, provides a measure of how well observed outcomes are replicated by the regression line fitted. It ranges from 0 to 1, 1 being a perfect fit.

Using the daily current climate baseline precipitation, the PMP is calculated according to Hershfield Method (Chapter 4 in WMO 2009) and the DAD (duration-area-depth) curves discussed in Appendix A of this report. A second method (the Transposition method) relies on observations of significant storms nearby the study area and is accomplished by construction of DAD curves. Using the same daily current climate baseline precipitation, IDF values are then calculated for various durations (1-day through 120-day) and return periods (1 in 100 years and 1 in 500 years). PMP is calculated for 1-day, 2-day, and 3-day durations. The IDF values for the current climate are calculated by adjusting a statistical distribution to the Annual Maximum Series (AMS) based on daily observed data. The AMS is a record of the largest 1-day rainfall for each year in a series and is calculated by extracting the maximum value of the daily precipitation series for each year. Three statistical distributions (Gumbel, Generalized Extreme Value – GEV, Pearson/Log-Pearson Type 3) are tested against the available data and the parameters are estimated using the method of L-moments (Hosking and Wallis 1997), following the approach adopted by Environment and Climate Change Canada - ECCC (ECCC 2019). A high-level flowchart with the analyses conducted and presented in this report are presented in Figure 2.

The detailed description of the methods is presented in Appendix A.2.

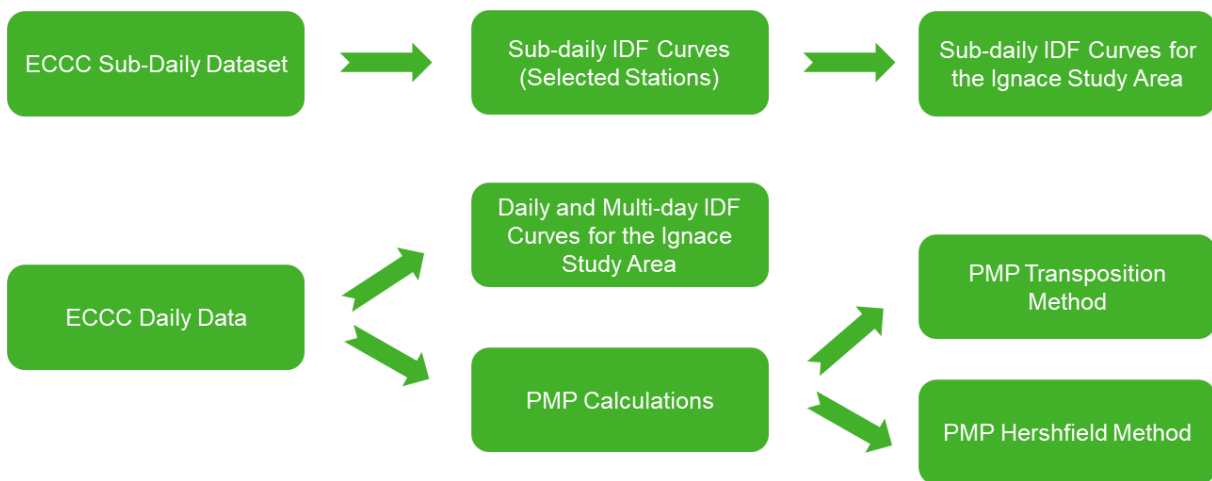


**Figure 2: High-Level Summary of Evaluation of Current Climate on PMP and IDF Analyses**

## 2.2 Climate Methodology on PMP and IDF Analyses

The approach to evaluating future climate impacts on precipitation uses the state of science and publicly available climate projections to complete the climate change impact assessment on the PMP and the IDF values. The range of projected future climate depends on the emission scenario used to project the future climate conditions as well as selected global climate model (GCM). Since no one model or climate scenario can be viewed as completely accurate, the Intergovernmental Panel on Climate Change (IPCC) recommends that climate change assessments use as many models and climate scenarios as possible, or a “multi-model ensemble”. For this reason, the multi-model ensemble approach is used here to describe the probable range of results and present changes to PMP and IDF curves expressed as percent change and percentile levels.

For this study, Golder developed methods to extract climate data (precipitation and temperature) from the multi-model ensemble for model baseline (1950-1993), the mid-century (2041- 2070), and end-of-century (2071 through to 2100) time periods for the PMP and IDF. The baseline period of 1950 to 1993 was selected based on a combination of data availability constraints (observed data from relevant climate stations has data only until the year 1993), as well as the need for a long observation period to allow for more accurate analysis of precipitation extremes in the form of PMP and IDF curves. The future time periods of 2041 to 2070 (2050s) and 2071 to 2100 (2080s), chosen to be a length of 30 years (minimum number of years needed to represent a climate normal as recommended by the World Meteorological Organization (WMO)), represent the changes in climate for mid-century and end of century time periods and are applicable to the site characterization, construction and operational periods. Currently, downscaled climate projections only extend out to the year 2100, making the 2071 to 2100 time period the furthest point into the future for detailed assessment. A qualitative assessment is provided for time periods beyond 2100 to cover the monitoring and decommissioning periods for the project. Emission scenarios RCP 2.6, RCP 4.5, and RCP 8.5 from the IPCC Fifth Assessment Report (AR5) (IPCC 2013) are used to describe the model baseline, mid-century and end-of-century time periods. The qualitative assessment past 2100 relies on projections available in literature.

Daily downscaled climate projections for precipitation and minimum and maximum temperature are obtained for the multi-model ensemble. This ensemble consists of statistically downscaled climate scenarios that correspond to a particular GCM for a given Representative Concentration Pathway (RCP). These daily time-series are then used in conjunction with methods for estimating PMP, snowfall, and moisture to establish initial ranges for PMP-related variables (based on literature values and results from historic analysis of PMPs), including precipitable water and moisture content, and rainfall. Ranges for previously identified ancillary factors (such as snowpack and snowmelt) are also established. The ranges are then presented as percent changes between the baseline period and the selected future periods across all GCMs and RCPs.

Using the historic data and GCM ensemble results, projections for future IDF values are developed. These projections can be used to understand aspects of the PMP storm (including sub-daily rainfall distribution) and how the PMP storm compares to more frequent design storms typically used in non-critical infrastructure design. These IDF values are done using two methods currently used by Golder to estimate the changes to IDF distributions: (1) Quantile Delta Mapping (QDM) method and; (2) the Ratio Method (RM).

The future projected changes in PMP are calculated using the moisture maximization method and the Hershfield method. The moisture maximization method is not used for current climate conditions, since it produces an analogous vapour pressure result (rather than an absolute rainfall depth value), and can only be used to estimate the change in PMP (i.e., based on change in vapour pressure) rather than provide an absolute value. Comparing the modelled future climate to modelled baseline produces changes in relative humidity, so it can be used to estimate percent change in PMP depths between baseline and future conditions. Ensemble statistics in terms of percentiles are calculated across the results from both methods. The daily rain and snowmelt projected changes are calculated using the same methodology as for the current climate but applied to all ensemble members and presented using percentiles across the ensemble.

A high-level flowchart with the analyses conducted and presented in this report are presented in Figure 3. The detailed description of the methods is presented in Appendix A.3.

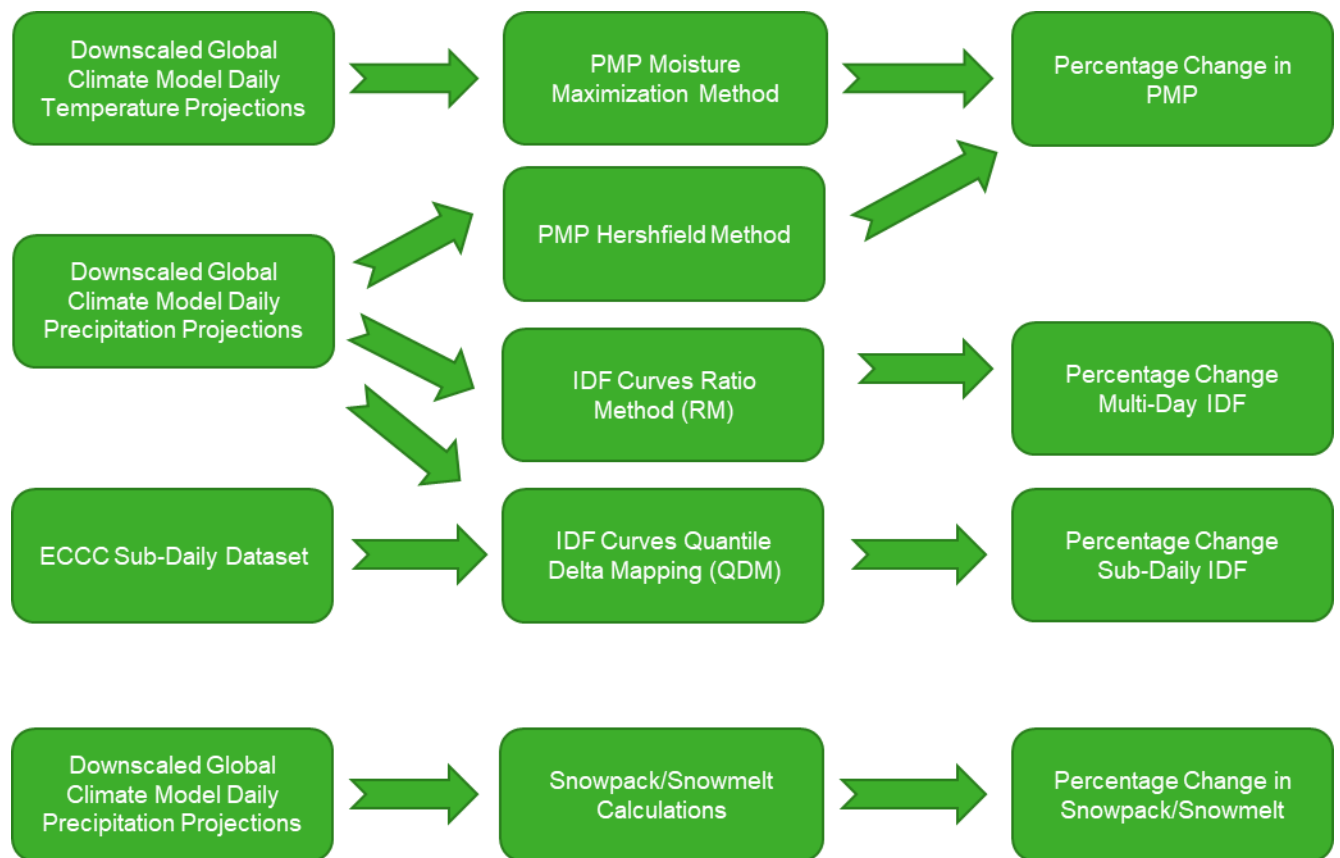


**Figure 3: High-Level Summary of Evaluation of Future Climate on PMP and IDF Estimates**

### 3. ANALYSES OF CURRENT CLIMATE ON PMP AND IDF

The following sections outline the development of the climate baseline and calculations of the baseline IDF curves and PMP. The baseline was developed using the methodology described in Section 3.1 to calculate the IDF curves and PMP based on the approach and methodology provided in Section 2.1. The detailed description of the methods is presented in Appendix A2. Select tables presented in this section are colored using a gradient to aid in the visual representation of the values. The color gradients provide a relative indication of the highest (red) and lowest (green) values with transitional colors in between. Colors cannot be compared between tables, as the color scale is relative for each.

#### 3.1 Climate Baseline Development

The current climate baseline was developed using publicly available regional climate stations using the methodology presented in Appendix A.2.

The following sections describe the three climate datasets used for the various analyses in this report:

- 1) Daily dataset to screen for significant storms for the Transposition method and the construction of the DAD curves as used in Wood (2019).
- 2) Daily infilled dataset at the Ignace study area for the analysis of daily and multi-day IDF curves, the PMP statistical (Hershfield) method, and the analysis of rainfall on snow and snowpack.
- 3) Data from the ECCC Engineering Database for the calculation of the sub-daily IDF curves.

##### 3.1.1 Daily climate dataset

The main criteria for the climate stations selected were the length of record (minimum 30 years of data), proximity to the study area, and the availability of continuous precipitation data. Other criteria are listed in Appendix A.2. All publicly available stations within about 100 km from the study area were considered for the analysis of regional storms. The candidate stations with daily data for the Ignace study area were collected from Environment and Climate Change Canada (ECCC 2019). The list of the selected stations is presented in Table 1. These stations were primarily used to screen for significant storms in the study area and to assist in calculating the DAD curves. The data available for the DAD analysis are less critical, since the interest is in specific (large) events.

Two of the stations listed, Ignace - 6033690 and Ignace TCPL 58 - 6033697 located in the center of the study area, were analyzed further to create a consolidated baseline for the Ignace study area. Although these stations only provide data up to 1993, together they provide 81 years of continuous data, allowing for more reliable estimates of extreme rainfall statistics including PMP and IDF. The geographical siting of the other stations was deemed to be too dissimilar to the Ignace area to be considered for correlation (e.g., differences in factors such as distance from the site, elevation difference, proximity to water bodies). Due to the localized nature of precipitation, these factors are considered important in order to develop a more reliable current climate dataset.

Table 1: Climate Station Properties

Station Name	Climate ID	Latitude and Longitude	Elevation (masl <sup>(2)</sup> )	Distance from Ignace Study Area (km)	Years Available	Notes
ATIKOKAN (AUT) <sup>(3)</sup>	6020LPQ	48.76, -91.63	389.3	73.5	2000-2019	Used to screen for large storms and Sub-daily IDF
ATIKOKAN	6020379	48.75, -91.62	395.3	74.6	1966-1988	Used to screen for large storms
DRYDEN	6032117	49.78, -92.83	371.9	93.4	1914-1997	Used to screen for large storms
DRYDEN A <sup>(1)</sup>	6032119	49.83, -92.75	412.7	90.9	1970-2005	Used to screen for large storms
DRYDEN REGIONAL	6032125	49.83, -92.74	412.7	90.3	2010-2019	Used to screen for large storms
IGNACE	6033690	49.42, -91.65	446.5	0.7	1889-1971	Used to screen for large storms and define the baseline at Ignace study area, PMP estimates and daily IDF Curves
IGNACE TCPL 58	6033697	49.48, -92	473	25.5	1969-1993	Used to screen for large storms and define the baseline at Ignace study area, PMP estimates and daily IDF Curves
KENORA RCS <sup>(3)</sup>	6034073	49.79, -94.38	412.7	200.5	2008-2019	Used to screen for large storms and Sub-daily IDF
MARTIN TCPL 60	6035002	49.28, -91.23	470.6	34.9	1969-1984	Used for screen large storms
MINE CENTRE	6025203	48.77, -92.62	342.9	100.7	1914-2005	Used for screen large storms
SIOUX LOOKOUT A <sup>(1, 3)</sup>	6037775	50.12, -91.9	383.1	79.8	1938-2013	Used to screen for large storms and Sub-daily IDF
SIOUX LOOKOUT A	6037776	50.11, -91.91	383.1	78.9	2013-2019	Used to screen for large storms
GERALDTON A <sup>(1, 3)</sup>	6042716	49.78, -86.93	348.4	343.6	1981-2015	Used to screen for large storms
GRAHAM A	6042975	49.27, -90.58	503.2	80.1	1948-1967	Used to screen for large storms
QUORN	6046811	49.42, -90.9	444.7	55.0	1915-1960	Used to screen for large storms
THUNDER BAY CS <sup>(3)</sup>	6048268	48.37, -89.33	199.4	206.7	2003-2019	Used to screen for large storms and Sub-daily IDF
UPSALA (AUT)	6049095	49.03, -90.47	488.5	96.8	1973-2019	Used to screen for large storms
UPSALA	6049096	49.05, -90.47	483.7	95.8	1947-1972	Used to screen for large storms
UPSALA TCPL 62	6049098	49.03, -90.52	492.9	93.6	1970-1986	Used to screen for large storms
WIARTON A <sup>(1, 3)</sup>	6119500	44.75, -81.11	222.2	954.1	1947-2014	Used to screen for large storms and Sub-daily IDF

Notes: <sup>(1)</sup> Stations available in the AHCCD dataset.

<sup>(2)</sup> Meters above sea level.

<sup>(3)</sup> Included in the Engineering Dataset for Sub-Daily IDF curves analysis – See Table 4.

A third subset of stations was selected from the ECCC Engineering Database for the sub-daily IDF curves as noted in Table 1 (notes column) and listed separately in Table 4. The selected stations for sub-daily IDF analysis are discussed in Section 3.1.3.

Some of the stations listed in Table 1 are available in the daily precipitation AHCCD dataset from Environment and Climate Change Canada (ECCC 2019). For the investigations of candidate storms for the calculation of the PMPs and the DAD curves, the data from the AHCCD were compared to the original (raw) records from ECCC and the higher value was selected if concurrent records are found.

### **3.1.2 Daily infilled dataset series for the Ignace study area**

A daily dataset was defined for the Ignace study area using stations Ignace (6033690) and Ignace CPL 58 (6033697) to calculate the daily and multi-day IDF curves, the PMP Hershfield method, and the rainfall on snow analysis.

The Ignace (6033690) station has long records dating back to 1889 and ending in 1971. Only years and months with at least 90% of the data available were considered. Another nearby station, Ignace TCPL 58 (6033697), was also considered using the same data completeness criteria.

After applying the data completeness criteria, 54 years of the data were available for the analysis. Of those, four years (1916, 1950, 1955 and 1959) have missing data higher than 5% (less than 10%) and were removed from the series given that some of the months did not meet the completeness criteria. The year 1891 was also removed due to missing temperature data.

Infilling for the Ignace (6033690) station was not possible, as the reanalysis data from MERRA-2 and ERA5 are only available from 1979 and 1981 onwards. For Ignace TCPL 58 (6033697) station, ERA5 and MERRA-2 were both tested against the concurrent period from 1979 and 1981 to 1993. MERRA-2 presented a better agreement with observations from Ignace TCPL 58 (6033697) station, with R-squared ( $R^2$ ) statistics for a linear regression of 0.82, while ERA5 was lower at 0.63. (The infilling process is discussed in Appendix A.2.1).

For Ignace TCPL 58 (6033697) station, data records were available from 1969 to 1993. After applying the data completeness analysis, only 12 years of data were available. The data completeness levels were below 90% for the years 1984 to 1993. Some of the missing records during the wet months from May to October were infilled using reanalysis data (MERRA-2) with the regression equations presented in Table 2. The MERRA-2 reanalysis data are available past 1992 up to present; however, no observations are available from the stations at the Ignace area to support the extension of the data series only using the modelled data.

Given the proximity of the two stations and similar elevation and latitude, a combined series was created after infilling procedure to represent the Ignace study area resulting in a lengthy series with records from 1914 to 1992. The annual maximum of the daily total precipitation (PPT) of the combined series is presented in Figure 4 and Table 3.

The dashed gray trend line in Figure 4 represents the combined series and the solid black trend line represents Ignace (6033690) station. The trends align well, validating the use of the combined longer series. Although more recent observations are missing, the series has 72 years of valid records that were used for the extreme precipitation analysis (daily and multi-day IDF curves, PMP Hershfield (statistical) method, and the rainfall on snow analysis) presented in the following sections.

**Table 2: Correlation between Ignace TCPL 58 Station and MERRA-2 Data during 1981-1992**

Climate Variable	Percentage Infilled <sup>(1)</sup>	Daily R <sup>2</sup>	Infilling Equation
Daily Maximum Temperature	7%	0.97	Infilled=0.960 x MERRA-2
Daily Minimum Temperature	7%	0.97	Infilled=0.956 x MERRA -2
Daily Mean Temperature	7%	0.99	Infilled=0.967 x MERRA -2
Daily Total Precipitation	8%	0.82	Infilled=0.733 x MERRA -2

Note: <sup>(1)</sup> Observations from Ignace TCPL 58 station are available from 1969 through to 1993. MERRA-2 is available from 1981.

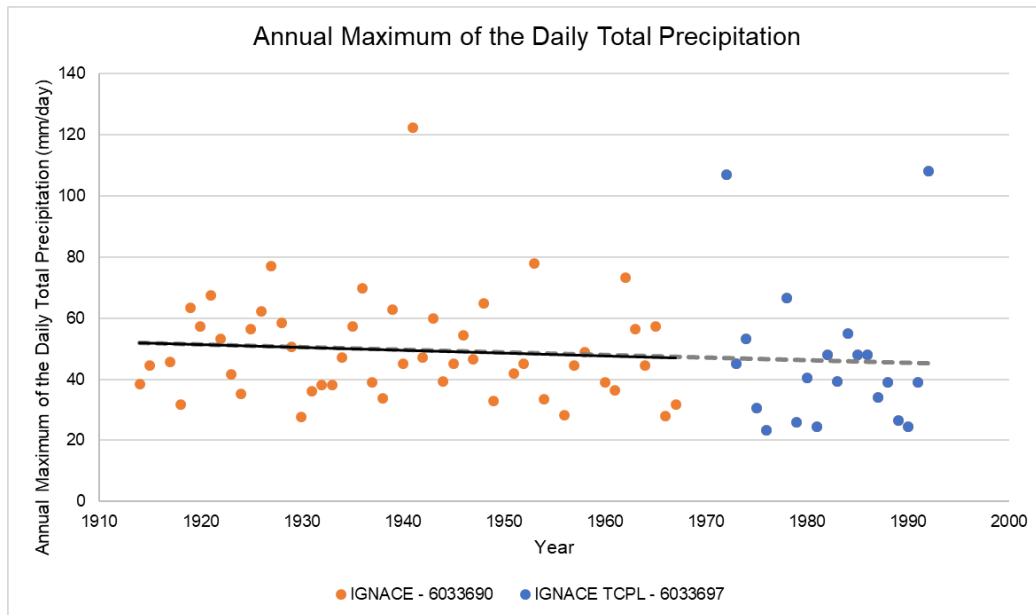


**Figure 4: Annual Maximum of the Daily Total Precipitation Series for Ignace and Ignace TCPL 58**

**Table 3: Annual Maximum of the Daily Total Precipitation Series for Ignace and Ignace TCPL 58**

Year	PPT (mm)	Year	PPT (mm)	Year	PPT (mm)	Year	PPT (mm)
1914	38.4	1933	38.1	1952	45.2	1976	23.4
1915	44.5	1934	47.0	1953	78.0	1978	66.7
1917	45.7	1935	57.2	1954	33.5	1979	26.0
1918	31.8	1936	69.9	1956	28.2	1980	40.4
1919	63.5	1937	38.9	1957	44.5	1981	24.5
1920	57.2	1938	33.8	1958	49.0	1982	48.0
1921	67.6	1939	62.7	1960	38.9	1983	39.4
1922	53.3	1940	45.2	1961	36.3	1984	55.0
1923	41.7	1941	122.4	1962	73.2	1985	48.1
1924	35.1	1942	47.2	1963	56.4	1986	48.0
1925	56.4	1943	59.9	1964	44.5	1987	34.0
1926	62.2	1944	39.4	1965	57.4	1988	39.0
1927	77.0	1945	45.2	1966	27.9	1989	26.6
1928	58.4	1946	54.4	1967	31.8	1990	24.4
1929	50.5	1947	46.5	1972	106.9	1991	39.0
1930	27.7	1948	64.8	1973	45.2	1992	108.0
1931	36.1	1949	33.0	1974	53.3	---	---
1932	38.1	1951	41.9	1975	30.5	---	---

### 3.1.3 IDF engineering dataset

The list of stations used to support the analysis of the sub-daily IDF curves (Section 3.2) was obtained directly from the ECCC IDF Engineering Database (ECCC 2019). The stations were selected based primarily on the distance from the Ignace study area and the length of records of at least 30 years. The stations used are listed in Table 4. It is worth noticing that some of the stations Geraldton A, Thunder Bay CS and Wiarton A are located farther from the Ignace area.

The data from the ECCC IDF Engineering are provided in the form of preprocessed annual maximum series (AMS) for selected sub-daily durations and they are verified by ECCC for quality assurance (ECCC 2019).

**Table 4: Stations from the Engineering Data Set for Sub-daily IDF Curves**

Name	Climate ID	Years Available	Elevation (masl)	Latitude and Longitude	Distance from Ignace Study Area (km)
ATIKOKAN (AUT)	6020LPQ	1967-2007	389	48.76, -91.63	73.5
KENORA RCS	6034073	1966-2011	412	49.79, -94.38	200.5
SIOUX LOOKOUT A	6037775	1963-2007	383	50.12, -91.9	79.8
GERALDTON A	6042716	1952-2007	348	49.78, -86.93	343.6
THUNDER BAY CS	6048268	1952-2012	199	48.37, -89.33	206.7
WIARTON A	6119500	1976-2007	222	44.75, -81.11	954.1

### 3.2 Baseline IDF Curves

IDF curves were calculated using the selected stations in the baseline development for selected return periods including 100-year and 500-year return periods. The IDF curves were compared to other available IDF calculations for the region, including historical precipitation trends. Two distinct analyses are presented in the next sections. The first analysis (Sections 3.2.1 to 3.2.3) using the sub-daily ECCC Engineering Database is an interpolated sub-daily IDF curves from selected stations for the Ignace study area and includes a comparison to other sources. The second analysis using the Annual Maximum of the Daily Total Precipitation time series (Section 3.1.2) calculates the daily and multi-day IDF curves for the Ignace study area (Section 3.2.4).

#### 3.2.1 Sub-daily IDF curves for the selected stations

For each of the selected stations listed in Table 4, three statistical tests including the Anderson-Darling, Chi-squared and Kolmogorov-Smirnov tests were used to select the best statistical distribution to fit the data from the four distributions- Gumbel (EV1), Generalized Extreme Value (GEV), Pearson Type 3 (PE3), and Log-Pearson type 3 (LP3) as described in Appendix A.2.2.3. This approach ensures that the most suitable distribution is used for each of the station to fit the IDF curves, i.e., better fitted to the observations. Table 5 presents the results of each statistical test for each of the five stations. The table shows how many times the distribution was selected for each of the sub-daily durations. The most frequent distribution was then used for that specific station for all sub-daily durations and the selected return periods including 100 and 500-years. The summary of the IDF curves for selected return periods, including 100 and 500-year, is presented in Table 6. The colour scale assists in the reading of the results and the analysis of the magnitude of the projections. The scale is presented for each of the sub-daily durations and grouped for the five stations. The cell space filled by the colour bars are relative to the correspondent precipitation amounts and proportional to the maximum for that duration. The GEV distribution was the most often selected for three of the stations, the Log-Pearson Type 3 for two stations, and the Gumbel and Pearson Type 3 for one station each. For Wiarton A station, the GEV and LP3 distributions yielded inconsistent estimates for 2, 6 and 12- hours durations compared to the 24-hour duration for higher return periods (greater than 100-years), and therefore, the Gumbel distribution was used. A detailed analysis of the raw data ordered from ECCC would be required to analyze sub-daily durations of 2, 6 and 12 hours, which is out of the scope of this study.

Table 7 through Table 12 present the detailed IDF curve calculations for stations near the Ignace study area.

**Table 5: Best Distribution for Each Climate Station (Number of Times Selected for the Sub-Daily Durations)**

Station	Distributions			
	GEV	EV1	PE3	LP3
6020LPQ - ATIKOKAN (AUT)	3	1	0	5
6037775 - SIOUX LOOKOUT A	3	4	1	1
6042716 - GERALDTON A	5	1	2	1
6034073 - KENORA RCS	1	0	5	3
6048268 - THUNDER BAY CS	5	0	2	2
6119500 - WIARTON A	6	0	0	3

Table 6: IDF Curves Summary – Rainfall Accumulation (mm)

Station	Duration	Return Period (years)						
		10	20	50	100	500	1000	2000
ATIKOKAN (AUT)	5 min	12.3	13.9	16.0	17.7	21.8	23.7	25.7
SIOUX LOOKOUT A	5 min	13.7	15.9	18.6	20.7	25.5	27.5	29.6
WIARTON A	5 min	10.7	12.1	13.8	15.2	18.3	19.6	20.9
THUNDER BAY CS	5 min	12.1	14.1	16.7	18.7	23.7	25.9	28.1
KENORA RCS	5 min	14.9	16.5	18.4	19.7	22.4	23.5	24.6
GERALDTON A	5 min	10.3	11.4	12.7	13.6	15.2	15.8	16.4
ATIKOKAN (AUT)	10 min	17.2	18.8	20.7	22.1	25.2	26.5	27.8
SIOUX LOOKOUT A	10 min	20.0	23.2	27.3	30.3	37.4	40.4	43.5
WIARTON A	10 min	15.2	17.0	19.4	21.3	25.4	27.2	29.0
THUNDER BAY CS	10 min	17.7	20.3	23.8	26.3	32.3	34.9	37.5
KENORA RCS	10 min	20.8	23.2	26.1	28.1	32.6	34.4	36.1
GERALDTON A	10 min	15.8	18.0	20.8	22.8	27.4	29.3	31.2
ATIKOKAN (AUT)	15 min	22.4	24.9	28.1	30.5	36.1	38.5	41.0
SIOUX LOOKOUT A	15 min	23.2	26.8	31.5	34.9	43.0	46.4	49.9
WIARTON A	15 min	19.2	21.6	24.8	27.1	32.6	34.9	37.3
THUNDER BAY CS	15 min	21.9	25.7	30.9	35.0	45.6	50.6	55.8
KENORA RCS	15 min	26.2	29.8	34.3	37.6	44.8	47.9	50.9
GERALDTON A	15 min	19.5	22.3	25.8	28.3	33.9	36.3	38.6
ATIKOKAN (AUT)	30 min	28.3	31.5	35.8	39.1	47.1	50.8	54.5
SIOUX LOOKOUT A	30 min	29.7	34.3	40.2	44.7	55.0	59.5	63.9
WIARTON A	30 min	25.7	29.1	33.5	36.8	44.5	47.8	51.1
THUNDER BAY CS	30 min	29.3	34.5	41.7	47.4	61.9	68.6	75.8
KENORA RCS	30 min	35.3	40.7	47.7	52.8	64.2	69.1	73.9
GERALDTON A	30 min	23.8	26.1	28.6	30.1	33.1	34.1	35.0
ATIKOKAN (AUT)	1 hr	34.2	38.0	43.0	46.9	56.4	60.8	65.4
SIOUX LOOKOUT A	1 hr	34.9	40.1	46.7	51.8	63.3	68.3	73.3
WIARTON A	1 hr	35.2	40.5	47.4	52.6	64.5	69.6	74.7
THUNDER BAY CS	1 hr	37.5	45.6	57.8	68.5	99.2	115.6	134.3
KENORA RCS	1 hr	45.2	52.5	61.7	68.5	83.6	90.0	96.3
GERALDTON A	1 hr	29.7	33.4	37.9	41.1	48.0	50.7	53.4
ATIKOKAN (AUT)	2 hr	43.0	48.3	55.7	61.5	76.5	83.6	91.2
SIOUX LOOKOUT A	2 hr	46.1	53.4	62.7	69.7	86.0	92.9	99.9
WIARTON A	2 hr	46.1	53.4	62.8	69.9	86.2	93.2	100.2
THUNDER BAY CS	2 hr	45.2	54.8	69.7	82.9	122.0	143.3	168.0
KENORA RCS	2 hr	61.9	76.2	95.2	109.5	143.0	157.5	171.9
GERALDTON A	2 hr	34.7	39.4	45.6	50.4	62.1	67.3	72.6
ATIKOKAN (AUT)	6 hr	62.4	75.1	94.6	111.7	161.5	188.2	218.8
SIOUX LOOKOUT A	6 hr	59.1	67.9	79.2	87.7	107.3	115.7	124.1
WIARTON A	6 hr	57.5	65.6	76.0	83.8	102.0	109.7	117.5
THUNDER BAY CS	6 hr	56.8	68.7	87.4	104.5	156.6	185.9	220.5
KENORA RCS	6 hr	81.1	98.9	122.8	140.9	183.2	201.4	219.7
GERALDTON A	6 hr	47.0	55.4	68.6	80.6	117.6	138.5	163.2
ATIKOKAN (AUT)	12 hr	76.1	91.8	115.8	136.8	197.6	230.2	267.4
SIOUX LOOKOUT A	12 hr	66.9	76.3	88.6	97.8	119.0	128.2	137.3
WIARTON A	12 hr	64.6	73.7	85.4	94.2	114.5	123.3	132.0
THUNDER BAY CS	12 hr	67.4	80.9	101.5	119.6	172.1	200.4	232.7
KENORA RCS	12 hr	97.3	118.0	145.3	165.9	213.8	234.4	255.0
GERALDTON A	12 hr	55.8	65.2	79.9	93.0	132.2	153.9	179.2
ATIKOKAN (AUT)	24 hr	80.4	96.0	119.7	140.5	200.5	232.6	269.3
SIOUX LOOKOUT A	24 hr	75.2	85.7	99.1	109.2	132.6	142.6	152.6
WIARTON A	24 hr	69.7	77.9	88.5	96.5	114.9	122.8	130.7
THUNDER BAY CS	24 hr	75.8	92.5	119.8	145.3	226.7	274.4	332.1
KENORA RCS	24 hr	105.7	126.1	152.6	172.4	217.8	237.2	256.5
GERALDTON A	24 hr	70.7	82.7	100.5	115.6	157.8	179.5	203.8

**Table 7: IDF Curves for 6020LPQ ATIKOKAN (AUT) – Gumbel Distribution (mm)**

<b>Return Period (years)</b>	<b>5min</b>	<b>10 min</b>	<b>15 min</b>	<b>30min</b>	<b>1h</b>	<b>2h</b>	<b>6h</b>	<b>12h</b>	<b>24h</b>
2	8.4	12.6	15.6	20.0	24.7	30.4	37.0	44.5	49.2
5	10.7	15.4	19.8	24.9	30.4	37.8	50.9	61.9	66.4
10	12.3	17.2	22.4	28.3	34.2	43.0	62.4	76.1	80.4
20	13.9	18.8	24.9	31.5	38.0	48.3	75.1	91.8	96.0
50	16.0	20.7	28.1	35.8	43.0	55.7	94.6	115.8	119.7
100	17.7	22.1	30.5	39.1	46.9	61.5	111.7	136.8	140.5
200	19.4	23.4	32.9	42.5	50.9	67.7	131.3	160.7	164.1
500	21.8	25.2	36.1	47.1	56.5	76.5	161.5	197.7	200.5
1,000	23.7	26.5	38.5	50.8	60.8	83.6	188.2	230.2	232.6
2,000	25.7	27.8	41.0	54.5	65.4	91.2	218.8	267.4	269.3

**Table 8: IDF Curves for 6037775\_SIOUX\_LOOKOUT\_A - Gumbel Distribution (mm)**

<b>Return Period (years)</b>	<b>5min</b>	<b>10 min</b>	<b>15 min</b>	<b>30min</b>	<b>1h</b>	<b>2h</b>	<b>6h</b>	<b>12h</b>	<b>24h</b>
2	8.1	11.8	13.9	17.6	21.4	27.2	36.2	42.1	48.0
5	11.5	16.7	19.5	24.9	29.5	38.6	50.0	57.0	64.4
10	13.7	20.0	23.2	29.7	34.9	46.1	59.1	66.9	75.3
20	15.9	23.2	26.8	34.3	40.1	53.4	67.9	76.3	85.7
50	18.6	27.3	31.5	40.2	46.7	62.7	79.2	88.6	99.1
100	20.7	30.3	34.9	44.7	51.8	69.7	87.7	97.8	109.2
200	22.8	33.4	38.4	49.1	56.7	76.7	96.1	106.9	119.3
500	25.5	37.4	43.0	55.0	63.3	86.0	107.3	119.0	132.6
1,000	27.5	40.4	46.4	59.5	68.3	92.9	115.7	128.2	142.6
2,000	29.6	43.5	49.9	63.9	73.3	99.9	124.1	137.3	152.6

**Table 9: IDF Curves for 6119500 WIARTON A – Gumbel Distribution (mm)**

<b>Return Period (years)</b>	<b>5 min</b>	<b>10 min</b>	<b>15 min</b>	<b>30 min</b>	<b>1h</b>	<b>2h</b>	<b>6h</b>	<b>12h</b>	<b>24h</b>
2	7.1	10.3	12.8	16.7	21.3	27.1	36.3	40.9	48.2
5	9.3	13.3	16.7	22.1	29.7	38.5	49.1	55.2	61.1
10	10.7	15.2	19.2	25.7	35.2	46.1	57.5	64.6	69.7
20	12.1	17.0	21.6	29.1	40.5	53.4	65.6	73.7	77.9
50	13.8	19.4	24.8	33.5	47.4	62.8	76.0	85.4	88.5
100	15.2	21.3	27.1	36.8	52.6	69.9	83.8	94.2	96.5
200	16.5	23.0	29.5	40.1	57.7	76.9	91.7	103.0	104.4
500	18.3	25.4	32.6	44.5	64.5	86.2	102.0	114.5	114.9
1,000	19.6	27.2	34.9	47.8	69.6	93.2	109.7	123.3	122.8
2,000	20.9	29.0	37.3	51.1	74.7	100.2	117.5	132.0	130.7

**Table 10: IDF Curves for 6048268\_THUNDER BAY CS – GEV Distribution (mm)**

<b>Return Period (years)</b>	<b>5 min</b>	<b>10 min</b>	<b>15 min</b>	<b>30 min</b>	<b>1h</b>	<b>2h</b>	<b>6h</b>	<b>12h</b>	<b>24h</b>
2	7.2	10.8	13.1	17.0	20.9	25.8	33.9	39.9	44.8
5	10.1	15.0	18.3	24.2	30.2	36.5	46.4	55.2	61.5
10	12.1	17.7	21.9	29.3	37.5	45.2	56.8	67.4	75.8
20	14.1	20.3	25.7	34.5	45.6	54.8	68.7	80.9	92.5
50	16.7	23.8	30.9	41.7	57.8	69.7	87.4	101.5	119.8
100	18.7	26.3	35.0	47.4	68.5	82.9	104.5	119.6	145.3
200	20.8	28.9	39.4	53.4	80.6	98.2	124.5	140.2	176.0
500	23.7	32.3	45.6	61.9	99.2	122.0	156.6	172.1	226.7
1,000	25.9	34.9	50.6	68.6	115.6	143.3	185.9	200.4	274.4
2,000	28.1	37.5	55.8	75.8	134.3	168.0	220.5	232.7	332.1

**Table 11: IDF Curves for 6034073 KENORA RCS – PE3 Distribution (mm)**

<b>Return Period (years)</b>	<b>5 min</b>	<b>10 min</b>	<b>15 min</b>	<b>30 min</b>	<b>1h</b>	<b>2h</b>	<b>6h</b>	<b>12h</b>	<b>24h</b>
2	10.0	13.7	16.3	20.9	25.8	29.2	40.7	49.0	55.6
5	13.1	18.1	22.3	29.5	37.5	47.7	63.4	76.6	84.8
10	14.9	20.8	26.2	35.3	45.2	61.9	81.1	97.3	105.7
20	16.5	23.2	29.8	40.7	52.5	76.2	99.0	118.0	126.1
50	18.4	26.1	34.3	47.7	61.7	95.2	122.8	145.3	152.6
100	19.7	28.1	37.6	52.8	68.5	109.5	140.9	165.9	172.4
200	20.9	30.1	40.8	57.8	75.1	123.9	159.1	186.6	192.0
500	22.4	32.6	44.8	64.2	83.6	143.0	183.2	213.8	217.8
1,000	23.5	34.4	47.9	69.1	90.0	157.5	201.4	234.4	237.2
2,000	24.6	36.1	50.9	73.9	96.3	171.9	219.7	255.0	256.5

**Table 12: IDF Curves for 6042716 GERALDTON A – GEV Distribution (mm)**

Return Period (years)	5 min	10 min	15 min	30 min	1h	2h	6h	12h	24h
2	6.7	9.8	12.0	16.2	19.2	23.0	31.0	37.3	45.0
5	9.0	13.4	16.6	21.1	25.7	29.9	39.8	47.5	59.5
10	10.3	15.8	19.5	23.8	29.7	34.7	47.0	55.8	70.7
20	11.4	18.0	22.3	26.1	33.4	39.4	55.4	65.2	82.7
50	12.7	20.8	25.8	28.6	37.9	45.6	68.6	79.9	100.5
100	13.6	22.8	28.3	30.2	41.1	50.4	80.6	93.0	115.7
200	14.3	24.8	30.8	31.5	44.2	55.4	94.8	108.2	132.5
500	15.2	27.4	33.9	33.1	48.0	62.1	117.6	132.2	157.8
1,000	15.8	29.3	36.3	34.1	50.7	67.3	138.5	153.9	179.5
2,000	16.4	31.2	38.6	35.0	53.4	72.6	163.2	179.2	203.8

### 3.2.2 Spatial interpolation to the Ignace study area

The stations located at the study area do not have short duration (sub-daily) rainfall records. A spatially interpolated (linearly scaled with distance) IDF curve was calculated using the station results from the two closest stations to the study area, 6020LPQ ATIKOKAN (AUT) and 6037775 – SIOUX LOOKOUT A (Table 4). The resulting sub-daily IDF is presented in Table 13. The results agree with the values calculated for other stations in the region. The 24-hour, 100-year return period precipitation is estimated at 125.5 mm and the 500-year return period at 167.9 mm.

**Table 13: Spatially Interpolated IDF Curves for the Ignace Study Area (mm)**

Return Period (years)	5 min	10 min	15 min	30 min	1 h	2 h	6 h	12 h	24 h
2	8.3	12.2	14.8	18.8	23.1	28.9	36.6	43.3	48.6
5	11.1	16.1	19.6	24.9	30	38.2	50.5	59.5	65.4
10	13	18.5	22.8	28.9	34.5	44.5	60.8	71.6	77.9
20	14.8	20.9	25.8	32.8	39	50.7	71.6	84.4	91
50	17.3	23.8	29.7	37.9	44.8	59	87.2	102.7	109.8
100	19.1	26	32.6	41.8	49.2	65.5	100.2	118.1	125.5
200	21	28.2	35.5	45.7	53.7	72	114.4	134.9	142.6
500	23.6	31	39.4	50.9	59.7	81	135.5	160	167.9
1,000	25.5	33.2	42.3	54.9	64.4	88.1	153.5	181.3	189.5
2,000	27.6	35.3	45.2	59	69.2	95.3	173.4	205	213.3

### 3.2.3 Comparison with other sources

The above stations were compared with publicly available external tools and portals to confirm the results presented in the previous section were in line with other sources. The following sources were used in the comparison:

- **IDF\_CC Tool:** The tool used Gumbel and GEV distribution with the method of moments and L-moments respectively to calculate the baseline values. The tool only calculates return periods up to 100-year.
- **MTO Lookup tool:** The tool used Gumbel with the method of moments to calculate the baseline values for the IDF curves. The tool only calculates return periods up to 100-year and uses an interpolation methodology.

Only select return periods and 24-hour durations were used for comparison, as presented in Table 14. The estimates generated by Golder are in line with the IDF tool, with a higher projection for Atikokan (AUT) and Kenora RCS, and similarly for the other stations. The comparison with the MTO tool shows larger variations that may be attributed to the spatial interpolation of the MTO tool. The projected values are shown not to change significantly from one station to the others.

**Table 14: IDF Curves Comparison with Other Sources – 100-Year Return Period for 24-Hour Duration**

Station	Golder (mm)	IDF_CC Tool		MTO IDF Tool	
		(mm)	(%)	(mm)	(%)
6020LPQ - ATIKOKAN (AUT)	140.5	114.5	22.6%	130.9	7.3%
6037775 - SIOUX LOOKOUT A	109.2	113.0	-3.4%	128.1	-14.7%
6119500 - WIARTON A	96.5	95.9	0.6%	127.3	-24.2%
6048268 - THUNDER BAY CS	145.3	145.4	-0.1%	121.3	19.7%
6034073 - KENORA RCS	172.4	158.6	8.7%	133.0	29.6%
6042716 - GERALDTON A	115.6	115.7	-0.1%	118.4	-2.3%
Ignace study Area <sup>(1)</sup>	125.5	—	—	128.6	-2.5%

Note: <sup>(1)</sup> Interpolated IDF curve calculated in Section 3.2.2.

### 3.2.4 Daily and multi-day IDF curve for the Ignace study area

The data source for this analysis is the daily baseline time series defined in Section 3.1.2. The daily and multi-day IDF curves were calculated for the same return periods used for the IDF curves in the previous section. Based on the goodness of fit tests, the Pearson Type 3 distribution was selected to calculate the curves. The results are shown in Table 15 for selected durations up to 120-days. The 1-day IDF curve is converted to 24-hours duration (using the 1.13 ratio recommended by the World Meteorological Organization 2019). Daily rainfall can be calculated for two different periods: 24-hour rainfall and 1-day rainfall. The 24-hour rainfall is calculated as the maximum rainfall during a moving block of 24 hours, while the 1-day rainfall is calculated as the maximum rainfall during the period from midnight of one day to midnight of the next. Due to the differences in the method of calculation, there are typically differences in the values, with the 24-hour rainfall often being higher (moving block allows for greater capture of storms). As seen in Table 16, the interpolated IDF curve (calculated in Section 3.2.2) shows good agreement, with higher differences for longer return periods due to uncertainties in the extrapolation.

**Table 15: Daily and Multi-day IDF Curves for the Ignace Study Area (mm)**

Return Period (years)	1-Day	2-Day	3-Day	4-Day	5-Day	6-Day	7-Day	10-Day	20-Day	30-Day	50-Day	75-Day	90-Day	120-Day
2	44.3	54.8	64.1	69.6	74.5	77.8	82.8	95.8	135.8	167.4	220.9	291.6	332.7	407
5	61.6	78	89	95.6	100.7	104.6	110.4	126.9	168.9	203.6	264.3	350.1	398.8	486.1
10	73.4	94.1	105.2	112.1	117.2	122	128.1	147	188.2	224	288.1	382.1	434.8	530.2
20	84.7	109.6	120.4	127.5	132.4	138.2	144.4	165.7	205.3	241.5	308.1	409.2	465.3	567.9
50	99.1	129.5	139.5	146.6	151.2	158.5	164.7	189.1	225.8	262.1	331.3	440.6	500.4	612
100	109.8	144.3	153.4	160.5	164.7	173.2	179.5	206.2	240.2	276.3	347.1	462	524.3	642.3
200	120.4	158.8	166.9	173.9	177.9	187.7	193.8	222.8	253.8	289.6	361.8	481.9	546.6	670.6
500	134.1	177.9	184.5	191.3	194.8	206.3	212.2	244.2	271.1	306.2	379.9	506.4	574	705.8
1,000	144.4	192.1	197.6	204.2	207.2	220.2	225.8	260.1	283.6	318.2	392.8	523.9	593.5	731.1
2,000	154.6	206.3	210.4	216.8	219.5	233.8	239.3	275.8	295.8	329.7	405.1	540.6	612.1	755.4

**Table 16: Comparison of the IDF Curves at Ignace Study Area**

Return Period (years)	Daily to 24-Hours <sup>(1)</sup> (mm)	Interpolated to Ignace Study Area, 24-Hours (mm)
2	50.1	48.6
5	69.6	65.4
10	82.9	77.9
20	95.7	91.0
50	112.0	109.8
100	124.1	125.5
200	136.0	142.6
500	151.5	167.9
1,000	163.1	189.5
2,000	174.7	213.3

Note: <sup>(1)</sup> Converted to 24-hours duration using the 1.13 WMO ratio.

### 3.3 Baseline PMP Calculations

Using the stations listed in Table 1 that were involved in the baseline development, DAD curves and PMP values were calculated for the desired duration periods (1-day, 24-hour, 2-day, and 3-day). The PMP values were calculated specifically for the Ignace study area using the precipitation series defined in Section 3.1.2 and Figure 4 of this report for the Hershfield method and cross validated using two different methods, the PMP Hershfield and the Transposition (DAD curves).

#### 3.3.1 Historical storms for the Transposition Method

All periods for the stations (Table 1) were screened for large events, including the most recent observations. The periods covered by the stations is from the early 1900s to 2019. All precipitation events higher than 100 mm/day were preselected and screened. One event registered at Ignace (6033690) station in September 1941, and two other stations were investigated. The total 1-day precipitation registered at Ignace was 122.4 mm on September 21<sup>st</sup>, 115.8 mm on September 20 at Sioux Lookout A Station (6037775), and 106.7 mm at Quorn Station (6046811). The 3-day accumulation from September 19<sup>th</sup> to 21<sup>st</sup>, 1941 was registered as 138.4, 134.8 and 129.8 mm, respectively.

The second major event in the study area was registered on June 2002; a large storm was registered on the northern region of Northwestern Ontario, parts of Manitoba and Minnesota (USA). This storm was named the 49<sup>th</sup> Parallel storm and it was the largest recorded for some of the stations including Mine Centre and Atikokan AUT. The amount recorded from June 8<sup>th</sup> to 11<sup>th</sup>, 2002, was 293.2 mm at Mine Centre (6025203) and 194.0 mm in Atikokan AUT (6020LPQ). Other stations farther north also registered significant amount on the same days, Sioux Lookout A (6037775) with 90.8 mm (92.88 mm from the AHCCD dataset) in the three days, Dryden A (6032119) with 113.1mm. Other stations farther away from the study area, such as Geraldton A (6042716) and Wiarton A (6119500) only registered 43.8 mm, and 9.1mm, respectively for this event.

According to Murphy et al. (2003), severe flooding, record precipitation, and high river flows were registered from the above-mentioned storm. A series of Mesoscale Convective Systems (MCS) moved through southern portions of northwestern Ontario, southeastern Manitoba, and northern Minnesota from the evening of June 8, 2002 through the morning hours of June 11, 2002. The highest rainfall rates occurred on June 9<sup>th</sup> and 10<sup>th</sup> associated with intense thunderstorms that were continuously generating and moving across the area from the Roseau River to just southwest of Upsala, Ontario and resulted in a swath having rainfall accumulations in the 200-400 mm range (Figure 1 in Murphy et al. 2003).

No significant storm events were registered on the stations from 2002 to present (based on the observations screened). The storm registered on September 1941 was deemed to not be large enough to affect the PMP in the study compared to the 49<sup>th</sup> parallel event. The DAD curve is constructed for this specific storm and compared to the results from the site specific Hershfield method for the study area.

### 3.3.2 Estimates of PMP with the Hershfield method

For the estimate of the PMP using the Hershfield method as described by the World Meteorological Organization (WMO 2009), the daily baseline time series prepared for the Ignace study area as described in Section 3.1.2 was used. The results using the baseline time series were compared to the calculations from the DAD curves for the Transposition method in the next section. The 1-day PMP value found was 364.3 mm (Table 17), which is equivalent to 411.7 mm for the 24-hour duration PMP using the 1.13 conversion factor (from daily to 24-hour rainfall events) recommended by the WMO. The 2-day and 3-day PMP values for the same location were calculated as 482.2 mm and 510.1 mm respectively.

**Table 17: PMP Summary for Statistical Method for the Ignace Study Area**

Duration	PMP (mm)
1-Day	364.3
24-Hour <sup>(1)</sup>	411.7
2-Day	482.2
3-Day	510.1

<sup>(1)</sup> Converted from daily to 24-hour duration using the 1.13 ratio recommended by the WMO (2009).

### 3.3.3 Development of DAD Curves in Estimate of PMP with the Transposition Method

The DAD curves were developed using the Transposition method described in Appendix A.2.3. For the development of the DAD curves for the Ignace study area, the focus was on the 49<sup>th</sup> Parallel storm in June 2002. This storm was the most intense observed near the Ignace area, based on the records extracted from the stations listed in Table 1. Additionally, previous analysis conducted by OMNR (2006) concluded that the 49<sup>th</sup> Parallel storm was found to be larger than the Timmins and Hazel events for all durations above 12 hours and comparable to the Hazel event and comparable for smaller durations.

The DADs were constructed for 1-day, 2-day and 3-day, and the areal average determined the envelopment curves. Figure 5 presents the curves constructed for 1-day, 2-day and 3-day from the data collected from the stations listed in Table 1 and the data points are given in Table 18. The dots in Figure 5 represent the total precipitation for each of the events registered on the stations screened and the area of influence for the corresponded rainfall amounts using the method described in Appendix A.2.3.1. The dashed lines represent the envelopment for both durations (1-day and 3-day) as indicated. The resulting DAD curves show little change in total precipitation from 25 km<sup>2</sup> to 1,000 km<sup>2</sup>. This is due to the nature of the 49<sup>th</sup> Parallel storm in the region, which produced a line of mesoscale convective systems passing over the area resulting in a large storm radius.

The original DAD curves were constructed as shown in Figure 5. The original DAD curves and consequent PMP values were multiplied by the maximization factor (used to maximize the screened observed storm) and transposition factor (used to transpose the values of the PMP to the Ignace study area), using the precipitable water content as described in Appendix A.2.3.2. . The maximization factor was estimated for Mine Centre Station as 2.21 (following the methodology described in Appendix A.2.3.2), using the 12-hours persistent dew point map from Figure 3.6 in OMNR (2006) for the month of June and the maximum daily mean temperature as a proxy for the dew point of the 49<sup>th</sup> Parallel storm of June 2002. The transposition factor (as defined in Appendix A.2.3.2) was estimated as 0.92, also using the map from Figure 3.6 in OMNR (2006); the approximate values of the 12-hours, 100-year return period dew point temperature were extracted for the locations of Mine Centre station and the Ignace study area.

The storm maximization for the 1-Day PMP was then calculated as 2.033 ( $2.21 \times 0.92$ ) to obtain the adjusted DAD curve and PMP for Ignace (Table 20). For the 2- and 3- Day PMP, the maximization delta of the 1-Day PMP was added to the original 2- and 3-Day DAD curve (Table 19).

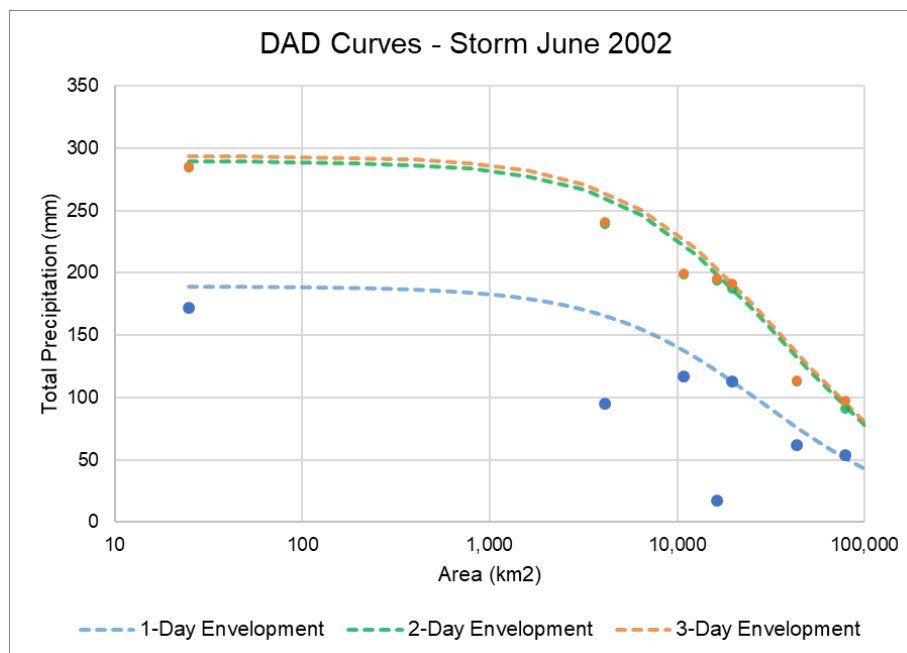


**Figure 5: DAD Curves for 49<sup>th</sup> Parallel Storm, 1-, 2- and 3-Day Duration (Non-Maximized Storm)**

**Table 18: Data Points Used to Obtain the DAD Curves**

Station / Points	Area (km <sup>2</sup> )	2002-06-09 1-Day	2002-06-09 and 10 2-Day	2002-06-09 to 11 3-Day
		PPT <sup>(1)</sup> (mm)	PPT (mm)	PPT (mm)
6020LPQ	16,367.4	17.6	194.0	195.8
Midpoint 6025203 to 6020LPQ	4,091.8	94.8	239.4	240.6
6025203	25.0	172.0	284.8	285.4
6032119	43,446.8	61.6	113.1	114.0
Midpoint 6025203 to 6032119	10,861.7	116.8	199.0	199.7
6037775	78,442.0	54.0	90.8	97.5
Midpoint 6025203 to 6037775	19,610.5	113.0	187.8	191.5

<sup>(1)</sup> PPT = Total Precipitation

**Table 19: Original DAD Curves for the 49<sup>th</sup> Parallel Storm**

Area (km <sup>2</sup> )	PMP (mm)		
	1-Day	2-Day	3-Day
25	188.8	289.6	293.7
100	188.4	289	293.1
500	186.4	286.7	290.8
1,000	183.9	283.6	287.7
2,000	179.1	277.6	281.8
5,000	170.3	266.4	270.7
10,000	154.9	246.6	250.9

**Table 20: Adjusted DAD Curves for the Ignace Study Area**

Area (km <sup>2</sup> )	PMP (mm)			
	1-Day	2-Day	3-Day	24-hour <sup>(1)</sup>
25	383.9	484.7	488.8	433.9
100	383	483.6	487.7	432.7
500	379.1	479.3	483.4	428.3
1,000	374	473.6	477.8	422.6
2,000	364.2	462.7	466.9	411.6
5,000	346.2	442.3	446.6	391.2
10,000	314.9	406.6	411	355.9

<sup>(1)</sup> Converted to 24-hour using 1.13 ratio recommend by the WMO (2009).

### 3.3.4 PMP comparison

This estimated 1-Day PMP value from the DAD curves for 1,000 km<sup>2</sup> (374.0 mm) in the Transposition method is slightly higher than that obtained by the Hershfield method (364.3 mm). The values of the PMP calculated were compared with other sources, including OMNR (2006), for validation. The PMP values were calculated by OMNR as an average by group of watersheds in Ontario as opposed to specific locations or specific storms. The Ignace study area is located in the English/Lake St. Joseph watershed and the 24-hour PMP is estimated at 436 mm. This is in line with the estimated calculation of 422.6 mm in Table 20.

If the Agimak River into Sandbar Lake is considered, the Ignace study area is only 126 km<sup>2</sup>. If the watershed for Agimak River into Barrel Lake is considered, the Ignace study area is approximately 812 km<sup>2</sup> using the Ministry of Natural Resources and Forestry (MNRF) Ontario Flow Assessment Tool (OFAT; MNRF 2020). Therefore, if the largest area is considered, the Ignace study area would be below 1,000 km<sup>2</sup>.

### 3.3.5 Sub-daily PMP estimates

The hourly precipitation data are not available from ECCC and therefore the sub-daily PMP was estimated using ratios obtained for the IDF curves for the sub-daily durations, from 5 minutes to 12 hours as described in Appendix A.2.3.3 (Table 21). The ratios were calculated using 24-hour duration and 100-year return period from the IDF curve calculated for the Ignace study area in Section 3.2.2. The 100-year return period is selected since it provides a more realistic and reliable estimate among sub-daily durations than higher return periods. The ratios were applied to the 24-hours PMP values obtained by the Hershfield method (Section 3.3.2) and the Transposition method (Section 3.3.3); the results are presented in Table 22 and Table 23. As noted in the previous sections, the values of the sub-daily PMP calculated by the Hershfield methods are similar to the values from the Transposition method for areas up to 1,000 km<sup>2</sup>. There are some uncertainties associated with the approach used to come up with the sub-daily values, since the actual sub-daily storm distribution may differ from the storm distribution derived using the adopted method.

**Table 21: Conversion Ratios from 24-hour to Sub-daily PMP**

Duration	5-min	10-min	15-min	30-min	1-hour	2-hour	6-hour	12-hour
Ratio	0.152	0.208	0.260	0.333	0.392	0.522	0.798	0.941

**Table 22: Estimated Sub-Daily PMP Values for the Ignace Study Area – Hershfield Method**

Duration	PMP (mm)
5-Min	62.7
10-Min	85.4
15-Min	107.0
30-Min	137.0
1-Hour	161.5
2-Hour	214.7
6-Hour	328.7
12-Hour	387.4
24-Hour	411.7
1-Day	364.3

**Table 23: Estimated Sub-Daily PMP Values for the Ignace Study Area – Transposition Method**

Area (km <sup>2</sup> )	PMP (mm)									
	1-Day	24-Hour	12-Hour	6-Hour	2-Hour	1-Hour	30-Min	15-Min	10-Min	5-Min
25	383.9	433.9	408.3	346.4	226.3	170.2	144.4	112.8	90	66.1
100	383	432.7	407.3	345.6	225.8	169.8	144.1	112.5	89.8	66
500	379.1	428.3	403.2	342	223.5	168.1	142.6	111.4	88.9	65.3
1,000	374	422.6	397.7	337.4	220.4	165.8	140.7	109.9	87.7	64.4
2,000	364.2	411.6	387.3	328.6	214.7	161.5	137	107	85.4	62.7
5,000	346.2	391.2	368.2	312.4	204.1	153.5	130.2	101.7	81.2	59.6
10,000	314.9	355.9	334.9	284.1	185.6	139.6	118.5	92.5	73.8	54.2

### 3.4 Rainfall on Snow

The analysis of rain on snow included the combined effect of precipitation as rainfall and the melting of accumulated snow. This analysis was conducted for the Ignace station using the baseline daily total precipitation and daily temperature time series defined for the Ignace study area as described in Section 3.1.2 in Table 3. The rain on snow requires the concurrent daily total precipitation and temperature data from the Ignace station. The procedure used for the calculation of the rainfall on snow results presented in this report follows the methodology adopted by ECCC (Louie and Hogg 1980), and the steps adapted are detailed in Appendix A.2.4. A snowpack accumulation and snowmelt model (Pysklywec et al. 1968) were used to estimate the depth of equivalent rainfall converted from the snowpack accumulation for the Ignace study area. A probability distribution (Gumbel) was used to calculate the estimates for selected return periods and presented in Table 24. The 1-day snowpack accumulation was calculated with the same distribution are presented in Table 25. The rain on snow projections can assist hydrological modeling to determine flood assessments, dam safety assessments, storage requirements and others. For shorter durations, i.e., the 1-day 100-year return period rain on snow event is calculated at 87 mm, indicating that extreme rainfall events are predominant over the snowmelt events based on the analysis of the historical observations. Longer duration events, however, 20-days or more and high return periods (100-year or more), may be useful for hydrological analysis when volumetric capacity is an important variable to consider.

**Table 24: Rainfall on Snow Projections for the Ignace Study Area (mm)**

<b>Return Period (years)</b>	<b>1-Day</b>	<b>2-Day</b>	<b>3-Day</b>	<b>4-Day</b>	<b>5-Day</b>	<b>6-Day</b>	<b>7-Day</b>	<b>10-Day</b>	<b>20-Day</b>	<b>30-Day</b>	<b>50-Day</b>	<b>75-Day</b>	<b>90-Day</b>	<b>120-Day</b>
<b>2</b>	38	54.2	69.5	83.5	96.2	106.5	117	146.8	208.3	245.7	295.7	328	332.7	342.3
<b>5</b>	51.1	71.8	91.6	110.5	128.5	144.4	160.9	206.8	300.8	354	412.8	449.9	453	455.5
<b>10</b>	59.8	83.5	106.2	128.4	150	169.5	190	246.5	362	425.7	490.4	530.6	532.7	530.4
<b>20</b>	68.2	94.7	120.2	145.5	170.5	193.6	217.9	284.6	420.7	494.5	564.8	608.1	609.2	602.3
<b>50</b>	79	109.2	138.3	167.7	197.2	224.8	254	334	496.7	583.5	661.2	708.3	708.1	695.4
<b>100</b>	87	120.1	151.9	184.4	217.1	248.2	281	371	553.7	650.2	733.3	783.3	782.3	765.1
<b>200</b>	95.1	130.9	165.5	200.9	237	271.5	308	407.8	610.4	716.7	805.3	858.2	856.1	834.6
<b>500</b>	105.7	145.1	183.3	222.8	263.2	302.2	343.6	456.4	685.3	804.4	900.1	956.9	953.6	926.2
<b>1,000</b>	113.8	155.9	196.8	239.3	283	325.4	370.5	493.1	741.9	870.7	971.8	1031.5	1027.3	995.5
<b>2,000</b>	121.8	166.7	210.3	255.9	302.8	348.6	397.3	529.9	798.4	937	1043.5	1106	1100.9	1064.7

**Table 25: 1-Day Snowpack Accumulation for the Ignace Study Area (mm)**

<b>Return Period (years)</b>	<b>2</b>	<b>5</b>	<b>10</b>	<b>20</b>	<b>50</b>	<b>100</b>	<b>200</b>	<b>500</b>	<b>1,000</b>	<b>2,000</b>
<b>1-Day</b>	207.1	301.3	363.6	423.4	500.8	558.7	616.5	692.8	750.4	808.0

#### **4. ANALYSES OF FUTURE CLIMATE ON PMP AND IDF ESTIMATES**

The following sections build on the current climate descriptions in Section 3 by providing the projected changes under future climate conditions for two future time horizons (2050s and 2080s) relative to the model baseline period of 1950 to 1993. The model baseline is based on projections from the GCMs for the same time period as the observations used to form the current climate baseline. The projected changes in climate are presented as the percentage change from the model baseline with guidance on how to apply the changes to the observed current climate baseline in order to obtain absolute values for future climate. Section 4.1 provides a description of future climate conditions used to estimate the potential changes in IDF curve and PMP estimates, which are later discussed in Sections 4.2 and 4.3. In all sections, projections are provided in terms of percentiles measured over the 136-member multi-model ensemble. Select tables presented in this section are colored using a gradient to aid in the visual representation of the values. The color gradients provide a relative indication of the highest (red) and lowest (green) values with transitional colors in between. Colors cannot be compared between tables, as the color scale is relative for each.

The following sections focus on the 50<sup>th</sup> percentile to illustrate general trends. The remaining percentiles are included in Appendix B. Guidance on applying the percentile changes to the observed current climate basis is provided in Section 4.1.

##### **4.1 Future Climate Projections**

Climate change has the potential to change future precipitation and temperature regimes that are important inputs for design purposes. Golder has developed a standardized approach to complete climate change assessments, which has been applied in the following sections to aid in the design of deep geological repositories for nuclear waste. The development of a detailed future climate assessment helps support the consideration of climate change in such designs. This climate change assessment report summarizes future projected changes in climate with a focus on extreme precipitation events. Future projected changes in daily and sub-daily IDF curves, PMP, combined rainfall and snowmelt statistics, and peak snowpack accumulation are estimated based on the best available climate science.

The IPCC is generally considered to be the definitive source of information related to past and future climate change as well as climate science. As an international body, the IPCC provides a common source of information relating to emission scenarios, provides third party reviews of models, and recommends approaches to document future climate projections. Periodically, the IPCC issues assessment reports summarizing the most current state of climate science. The Fifth Assessment Report (AR5) (IPCC 2013) represents the most current complete synthesis of information regarding climate change to date. The next assessment report (Sixth Assessment Report) is anticipated in 2022 and will build on the results from AR5. Future climate is typically projected using GCMs that involve the mathematical representation of global land, sea, and atmosphere interactions over a long time period. These GCMs have been developed by different government agencies but share common elements described by the IPCC. The IPCC does not run the models but acts as a clearinghouse for the distribution and sharing of the model forecasts. Future climate projections are made using scenarios that incorporate different representative concentrations pathways (RCPs) to drive the GCM simulations. The RCPs represent different trajectories for radiative forcing due to mainly anthropogenic influence on the climate cycle. The pathways are named after the radiative forcing projected to occur by 2100.

Future climate projections are available from about 30 GCMs and four representative concentration pathways (RCP 2.6, RCP 4.5, RCP 6.0, and RCP 8.5) in AR5.

Downscaling procedures allow for GCM model output to be represented at a finer spatial scale which better represents local climate. Statistical downscaling refines GCM projections by incorporating observed data and statistical methods are applied to allow for a better match between local observed climate and historical GCM model output. These methods are then applied to future GCM projections which are assumed to be more representative of local climate. This report focuses on analysis using the statistically downscaled daily data using the Bias Correction/Construction Analogues with Quantile mapping reordering version 2 (BCCAQv2) model from ClimateData.ca (ClimateData 2019), and the Localized Constructed Analogues (LOCA) model from the GDO-DCP archive (Pierce et al. 2014; Reclamation 2013). Climate variables of daily minimum and maximum temperature and precipitation are obtained from these datasets. Three RCP scenarios (RCP 2.6, RCP 4.5, and RCP 8.5) are currently available from ClimateData.ca for the BCCAQv2 model and are used in this report, while only two RCP scenarios (RCP 4.5 and RCP 8.5) are available for LOCA. Details regarding the methodology, number of model projections, and resolution of both the BCCAQv2 and LOCA datasets are included in Appendix A.

Since no one model or climate scenario can be viewed as completely accurate, the IPCC recommends that climate change assessments use as many models and climate scenarios as possible, or a “multi-model ensemble”. For this reason, the multi-model ensemble approach is used to delineate the probable range of results using percentiles. The percentiles are used to show the distribution of projected changes. This allows for uncertainty in the projections to be understood, while the 50<sup>th</sup> percentile is used to illustrate general trends. For critical infrastructure, selection of future projections at higher percentiles and higher return periods should be considered. For example, for critical infrastructure whose failure is considered unacceptable, a 95<sup>th</sup> percentile could be considered over the typical 50<sup>th</sup> percentile. The projected changes in climate for the site are calculated using three separate time periods including:

- Model baseline (1950 to 1993) – this time-period represents the current climate conditions for which the changes are estimated using each member of the multi-model ensemble.
- Mid-century (2041 to 2070) – used to represent changes in climate projected for the near future.
- End-of-century (2071 to 2100) – used to represent the furthest projections into the future possible with the available climate model scenarios. Changes in climate are typically greater for this period compared to the mid-century for the RCP4.5 and RCP8.5 scenarios.
- Beyond 2100 - qualitative climate assessment (climate projections beyond 2100 are not currently available from ClimateData.ca) provided using the projected trends from the mid-century and end-of-century periods guided by literature.

Changes in climate for the mid-century and end-of-century future periods are calculated as percentage changes from the model baseline to avoid model bias influencing the results. Absolute values for the future climate projections can be obtained by applying the percentage changes to the observed data for a given percentile level from the multi-model ensemble as outlined in Appendix A (Sections A3.3 and A3.4).

The planned Project phases and how they correspond to the selected time periods are shown in Figure 6. The mid-century period coincides with part of the site characterization, preparation, and construction phase. The mid-century and part of the end of century time periods coincide with the operational period phase. Part of the end of century time period coincides with the extended monitoring period, and the qualitative climate assessment period corresponds with both the extended monitoring and decommissioning period Project phases. The extended monitoring and decommissioning periods extend past the year 2100 up to 2180.

Each of the Project phases coincide with part of the selected climate assessment periods. Percentiles from the multi-model ensembles for mid- and end-of-century may be selected in a way that accounts for how the Project phases and climate periods overlap. For example, a lower percentile may be used to cover the site characterization, preparation, and construction phase, as the mid-century period represents time horizon beyond this project phase. Similarly, a higher percentile may be used for the extended monitoring phase as it takes place after the end-of-century period. The 50<sup>th</sup> percentile level may be selected from the end-of century climate period to represent the operational project phase. Different percentile levels may be selected from the climate projections based on the level of associated risk for design purposes. For designs that are associated with a high level of risk, the 95<sup>th</sup> or 99<sup>th</sup> percentile level may be used. For project phases past 2100, a high percentile from the end-of-century climate period can be used for screening purposes. The qualitative climate assessment provides further guidance on how the climate may change past the year 2100.

The qualitative climate assessment period takes into consideration both the mid-century and end-of-century periods, as well as Extended Concentration Pathways (ECPs). ECPs have been developed by extending the RCP scenarios until the year 2300 using Earth Models of Intermediate Complexity (EMICs). The results of the EMIC extensions are consistent until 2300 with atmospheric-ocean general circulation models used in the IPCC fifth assessment report. Only global values are provided and are not directly applicable to the site; however, they provide qualitative trajectories of changes in temperature and precipitation in the far future.

The future projected changes in PMP are calculated using the Hershfield and moisture maximization methods. Future projected changes in IDF curves for sub-daily, daily, and multi-day durations were estimated using the Equidistant Quantile Mapping (EQM) method and the Ratio method. The same approach for estimating changes in IDF curves is applied to combined daily rain and snowmelt. The ensemble approach is used for all future projections, providing the results for a range of percentiles which takes multiple climate models, emission scenarios, and calculation methodologies into account. Details regarding the methodology for all the analyses provided in this report can be found in Appendix A. The following sections focus on the 50<sup>th</sup> percentile to illustrate general trends. The remaining percentiles are included in Appendix B.

## **4.2 Climate Change Impacts on IDF Curves**

The percent changes in IDF conditions (future periods relative to model baseline) were estimated for different durations of extreme rainfall events. Selected results for the 50<sup>th</sup> percentile for the 2050s and 2080s climatic horizons are summarized in the following sub-sections. Detailed methodology for this section can be found in Section A3.3. Additional results have been included in Appendix B in an Excel spreadsheet format. This format was selected to allow for the results to be more easily accessible and improve the readability of the report.

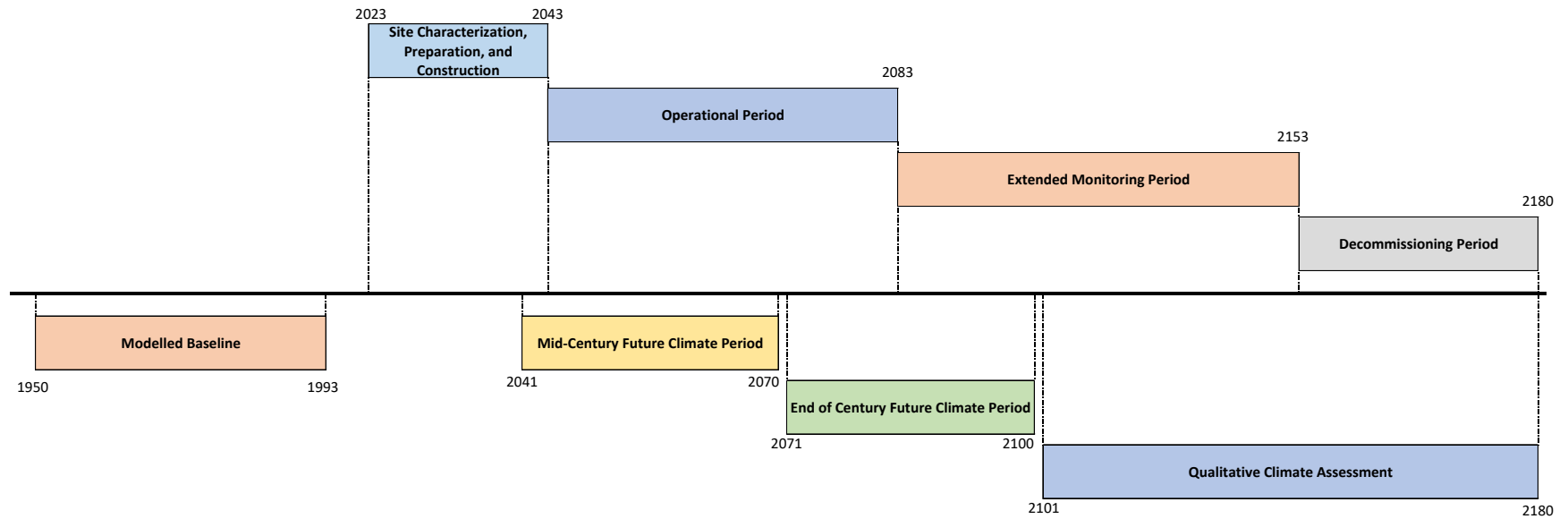


**Figure 6: Overview of Project Phases and Selected Future Climate Periods**

#### 4.2.1 Percent changes in sub-daily IDF curves

Sub-daily IDF curves are generally used to size site infrastructure for catchments small enough that runoff from the catchment would peak in less than 24 hours.

Daily rainfall amounts are provided in the climate model ensemble; however, sub-daily rainfall in the future projections are not available. The change in sub-daily rainfall statistics can be inferred by examining the projected changes for the 1-day duration. A summary of the projected changes in 1-day rainfall for the 2-, 5-, 10-, 25-, 50-, 100-, 1000-, and 2000-year return period are presented here for the 2050s and 2080s (Table 26 and Table 27). In the 2050s, the 1-day rainfall amount is projected to increase between 9.5% to 16.8% for the 50<sup>th</sup> percentile across return periods, while in the 2080s this is projected to increase between 11.8% to 18.1%. Based on these results, daily precipitation is expected to become more intense in the future. This is particularly true in the case of extreme rainfall events due to larger percentage increases shown as return period increases. Changes in sub-daily rainfall durations can be estimated by applying the changes in the 1-day rainfall amounts for the 2050s (Table 26) and 2080s (Table 27) to the observed sub-daily durations (Table 13).

Changes in atmospheric processes driving extreme rainfall will unlikely be uniform in the future climate for sub-daily rainfall durations. However, climate models are not yet able to fully resolve convective processes responsible for generating extreme precipitation amounts on finer spatial scales and contributing to extreme precipitation in larger scale synoptic systems (CSA 2012). Despite this fact, climate projections generally support an increase in short duration rainfall in future climate within Canada (CSA 2012). Therefore, the projected changes in sub-daily rainfall based on the 1-day projected changes should be used with caution. A higher percentile level may be used to account for uncertainty in sub-daily precipitation projections provided here.

**Table 26: Summary of the Projected Changes (%) in 1-day Rainfall in 2050s for Ignace Study Area**

Statistical indices	Return Period (years)									
	2	5	10	20	50	100	200	500	1000	2000
Minimum	-15.1%	-17.8%	-18.1%	-20.3%	-27.0%	-33.1%	-38.2%	-43.9%	-47.5%	-50.7%
5%	-6.7%	-4.8%	-7.3%	-11.5%	-15.2%	-17.4%	-20.0%	-23.1%	-25.1%	-27.1%
10%	-3.2%	-1.9%	-3.1%	-6.4%	-9.5%	-12.0%	-15.7%	-17.0%	-17.9%	-19.7%
25%	2.7%	4.0%	4.0%	3.6%	1.7%	0.5%	-1.0%	-1.6%	-2.2%	-2.9%
50%	9.5%	11.0%	12.2%	13.2%	14.3%	14.3%	14.4%	15.6%	16.3%	16.8%
75%	15.7%	18.5%	20.9%	24.1%	26.5%	28.7%	31.0%	33.8%	35.7%	37.0%
90%	23.7%	24.8%	30.0%	34.9%	41.8%	46.2%	50.0%	55.3%	59.9%	64.2%
95%	28.8%	29.5%	32.6%	43.4%	54.7%	62.6%	68.7%	76.2%	81.6%	86.5%
99%	32.1%	33.2%	46.1%	60.0%	86.0%	98.9%	108.6%	120.3%	131.0%	140.7%
Maximum	33.7%	37.9%	55.6%	72.1%	91.3%	107.7%	124.5%	144.1%	157.1%	168.9%
Mean	9.7%	11.4%	12.9%	14.3%	16.0%	17.1%	18.0%	19.2%	20.0%	20.7%
Standard deviation	10.3%	10.3%	12.9%	16.5%	21.3%	24.7%	27.7%	31.3%	33.7%	36.0%

**Table 27: Summary of the Projected Changes (%) in 1-day Rainfall in 2080s for Ignace Study Area**

Statistical indices	Return Period (years)									
	2	5	10	20	50	100	200	500	1000	2000
Minimum	-11.0%	-8.0%	-13.7%	-23.0%	-32.3%	-37.9%	-42.6%	-47.7%	-51.0%	-53.9%
5%	-6.6%	-5.0%	-4.3%	-5.2%	-8.1%	-11.0%	-13.9%	-16.6%	-18.8%	-20.7%
10%	-2.3%	-0.2%	-2.4%	-3.1%	-4.9%	-5.6%	-6.8%	-9.0%	-10.6%	-11.7%
25%	5.6%	7.4%	6.8%	5.4%	3.1%	1.8%	0.9%	-0.6%	-1.5%	-2.1%
50%	11.8%	14.7%	15.6%	16.1%	16.8%	17.8%	17.9%	18.0%	18.1%	18.1%
75%	20.1%	23.6%	26.6%	29.4%	30.3%	31.0%	32.4%	34.8%	35.6%	36.9%
90%	26.6%	31.2%	35.0%	42.7%	53.6%	60.7%	66.7%	73.2%	78.9%	83.2%
95%	31.1%	35.6%	46.2%	57.5%	69.2%	76.0%	83.1%	92.1%	96.7%	100.7%
99%	42.9%	43.4%	58.6%	77.4%	98.7%	112.1%	124.0%	137.6%	146.7%	155.0%
Maximum	47.1%	51.2%	65.1%	89.0%	119.4%	139.6%	157.8%	178.9%	193.1%	205.9%
Mean	12.8%	15.4%	17.2%	18.8%	20.6%	21.8%	22.9%	24.1%	24.9%	25.6%
Standard deviation	11.3%	11.8%	15.0%	19.0%	24.2%	27.7%	31.0%	34.8%	37.4%	39.7%

#### 4.2.2 Percent changes in daily and multi-daily IDF curves

Compared to sub-daily IDF values, the multi-day IDF values are used primarily to assess large catchments (where it takes more than 24 hours for flows to peak following a rainfall) and for water management systems (like dewatering and pumping).

The percent changes in daily and multi-day IDF conditions (future periods relative to the model baseline) were estimated for different durations of extreme rainfall events (ranging from 1 day to 120 days). Selected results for the 50<sup>th</sup> percentile are summarized in Table 28 and Table 29. The methodology is described in Section A.3.3. The remaining percentiles for all the duration periods are presented in Appendix B.

Note that the method used to produce the 24-hour results discussed in Section 4.2.1 (using sub-daily data and interpolating between Atikokan and Sioux Lookout) is different from the method used to produce the 1-day results in this section (fitting a curve to the daily projections for Ignace). The projected changes for the 50<sup>th</sup> percentile 1-day IDF curves range from 9.5% to 16.8% in the 2050s (Table 28) and 11.8% to 18.1% in the 2080s (Table 29). Generally, the longer durations show a smaller percentage increase (compared to the shorter durations) for both the 2050 and 2080 horizons. This suggests that shorter events are more sensitive to climate change effects, while longer events may be more likely to follow historic patterns.

**Table 28: Summary of the 50<sup>th</sup> Percentile of Projected Percent Changes in Rainfall in the 2050s for Ignace Study Area**

Return Period (years)	1-Day	2-Day	3-Day	4-Day	5-Day	6-Day	7-Day	10-Day	20-Day	30-Day	50-Day	75-Day	90-Day	120-Day
2	9.5%	9.3%	9.0%	8.5%	7.9%	7.8%	8.7%	8.1%	6.5%	6.1%	5.2%	5.4%	5.2%	4.5%
5	11.0%	12.3%	11.5%	9.9%	9.8%	10.0%	10.2%	9.7%	8.2%	7.0%	4.6%	3.6%	3.0%	2.9%
10	12.2%	13.5%	13.3%	11.6%	10.7%	10.0%	10.4%	10.1%	7.8%	7.5%	5.1%	3.7%	2.5%	3.0%
20	13.2%	15.7%	16.8%	13.8%	11.2%	9.2%	10.5%	9.6%	7.5%	8.2%	5.7%	4.6%	2.1%	3.1%
50	14.3%	18.7%	19.1%	15.2%	11.6%	10.8%	11.0%	10.0%	10.5%	8.4%	6.7%	4.8%	2.8%	3.8%
100	14.3%	20.9%	20.7%	15.4%	12.1%	11.6%	11.0%	10.2%	11.3%	9.5%	7.1%	5.0%	2.9%	4.0%
200	14.4%	22.1%	21.9%	16.6%	12.5%	12.3%	11.4%	9.6%	11.2%	10.0%	7.4%	6.1%	2.5%	3.7%
500	15.6%	24.0%	23.4%	17.3%	12.9%	12.3%	11.1%	9.6%	10.9%	10.4%	7.6%	6.2%	1.9%	3.7%
1,000	16.3%	24.8%	24.1%	17.8%	13.7%	12.4%	11.2%	9.9%	11.3%	10.6%	7.3%	6.4%	1.8%	3.8%
2,000	16.8%	25.1%	24.6%	18.1%	13.9%	12.8%	11.7%	9.9%	11.7%	10.8%	7.4%	6.7%	1.9%	3.6%

**Table 29: Summary of the 50<sup>th</sup> Percentile of Projected Percent Changes in Rainfall in the 2080s for Ignace Study Area (%)**

Return Period (years)	1-Day	2-Day	3-Day	4-Day	5-Day	6-Day	7-Day	10-Day	20-Day	30-Day	50-Day	75-Day	90-Day	120-Day
2	11.8%	11.5%	11.4%	11.2%	12.0%	11.1%	11.3%	10.0%	8.1%	7.6%	5.9%	5.4%	4.4%	3.8%
5	14.7%	15.1%	14.5%	12.6%	12.6%	12.2%	11.9%	10.8%	9.7%	8.7%	6.8%	5.6%	4.9%	4.3%
10	15.6%	18.1%	17.3%	15.3%	14.2%	12.8%	13.2%	11.9%	11.3%	9.9%	7.5%	6.2%	5.6%	4.0%
20	16.1%	19.4%	18.0%	15.9%	14.2%	13.6%	13.9%	13.3%	12.2%	11.0%	6.9%	6.6%	6.1%	4.3%
50	16.8%	22.6%	20.1%	16.4%	15.1%	14.0%	14.4%	14.0%	13.1%	13.0%	8.0%	7.2%	5.9%	4.7%
100	17.8%	23.3%	21.3%	16.5%	14.7%	13.6%	14.4%	15.3%	13.4%	13.6%	9.0%	7.2%	6.5%	5.2%
200	17.9%	24.2%	21.7%	17.0%	14.3%	13.6%	14.9%	16.3%	13.5%	14.4%	9.2%	7.9%	7.0%	5.5%
500	18.0%	25.1%	22.8%	17.4%	14.9%	14.1%	15.0%	17.8%	14.0%	15.2%	9.5%	8.9%	7.1%	5.1%
1,000	18.1%	26.0%	22.5%	17.7%	15.1%	14.2%	15.2%	18.6%	14.6%	15.1%	9.5%	9.1%	8.1%	4.8%
2,000	18.1%	26.6%	23.6%	18.0%	15.0%	14.3%	15.0%	19.3%	14.1%	15.9%	10.1%	9.6%	8.2%	4.8%

Projections for the 10-, 20-, and 50-year 24-hour events are available in Canada's Changing Climate report for Ontario using a multi-model ensemble 29 global climate models for comparison (Bush and Lemmen 2019). The report shows that the 24-hour event for the 10-, 20-, and 50-year return period is projected to change between 6% to 8.5%, 5.7% to 8.2%, and 4.9% to 8.5% respectively for the period of 2031 to 2050, and 5.3% to 20.5%, 5.1% to 20.1%, and 7.6% to 20.1% respectively for the period of 2081 to 2100 (Bush and Lemmen 2019). It should be noted that these values use global climate models that are not downscaled, have different time periods from those in this report, and present average values from the model ensemble as opposed to 50<sup>th</sup> percentile shown here. In general, the results shown in Table 28 and Table 29 are slightly higher than the range of projections made in Bush and Lemmen (2019) for the 2050s period, and are within the range for the 2080s period.

### 4.3 Climate Change Impacts on PMP Estimates

PMP values are typically used to assess the safety of critical infrastructure such as dams, where failure of the infrastructure would cause significant damage and or loss of life. The projected percentage changes in PMP shown here are point projections for the site that are not based on any specific watershed size. Therefore, these projected changes in PMP shown here are the same for the projected DAD curves of the corresponding event duration. Absolute values for future DAD curves can be obtained by applying the percentage changes in PMP to the DAD curves presented for current climate given in Section 3.3.3.

The percent changes in PMP estimates (future periods relative to model baseline) were estimated for future PMP using the Hershfield and Moisture Maximization methods. Both methods provide point estimates of PMP and require the use of annual maximum precipitation series for a given location. The annual maximum precipitation projections for the Ignace study area described in Section 4.1 are used; therefore, the PMP values provided are applicable to the study area and are not associated with a particular watershed or its size.

Sub-daily climate projections are not available, which are required to generate sub-daily estimates of PMP using these methods. Therefore, PMP is estimated for the 1-, 2-, and 3-day durations (**Error! Reference source not found.** and **Error! Reference source not found.**). The 50<sup>th</sup> percentile results suggest increases in the 1-day PMP of 18.7% for the 2050s and 25.4% for the 2080s. The results agree with the expectation that as temperature increases under future climate conditions, precipitation is expected to increase as more vapor becomes available in the atmosphere (Kunkel et al. 2013), resulting in a rise in the projected PMP. The range of results for the 1-day PMP (from -27.4% to +103.4% in 2050s and -24.6% and +126.0% in 2080s) suggest that significant flexibility may be required in the future for systems designed for the PMP event.

Kunkel et al. (2013) used seven GCMs from the CMIP5 to project changes in PMP for the 2050s and 2080s future time periods from the 1971 to 2000 baseline. It was found that ensemble average projected maximum precipitable water changes for Ontario were on the order of 25-35%. The 2080s projection for the 50<sup>th</sup> percentile in this report is within the range projection in Kunkel et al. (2013); however, the 2050s value is slightly below. Clavet-Gaumont et al. (2017) used an ensemble of 12 RCM runs to project the change in PMP between the periods of 1971 to 2000 and 2041 to 2070 time periods for 5 major Canadian water basins. The 24-, 48-, and 72-hour springtime changes in PMP for the Mattagami river basin (which drains a major portion of northern Ontario) were estimated as 8%, 4%, and 5% respectively, with no consensus in the

sign of the change, significantly lower than that of this report as well as Kunkel et al. (2013). The models used and time periods analyzed are different between this study and those in the literature. However, the comparison allows the number to be put into context with the range of those projected previously for a similar area.

**Table 30: Summary of Selected Percentiles of Projected Percent Changes in PMP Estimates in the 2050s for Ignace Study Area**

Percentiles	1-Day	2-Day	3-Day
Minimum	-27.4%	-30.9%	-28.0%
5%	-7.5%	-6.0%	-6.4%
25%	8.6%	11.2%	10.3%
<b>50%</b>	<b>18.7%</b>	<b>18.7%</b>	<b>18.5%</b>
75%	28.3%	30.0%	28.1%
95%	55.8%	54.8%	51.7%
Maximum	103.4%	79.6%	83.7%

**Table 31: Summary of Selected Exceedance Probabilities of Projected Percent Changes in PMP Estimates in the 2080s for Ignace Study Area**

Percentiles	1-Day	2-Day	3-Day
Minimum	-24.6%	-17.5%	-18.4%
5%	-4.5%	-4.0%	-4.9%
25%	12.4%	13.3%	11.5%
<b>50%</b>	<b>25.4%</b>	<b>27.4%</b>	<b>25.7%</b>
75%	40.2%	44.4%	41.3%
95%	69.8%	73.6%	71.8%
Maximum	126.0%	111.7%	111.4%

Note that the method used to estimate changes in PMP (using the Hershfield and Moisture Maximization methods) is again different from the methods to estimate sub-daily IDF (interpolating changes at Atikokan and Sioux Lookout) and the method used for multi-day IDFs (fitting a curve to the daily projections for Ignace). However, the projected changes in the 50<sup>th</sup> percentile for 1-day PMP (18.7% in the 2050s and 25.4% in the 2080s; see **Error! Reference source not found.** and **Error! Reference source not found.**) represent the most conservative estimate, as the changes are larger than projected changes for the 50<sup>th</sup> percentile 1-day IDF curves (9.5% to 16.8% in the 2050s and 11.8% to 18.1% in the 2080s; see Table 28 and Table 29). The larger percent change for the 1-Day PMP event is expected, as the PMP event represents a significantly more extreme event than a return period storm.

Daily rainfall amounts are provided in the climate model ensemble; however, timeseries of sub-daily rainfall in the future projections are not available. Therefore, the same approach used for projecting future sub-daily IDF curves in Section 4.2.1 is also used here. Future sub-daily PMP values can be estimated by applying the percentage changes in the 1-day PMP (**Error! Reference source not found.**), to the sub-daily PMP values (Table 22) for a given percentile level. This assumes that the changes in sub-daily PMP are the same for the 1-day PMP. Further justification for this approach can be found in Section 4.2.1.

#### 4.4 Climate Change Impacts on Rainfall on Snow

The daily snowpack/snowmelt analysis used the daily precipitation and temperature projections at Ignace (using the same ECCC method as for the baseline climate). These results are used to assess large catchments where peak flooding events may be driven by a combination of rain and melt events (rather than by rain alone, as is assumed the case in IDF and PMP). Previous studies have found that the use of combined rainfall and snowmelt statistics instead of only precipitation can help prevent over or under design, and that the impact of this varies based on the location considered (Yan et al. 2018). The projected changes in the 50<sup>th</sup> percentile are shown in Table 32 and Table 33 below (future periods relative to the model baseline). For short durations (1 to 3 days), there is a general increase; this is likely the result of larger one-day rainfall events (shown on Table 28 and Table 29 above), which are expected to continue dominating short duration rain-on-snow events. For mid-range durations (6 to 30 days), there is a general downward trend, with larger decreases in the 2080s than in the 2050s, suggesting a general decrease in future snowmelt events which are expected to play a more significant role in the mid-duration rain on snow events. This is also in agreement with an expected decrease in peak snowpack seen in Table 34 (relative to the model baseline from the GCM ensemble over 1950-1993). The longest duration events (120 days) generally match the expected increases in long-duration rainfall (as shown on Table 28 and Table 29) with a range of 5.1% to 6.9% in the 2050s and 2.3% to 5% in the 2080s.

**Table 32: Summary of the 50<sup>th</sup> Percentile of Projected Percent Changes in Rain on Snow Events in the 2050s for Ignace Study Area**

Return Period (years)	1-Day	2-Day	3-Day	4-Day	5-Day	6-Day	7-Day	10-Day	20-Day	30-Day	50-Day	75-Day	90-Day	120-Day
2	12.4%	7.4%	3.0%	-0.5%	-2.3%	-3.1%	-4.2%	-6.0%	-6.5%	-5.2%	-2.5%	1.1%	3.3%	6.9%
5	15.0%	10.4%	4.9%	1.7%	-1.4%	-2.9%	-3.0%	-4.5%	-5.3%	-4.3%	-2.4%	0.6%	3.1%	6.2%
10	16.7%	12.2%	6.5%	3.7%	-0.1%	-2.5%	-2.2%	-4.0%	-5.1%	-3.5%	-2.1%	0.8%	3.0%	6.1%
20	18.2%	12.5%	7.7%	5.3%	1.1%	-2.0%	-1.7%	-3.8%	-4.9%	-2.9%	-1.8%	1.1%	3.3%	5.7%
50	19.6%	13.6%	8.9%	6.5%	1.7%	-1.4%	-1.1%	-3.6%	-4.5%	-2.9%	-1.3%	0.9%	3.2%	5.2%
100	20.1%	14.2%	9.5%	6.8%	1.7%	-0.9%	-0.7%	-3.5%	-4.3%	-3.0%	-1.0%	1.4%	3.5%	5.1%
200	20.6%	14.9%	10.1%	7.3%	1.6%	0.1%	-0.1%	-3.2%	-4.0%	-2.4%	-0.7%	1.5%	2.7%	5.1%
500	21.3%	15.5%	11.0%	7.5%	2.1%	0.3%	0.2%	-3.1%	-3.8%	-1.8%	-0.1%	1.8%	3.0%	5.4%
1,000	21.8%	15.8%	11.6%	7.6%	3.0%	0.5%	0.6%	-3.0%	-3.5%	-1.6%	0.0%	1.8%	3.4%	5.3%
2,000	22.2%	16.0%	11.6%	8.0%	3.5%	0.8%	0.5%	-2.7%	-3.2%	-1.3%	-0.1%	1.4%	3.2%	5.2%

**Table 33: Summary of the 50<sup>th</sup> Percentile of Projected Percent Changes in Rain on Snow Events in the 2080s for Ignace Study Area (%)**

Return Period (years)	1-Day	2-Day	3-Day	4-Day	5-Day	6-Day	7-Day	10-Day	20-Day	30-Day	50-Day	75-Day	90-Day	120-Day
2	9.2%	4.9%	-1.7%	-6.5%	-9.1%	-10.5%	-12.3%	-13.9%	-15.5%	-12.8%	-9.0%	-5.7%	-3.1%	2.3%
5	12.5%	7.2%	-0.5%	-4.6%	-5.8%	-8.8%	-10.5%	-12.2%	-13.5%	-10.5%	-6.7%	-3.6%	-1.6%	2.6%
10	13.9%	8.9%	1.1%	-3.5%	-6.2%	-8.0%	-8.7%	-11.9%	-13.6%	-9.8%	-6.5%	-3.1%	-0.9%	3.2%
20	14.6%	10.2%	2.0%	-3.2%	-5.9%	-7.7%	-9.1%	-11.9%	-13.7%	-9.4%	-5.7%	-2.7%	-0.9%	3.6%
50	15.7%	11.5%	2.8%	-3.0%	-5.5%	-8.2%	-9.8%	-11.2%	-13.3%	-8.7%	-4.9%	-2.3%	-0.4%	4.5%
100	16.3%	12.6%	2.8%	-2.8%	-5.7%	-8.8%	-9.7%	-11.1%	-12.8%	-8.2%	-4.8%	-2.0%	-0.1%	4.5%
200	16.9%	12.9%	3.4%	-2.4%	-6.0%	-9.0%	-9.5%	-11.0%	-12.5%	-7.5%	-4.7%	-1.0%	0.3%	5.0%
500	17.8%	13.4%	3.9%	-1.8%	-6.3%	-8.9%	-9.8%	-10.3%	-12.2%	-6.4%	-4.7%	-0.4%	0.8%	4.9%
1,000	18.7%	13.7%	4.2%	-1.4%	-6.2%	-8.3%	-9.7%	-10.4%	-12.2%	-6.2%	-4.5%	0.0%	1.4%	4.8%
2,000	19.2%	14.2%	4.4%	-1.2%	-6.2%	-7.7%	-9.5%	-10.7%	-12.1%	-6.0%	-4.4%	0.3%	1.7%	4.6%

**Table 34: Percent Change in Peak Snowpack Accumulation for the Ignace Study Area (50<sup>th</sup> Percentile)**

Return Period (years)	2	5	10	20	50	100	200	500	1,000	2,000
Baseline to 2050s	-8.3%	-7.5%	-6.5%	-5.5%	-4.3%	-3.0%	-2.1%	-1.9%	-1.4%	-1.1%
Baseline to 2080s	-13.8%	-10.5%	-8.8%	-7.2%	-6.0%	-5.5%	-4.4%	-3.8%	-3.4%	-2.7%

## 5. QUALITATIVE CLIMATE ASSESSMENT BEYOND THE YEAR 2100

The daily future climate projections used in this report are only available to the year 2100. Future climate assessments beyond 2100 can only be made qualitatively based on the best available information from literature and an understanding of climate change trends up to 2100. Extended concentration pathways (ECPs) provide qualitative estimates of future temperature on a global scale up to the year 2500. It is generally accepted that with increased temperature (through increased radiative forcing), mean global precipitation will also increase by an estimated 1-3% per degree Celsius increase in temperature (IPCC 2013). With this information, the ECP projections can be used to qualitatively inform precipitation trends in the far future for the site.

The ECP global projections indicate that beyond 2100, the radiative forcing driven by greenhouse gas emissions will gradually slow down and stabilize (Figure 7). The ECP 8.5 scenario results in increasing radiative forcing which slows down and stabilizes by the year 2250. The ECP 4.5 scenario results in stabilized (no change) radiative forcing, while the ECP 3-PD shows gradually decreasing radiative forcing levels. As a conservative measure, projections are provided based on the ECP 8.5 scenario.

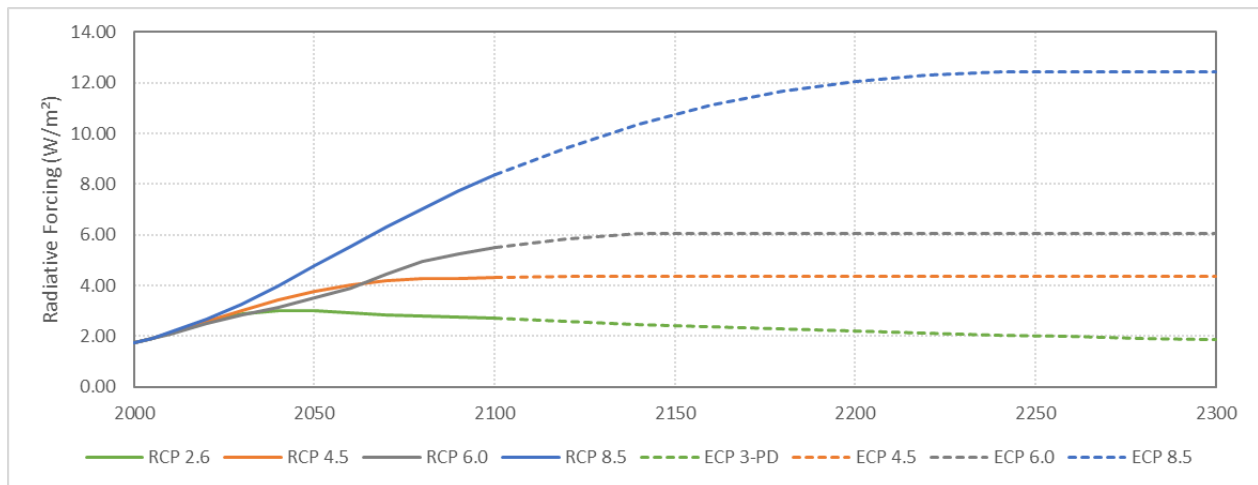


**Figure 7: Illustration of RCP and ECP Scenario Radiative Forcing from 2000 to 2300**

Two future climate periods (2050s and 2080s) have been used in this report, which allows for the trajectory of the projected changes to be estimated beyond these periods. Comparison of the differences between the percentage changes from the model baseline for the 2050s and 2080s time periods shows that on average across durations and return periods:

- Sub-daily IDF curves are projected to increase by 2.1%
- Daily and multi-day IDF curves are projected to increase by 2.4%
- PMP is projected to increase by 11.28%
- Rainfall on snow is projected to decrease by 5.6% (change of -5.6%)
- Peak snowpack accumulation is projected to decrease by 2.5% (change of -2.5%)

This indicates that the overall direction of change for extreme rainfall events is increasing and snowpack and combined rainfall and snowmelt are decreasing between the 2050s and 2080s time periods. Based on the ECP 8.5 scenario and the relationship between radiative forcing, temperature and precipitation, these changes may continue well into the future but may slow down and stabilize. There is a delay in the response of global temperatures to radiative forcing; therefore, changes in temperature and precipitation may continue past 2250 when the radiative forcing stabilizes. Due to the large range of radiative forcing in the ECP scenarios, there exists a large amount of uncertainty on how climate will change globally beyond the year 2100, and even more so at the scale of the study site. Updated climate assessments should be made throughout the project lifecycle to account for updated climate models and scenarios.

## 6. UNCERTAINTY OF CLIMATE CHANGE PROJECTIONS FOR PMP AND IDF

This assessment is based on the current available climate science. The nature of the work undertaken is stochastic with substantial inherent uncertainty around any given data points. The uncertainty associated with any projections or forecasts is increased with a longer time horizon into the future for the projected period. The projections are subject to change with future developments; therefore, this study should be updated, as new climate science is developed and after the release of the latest assessment report by the IPCC. The approach to reduce levels of uncertainty with the future climate projections for this study is based on using multiple projections from multiple models and scenarios (multi-model ensemble approach), as recommended by the IPCC (IPCC 2013), and discussed in Section 4.1. Overall, there is less variability and uncertainty (measured as the agreement within the ensemble or range of projected anomalies) during the 2050s, with variability/uncertainty increasing during the 2080s. In addition, precipitation projections typically have larger uncertainty than temperature projections due to the challenge of capturing precipitation in the climate models (temperature is well understood). Therefore, the level of uncertainty in this assessment, focused on PMP and IDF estimates, is generally higher than climate change studies focused on temperature.

The estimation of PMP (current and future projected) require moisture content and other variables, which were not readily available from the climate datasets. In order to calculate the moisture content for the model result datasets that do not provide these variables, Golder used the daily minimum temperature projections as a proxy for the dew point temperature and the surface specific humidity as a proxy for the precipitable water. Similar proxies were used to describe additional variables where they were not available from the climate datasets. The selection of proxy data to fill gaps in the climatic datasets added uncertainty around the estimation of PMPs.

## 7. USING THE RESULTS OF THIS ASSESSMENT IN DECISION MAKING

To better describe the uncertainty around future projections, the estimated percent changes to precipitation (PMP and IDF curves) are described in terms of percentiles, allowing for different levels of acceptable risk. The projections at 50<sup>th</sup> percentile represent the ensemble median.

When considering the impact of future projected climate on current design parameters, the level of acceptable risk can be selected by using the desired percentile. Selection of future projections for climate change risk assessment should be based on the balance between the extra investment and consequential risks.

Therefore, it is recommended that the results in this report be used as follows:

- For the ensemble mean projections, the projections at 50<sup>th</sup> percentile should be selected as the starting point, which NWMO should consider in regard to risk assessment and undertaking planning and engineering design applications of infrastructure in the future.
- To relate the Project phases to the climate assessment periods, the distribution of the projections should be considered by examining the percentiles from the multi-model ensemble. For screening purposes, the 50<sup>th</sup> percentile may be used from the mid-century climate period for the site characterization, preparation, and construction phase, and the end of century climate period for the operational project phase. For Project phases beyond 2100, a high percentile may be used from the end-of-century climate assessment period as a screening value. Other percentiles may be used to relate to the Project phases. For example, if conservatism is not required, then a lower percentile from the mid-century climate period could be used for the site characterization, preparation, and construction phase.
- For critical infrastructure, selection of future projections at higher percentile and higher return periods should be considered. For example, for critical infrastructure whose failure is considered unacceptable, a 95<sup>th</sup> percentile could be considered over the typical 50<sup>th</sup> percentile. With regards to the return period, the storm associated with a return period sufficiently larger than the planning horizon for the infrastructure should be used. In the case of the Project, the decommissioning phase is planned to conclude in 2180, which is approximately 160 years from the publication of this report. Therefore, a return period that is at least larger than 160 years should be used for future extreme rainfall projections. For critical infrastructure it may be more appropriate to select the 1000 or 2000-year return period.
- Where several results overlap specific parameter based on different methods (for instance, the change in 1-day rainfall for the sub-daily, multi-day, and rainfall on snow results), this report recommends that the most conservative method (i.e., the one that generates the largest future rainfall depth) be used.
- If a risk is identified for an infrastructure component for the area, then a more refined analysis should be performed to further define the risks using the projections at different percentile levels.

## 8. CONCLUSIONS AND RECOMMENDATIONS

The baseline assessment of the Ignace study area was completed using publicly available data in the region from ECCC. The 24-hours 100-year return period precipitation was estimated at 125.5 mm and the 500-year return period at 167.9 mm from the interpolated IDF curve at the Ignace study area (Table 13). The PMP calculation yielded a 1-day value of 364.3 mm, 411.7 mm for 24-hours, 482.2 mm for 2-day, and 510.1 mm for 3-day with the Hershfield method (Table 17). With the DAD curves in the Transposition method for 1,000 km<sup>2</sup> watershed area, the estimates were slightly higher being 374.0 mm for 1-day and 422.6 mm for 24-hours, and slightly lower being 473.6 mm for 2-day, and 477.8 mm for 3-day (Table 20). The values of IDF and PMP estimates were compared with literature sources and found in agreement with previous studies.

The results are presented for the range of models within the “ensemble” and expressed in terms of percentiles. When considering the impact of future projected climate on current design parameters, the level of acceptable risk can be selected by using the desired percentile.

The trends in future climate extremes follow a pathway that is consistent with the trends in climate normals for both the current and future climate projections. From the median (50<sup>th</sup> percentile) values for the 2050s and 2080s, the projected future climate extremes are indicating a future that is likely to be wetter. The 1-day PMP values are projected to increase between approximately 18.7% and 25.4% in the 2050s and in the 2080s, respectively, at the 50<sup>th</sup> percentile (**Error! Reference source not found.** and **Error! Reference source not found.**), relative to the model baseline from the GCM ensemble. The 1-day rainfall events are projected to increase by 9.5% to 16.8% in the 2050s (Table 28) and 11.8% to 18.1% in the 2080s (Table 29) at the 50<sup>th</sup> percentile, relative to the model baseline from the GCM ensemble.

Qualitative assessment of climate change beyond the year 2100 was made using the projections for the 2050s and 2080s time periods and the global ECP scenarios. Overall, extreme precipitation statistics (IDF and PMP) are likely to increase beyond the year 2100 based on the comparison of projections between the 2050s and 2080s time periods. These changes may continue well into the future, as the ECP 8.5 scenario shows increased radiative forcing until the year 2250. It is recommended additional climate assessments be made throughout the project life cycle, so that updated climate projections and scenarios are used to reduce uncertainty associated with projections made far into the future.

The nature of the study has substantial level of inherent uncertainty. The approach to address levels of uncertainty around future climate projections in this study relies on the multi-model ensemble approach recommended by IPCC. Furthermore, the uncertainty associated with any projections is increased with the far future of the projected period, resulting into less variability and uncertainty during the 2050s, when compared to the 2080s. To acknowledge the uncertainty around future projections, the estimate percent changes to precipitation (PMP and IDF curves) is described in terms of percentiles, allowing for different levels of acceptable risk. When considering the impact of future projected climate on current design parameters, the level of acceptable risk can be selected by using the desired percentile. Selection of future projections for climate change risk assessment should be based on the balance between the extra investment and consequential risks.

Based on Golder's experience in climate change projections, the proposed approaches as described in this study are considered best guidance for the industry. The observations available at the Ignace study area are limited to 1993; therefore, it is recommended that the meteorological station located in the study area (Ignace Station - 6033690) be reactivated or a new meteorological station be installed for continuous monitoring, should this study area be selected for the DGR location.

## REFERENCES

- AMEC. 2011. Maximum Flood Hazard Assessment. Nuclear Waste Management Organization Report DGR-TR-2011-35. Toronto, Canada. Available at [https://archive.opg.com/pdf\\_archive/Deep%20Geologic%20Repository%20Documents/DGR%20Submission%20Documents/D175\\_26.Maximum-Flood-Hazard-Assessment.pdf](https://archive.opg.com/pdf_archive/Deep%20Geologic%20Repository%20Documents/DGR%20Submission%20Documents/D175_26.Maximum-Flood-Hazard-Assessment.pdf).
- Bush, E. and Lemmen, D.S., editors. 2019. Canada's Changing Climate Report. Government of Canada, Ottawa, ON. 444p. Available at [https://www.nrcan.gc.ca/sites/www.nrcan.gc.ca/files/energy/Climate-change/pdf/CCCR\\_FULLREPORT-EN-FINAL.pdf](https://www.nrcan.gc.ca/sites/www.nrcan.gc.ca/files/energy/Climate-change/pdf/CCCR_FULLREPORT-EN-FINAL.pdf).
- Canadian Standards Association (CSA). 2012. Draft Standard Plus 4013-12 Technical Guide Development, interpretation and use of rainfall intensity-duration-frequency (IDF) information: Guideline for Canadian water resources practitioners.
- Clavet-Gaumont, J., Huard, D., Frigon, A., Koenig, K., Slota, P., Rousseau, A., Klein, I., Thiémonge, N., Houdré, F., Perdikaris, J., Turcotte, R., Lafleur, J. and B. Larouche. 2017. Probable maximum flood in a changing climate: An overview for Canadian basins. *Journal of Hydrology: Regional Studies*, 13, 11-25. doi:10.1016/j.ejrh.2017.07.003.
- Climatedata. 2019. Statistically Downscaled Climate Scenarios - BCCAQv2. Available at <https://climatedata.ca/>.
- Climatedata. 2019. Statistically Downscaled Climate Scenarios - BCCAQv2. Available at <https://climatedata.ca/>.
- Environment and Climate Change Canada (ECCC). 2019. Historical Climate Data. Available at [https://climate.weather.gc.ca/historical\\_data/search\\_historic\\_data\\_e.html](https://climate.weather.gc.ca/historical_data/search_historic_data_e.html). Accessed June 15, 2019.
- Hosking, J.R.M. and J.R. Wallis. 1997. *Regional Frequency Analysis*. Cambridge University Press, Cambridge, U.K.
- Intergovernmental Panel on Climate Change (IPCC). 2013. *Climate Change 2013: The Physical Science Basis*. Contribution of Working Group I to the Fifth Assessment Report of the Intergovernmental Panel on Climate Change. Retrieved on March 15, 2017 from <https://www.ipcc.ch/report/ar5/wg1/>.
- Kunkel, K.E. 2013. Probable Maximum Precipitation and Climate Change. *Geophysical Research Letters*, Vol.40, Issue 7. March 2013.
- Louie, P. Y. T. and W. D. Hogg. 1980. Extreme Value Estimates of Snowmelt. *Proceedings of Canadian Hydrology Symposium 80* (Toronto, ON: 64-78 National Research Council Canada).
- Ministry of Natural Resources and Forestry (MNRF). 2020. Ontario Flow Assessment Tool. Available at <https://www.gisapplication.lrc.gov.on.ca/OFAT/Index.html?site=OFAT&viewer=OFAT&locale=en-US>. Accessed March 2, 2020.
- Murphy, B., P. Campbell, J. Cummine, R.P. Ford, B. Johnson, A. Thompson, P. Pilon, and D. Brown. 2003. The 49<sup>th</sup> Parallel Severe Rainstorm, Flooding and High Water Events of June 2002. Meteorological Service of Canada, Environment Canada, Burlington, Ontario. 46 pp.
- Ontario Ministry of Natural Resources (OMNR). 2006. PMP for Ontario. Prepared by IBI Group. December 2006.

- Pierce, D. W., D. R. Cayan, and B. L. Thrasher, Statistical Downscaling Using Localized Constructed Analogs (LOCA), *Journal of Hydrometeorology*, 15(6), 2558-2585, 2014.; and Pierce, D. W., D. R. Cayan, E. P. Maurer, J. T. Abatzoglou, and K. C. Hegewisch, 2015: Improved bias correction techniques for hydrological simulations of climate change. *J. Hydrometeorology*, v. 16, 2421-2442. DOI: <http://dx.doi.org/10.1175/JHM-D-14-0236.1>.
- Pysklywec, D.W., K.S. Davar and D.I. Bray. 1968. Snowmelt at an Index Plot. *Water Resource*. 4(5), 937-946.
- Reclamation. 2013. Downscaled CMIP3 and CMIP5 Climate Projections: Release of Downscaled CMIP5 Climate Projections, Comparison with Preceding Information, and Summary of User Needs. U.S. Department of the Interior, Bureau of Reclamation, Technical Service Center, Denver, Colorado, 116 p. Available at: [http://gdo-dcp.ucllnl.org/downscaled\\_cmip\\_projections/techmemo/downscaled\\_climate.pdf](http://gdo-dcp.ucllnl.org/downscaled_cmip_projections/techmemo/downscaled_climate.pdf).
- Yan, H., Sun, N., Wigmosta, M., Skaggs, R., Hou, Z., and Leung, R. 2018. Next-generation Intensity-Duration-Frequency Curves for Hydrologic Design in Snow-Dominated Environments. *Water Resources Research*, 54, 1093-1108. doi: 10.1002/2017WR021290.
- Wood. 2019. Climate Change Impacts Review and Method Development. NWMO-TR-2019-05. Toronto, Canada. Retrieved from <http://rms.nwmo.ca/Sites/APM/Reports/NWMO-TR-2019-05.pdf>.
- World Meteorological Organization (WMO). 2009. Manual on Estimation of Probable Maximum Precipitation (PMP). World Meteorological Organization (WMO). WMO-No. 1045.

## APPENDIX A: DETAILED METHODOLOGY

### CONTENTS

	Page
<b>APPENDIX A: DETAILED METHODOLOGY .....</b>	<b>45</b>
<b>A.1 INTRODUCTION .....</b>	<b>47</b>
<b>A.2 CURRENT CLIMATE OBSERVED BASELINE DEVELOPMENT .....</b>	<b>47</b>
<b>A.2.1 Data Sources for Current Climate and Reanalysis .....</b>	<b>49</b>
<b>A.2.2 Calculation of Observed Baseline IDF Curves and Rainfall Statistics .....</b>	<b>49</b>
A.2.2.1 Sub-daily and daily precipitation .....	50
A.2.2.2 Multi-day precipitation .....	50
A.2.2.3 Statistical distributions .....	50
A.2.2.4 Parameter estimation methods .....	52
A.2.2.5 Goodness-of-Fit tests .....	54
<b>A.2.3 Calculation of Baseline Probable Maximum Precipitation (PMP) .....</b>	<b>55</b>
A.2.3.1 Construction of the DAD curves in the Hershfield method .....	57
A.2.3.2 Storm maximization and Transposition method .....	57
A.2.3.3 Converting daily PMPs to sub-daily .....	59
<b>A.2.4 Rain on Snow Procedure .....</b>	<b>59</b>
<b>A.3 FUTURE CLIMATE PROJECTIONS DEVELOPMENT .....</b>	<b>59</b>
<b>A.3.1 Data Sources for Future Climate .....</b>	<b>60</b>
<b>A.3.2 Global Climate Change Projections .....</b>	<b>60</b>
A.3.2.1 Regional climate change projections .....	61
A.3.2.2 Uncertainty of climate change downscaling methods .....	64
<b>A.3.3 Projecting Future Rainfall Statistics (IDF Curves) .....</b>	<b>65</b>
A.3.3.1 Quantile Delta Mapping (QDM) .....	66
A.3.3.2 Ratio Method (RM) .....	67
<b>A.3.4 Projecting Future Changes in PMPs .....</b>	<b>68</b>
<b>A.3.5 Projecting Future Changes in Rain on Snow and Snowpack .....</b>	<b>69</b>
<b>APPENDIX B: FUTURE RAINFALL STATISTICS .....</b>	<b>70</b>
<b>REFERENCES .....</b>	<b>71</b>

## LIST OF TABLES

	<b>Page</b>
Table A.1: Characterization of Representative Concentration Pathways .....	61
Table A.2: Global Climate Models used in BCCAQv2 and LOCA Downscaling Methods .....	62

## LIST OF FIGURES

	<b>Page</b>
Figure A.1: PMP and IDF Baseline Analyses Flowchart .....	47
Figure A.2: Baseline and Future PMP Analyses Flowchart .....	56
Figure A.3: Precipitable Water and Dew Point relationship (Adapted from: OMNR 2006). ....	58
Figure A.4: QDM Method Flowchart (Adopted from Schardong and Simonovic 2019).....	67
Figure A.5: Ratio Method Flowchart .....	68

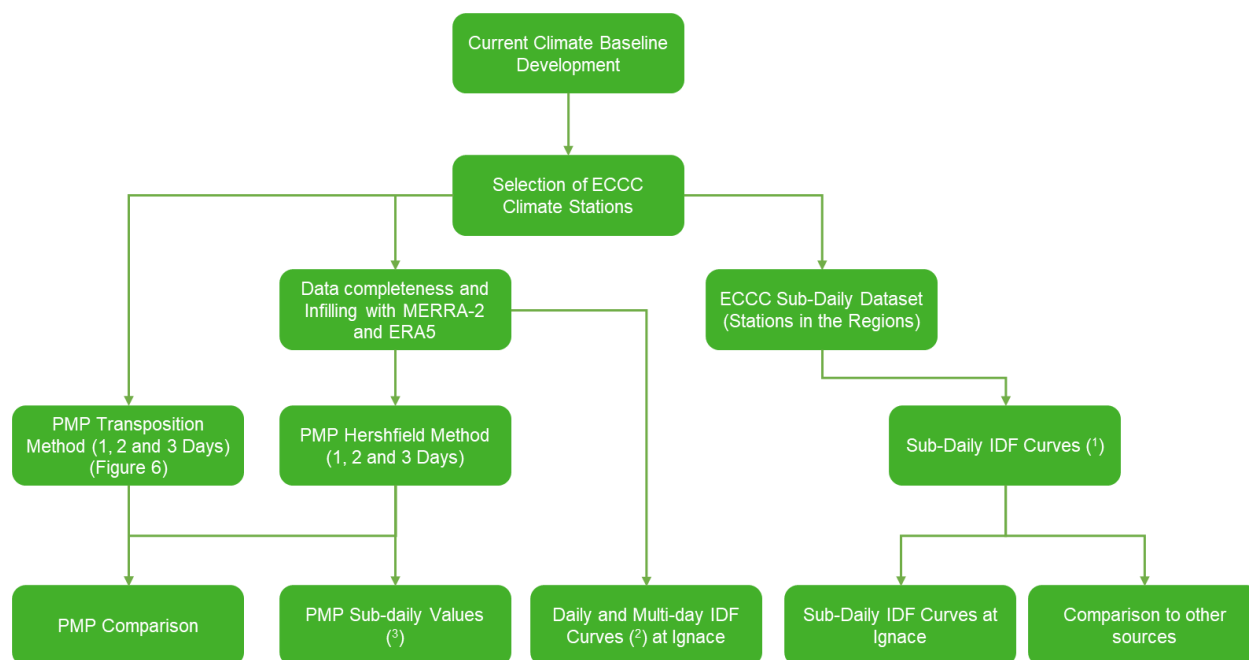
## A.1 INTRODUCTION

This appendix outlines in detail the PMP and IDF analyses approach and methodology applied to the Ignace study area and follows *Climate Change Impacts Review and Method Development* (NWMO-TR-2019-05 from Wood 2019) for PMP analyses. This stepwise approach combines information about the current climate conditions and publicly available projections of how the climate may change under future climate conditions to describe a range of future projections at the site of interest, and represents the most recent best guidance found in literature.

Section A.2 provides the detailed methodology followed to develop a current climate observed baseline for PMPs and IDFs in Section 3, and Section A.3 outlines the method based on GCM ensemble to develop future climate % change projections for PMPs and IDFs in Section 4.

## A.2 CURRENT CLIMATE OBSERVED BASELINE DEVELOPMENT

Understanding the current climate and current climate trends is important when evaluating current design parameters and developing the percentile levels using the future climate projections. The process to develop the observed baselines for PMPs and IDFs is outlined in Figure A.1 **Error! Reference source not found.** Where available, the climate baseline is grounded in observations from local climate stations. Publicly available observations are used to establish the baseline infilled with reanalysis data (to meet data completeness requirements including only considering months and years where at least 90% of the data is available).



Notes:

- 1) IDF curves were developed for the following durations: 5, 10, 15, 30 minutes, 1, 2, 6 and 12 hours, and 2, 5, 20, 50, 100, 200, 500, 1000 and 2000 years return period.
- 2) IDF curves were developed for the following durations: 1, 2, 3, 4, 5, 6, 7, 10, 20, 30, 50, 75, 90, 120 days, and 2, 5, 20, 50, 100, 200, 500, 1000 and 2000 years return period.
- 3) Sub-daily PMP values were calculated for the following durations: 5, 10, 15, 30 minutes, 1, 2, 6, 12 and 24 hours.

**Figure A.1: PMP and IDF Baseline Analyses Flowchart**

Before infilling, the reanalysis data is compared and correlated to the available regional climate station. This step is carried out to create a current climate baseline time series and is used to evaluate PMP and IDF values for the region of interest. Additional data stations from the region are screened for the study of the extreme events as well as series from the Engineering Dataset for the IDF curves (ECCC 2019). If available, the Adjusted and Homogenized Canadian Climate Data (AHCCD) are used to apply adjustments to the station observations (infilled if necessary) to account for non-climatic shifts in data, mainly due to the relocation of stations and wind undercatch correction (ECCC 2019). Wind undercatch describes the effects of wind on rain gauges that can cause underestimation of rainfall which contributes to inconsistencies in the rainfall dataset (Guo et al. 2001).

The climate station selection is based on the following selection factors to identify the station which best represents the Ignace study area, meteorologically:

- the length of record (minimum 30 years of data);
- availability of a continuous record;
- proximity to the area of interest;
- age of observations compared to the currently accepted normal period;
- latitude;
- elevation of station;
- geographic siting; and
- monthly data availability threshold of 90% for all years.

The available climate data from each station must be compared to, and pass, the selection criteria outlined above. Data from most climate stations are constrained by low numbers of observations or a limited life span for the station (data quantity), and varying data quality. Therefore, the station which matches the most selection criteria, with the first three criteria bearing the most weight, is selected. Meeting the monthly data availability is often a challenge over the desired, long observation period. When available climate observations are representative of a site but fail to meet the required data completeness, reanalysis data from the National Aeronautics and Space Administration's (NASA's) Modern-Era Retrospective analysis for Research and Applications, Version 2 (MERRA-2) is used to represent current climate or to infill the missing data.

After the station observations have been reviewed for data completeness, infilling, and any available adjustments, the PMP and IDF are calculated. The current climate observed baseline is discussed in Section 3.

### **A.2.1 Data Sources for Current Climate and Reanalysis**

The current climate is based on available long term daily meteorological observations from climate stations near the Ignace study area. For the Ignace study area, the selected current climate baseline period is from 1889 through 1993. Meeting the monthly data availability is often a challenge over the desired, long observation period. The data availability is necessary to properly capture the different cycles impacting the observations (e.g., diurnal, seasonal) and avoid potential biases in the analysis of the observations (e.g., consistently missing observations during the nighttime or winter). When available climate observations are representative of a site but fail to meet the required data completeness, reanalysis data from the National Aeronautics and Space Administration's (NASA's) Modern-Era Retrospective analysis for Research and Applications, Version 2 (MERRA-2) are used to represent current climate or to infill the missing data. MERRA-2 is a NASA's atmospheric reanalysis using the Goddard Earth Observing System Model, along with its atmospheric data assimilation system that simulates temperature and precipitation on an hourly basis (NASA 2019). Additionally, data from the European Centre for Medium-Range Weather Forecasts (ECMWF) Re-Analysis (ERA5) are used to represent current climate or to infill the missing data from observations. The R-squared ( $R^2$ ) statistics is used to select between MERRA-2 and ERA5 and complete missing historical observed dataset.

Infilling the missing data is a two-step process: the first step is to perform a correlation analysis for the concurrent period between the non-missing observations and MERRA-2 data, and the second step is to scale the reanalysis data using a linear relationship based on the correlation. Environment and Climate Change Canada (ECCC) has provided the AHCCD dataset that has adjusted measurements to account for non-climatic measurement issues (i.e., wind undercatch) and has combined observations from nearby stations to create longer time series that are useful for trend studies (Mekis and Vincent 2011). The AHCCD dataset includes daily observations for minimum, maximum and mean temperatures and total precipitation. The AHCCD dataset does not always include the most recent observations and as a result, a trending analysis is used to adjust the AHCCD dataset to match the infilled observations to account for any missing observations/years. This adjustment uses monthly factors based on the difference between the two datasets for the concurrent period. A sensitivity analysis is then conducted comparing the datasets to verify that the adjustments are consistent with the infilled dataset.

### **A.2.2 Calculation of Observed Baseline IDF Curves and Rainfall Statistics**

This subsection describes the methodology to calculate the IDF curves for the baseline, divided into different durations (i.e., 1-day, 2-day, and 3-day for the meteorological stations and sub-daily for the stations where sub-daily data is available). The methodology requires fitting curves for several statistical distributions whose parameters are estimated using standard statistical methods. The preferred statistical distribution is then selected based on the results of the goodness-of-fit tests. This section supports the results and summary presented in Section 3.2.

To estimate the IDF values under historical climate conditions, the statistical distribution based on 'goodness-of-fit' criteria are used. For this step, three different distributions are assessed, namely: Gumbel, GEV (Generalized Extreme Value) and Log-Pearson type 3, and based on three goodness-of-fit criteria: Anderson-Darling, Kolmogorov-Smirnov and Chi-Squared tests described on the following sub-sections.

### A.2.2.1 Sub-daily and daily precipitation

Sub-daily IDF curves apply only to stations with sub-daily observation records. The sub-daily rainfall data was obtained from the ECCC database.

Consistent with all future projections, the GCM ensemble approach are used. The 1-day rainfall amounts for return periods of 2, 5, 20, 10, 50, 100, 200, 500, 1,000, and 2,000 years in the future periods at different percentile levels are presented.

### A.2.2.2 Multi-day precipitation

Consistent with all future projections, the GCM ensemble approach is used. The 1-day, 2-day, 3-day, 4-day, 5-day, 10-day, 20-day, 30-day, 50-day, 75-day, 90-day and 120-day consecutive rainfall amounts for return periods of 2, 5, 20, 10, 50, 100, 200, 500, 1,000 and 2,000 years in the future periods at different percentile levels are presented.

### A.2.2.3 Statistical distributions

This subsection describes in detail the three candidate statistical distributions used to produce the IDF curve results. The distributions are: Gumbel, Generalized Extreme Value (GEV) and Pearson or Log Pearson Type 3.

#### A.2.2.3.1 Gumbel Distribution (EV1)

The EV1 distribution has been widely recommended and adopted as the standard distribution by Environment and Climate Change Canada for all the Precipitation Frequency Analyses in Canada. The EV1 distribution for annual extremes can be expressed as:

$$Q(T) = \mu + k_T \cdot \sigma \quad \text{Equation 1}$$

$$k_T = -\frac{\sqrt{6}}{\pi} \left[ 0.5772 + \ln \left( \ln \left( \frac{T}{T-1} \right) \right) \right] \quad \text{Equation 2}$$

where  $Q(T)$  is the exceedance value,  $\mu$  and  $\sigma$  are the population mean and standard deviation of the annual extremes;  $T$  is return period in years.

#### A.2.2.3.2 Generalized Extreme Value (GEV) Distribution

The GEV distribution is a family of continuous probability distributions that combines the three asymptotic extreme value distributions into a single one: Gumbel (EV1), Fréchet (EV2) and Weibull (EV3) types. GEV uses three parameters: location, scale and shape. The location parameter describes the shift of a distribution in each direction on the horizontal axis. The scale parameter describes how spread out the distribution is and defines where the bulk of the distribution lies. As the scale parameter increases, the distribution becomes more spread out. The shape parameter affects the shape of the distribution and governs the tail of each distribution. The shape parameter is derived from skewness, as it represents where most of the data lies, which creates the tail(s) of the distribution. The value of shape parameter  $k = 0$ , indicates the EV1 distribution. Value of  $k > 0$ , indicates EV2 (Fréchet), and  $k < 0$  the EV3 (Weibull). The Fréchet type has a longer upper tail than the Gumbel distribution and the Weibull type has a shorter tail (Overeem et al. 2007 and Millington et al. 2011).

The GEV cumulative distribution function  $F(x)$  is given by Equation 3 for  $k \neq 0$  (EV1).

$$F(x) = \exp \left\{ - \left[ 1 - \frac{k}{\alpha}(x - \mu) \right]^{1/k} \right\} \quad \text{for } k \neq 0 \quad \text{Equation 3}$$

$$F(x) = \exp \left\{ -\exp \left[ -\frac{1}{\alpha}(x - \mu) \right] \right\} \quad \text{for } k = 0 \quad \text{Equation 4}$$

where  $\mu$  is the location,  $\alpha$  is the scale and  $k$  is the shape parameter of the distribution, and  $y$  is the GEV reduced variate,  $y = -\ln(-\ln F)$ .

The inverse distribution function or quantile function is given by Equation 5 for  $k \neq 0$  and Equation 6 for  $k = 0$ .

$$Q(x) = \mu + \alpha \{ 1 - (-\ln F)^k \} / k \quad \text{for } k \neq 0 \quad \text{Equation 5}$$

$$Q(x) = \mu - \alpha \left\{ -\exp \left[ -\frac{1}{\alpha}(F - \mu) \right] \right\} \quad \text{for } k = 0 \quad \text{Equation 6}$$

#### A.2.2.3.3 Pearson and Log Pearson Type 3

The Pearson Type 3 (PE3) distribution is a member of the family of Pearson Type 3 distributions and is also referred to as the Gamma distribution. The PE3 is required for all Precipitation Frequency Analysis in the United States. Like GEV, the PE3 has three parameters, location ( $\mu$ ), scale ( $\sigma$ ) and shape ( $\gamma$ ). A problem arises with PE3 as it tends to give low upper bounds of the precipitation magnitudes, which is undesirable (Cunnane 1989). The CDF (Cumulative Density Function –  $F$ ) and PDF (Probability Density Function –  $f$ ) are defined in (Hosking and Wallis 1997) as:

$$\text{If } \gamma \neq 0, \text{ let } \alpha = 4/\gamma^2 \text{ and } \xi = \mu - 2\sigma/\gamma \quad \text{Equation 7}$$

If  $\gamma > 0$  then:

$$F(x) = G \left( \alpha, \frac{x - \xi}{\beta} \right) / \Gamma(\alpha) \quad \text{Equation 8}$$

$$f(x) = \frac{(x - \xi)^{\alpha-1} e^{-(x-\xi)/\beta}}{\beta \cdot \Gamma(\alpha)} \quad \text{Equation 9}$$

If  $\gamma < 0$  then:

$$F(x) = 1 - G \left( \alpha, \frac{\xi - x}{\beta} \right) / \Gamma(\alpha) \quad \text{Equation 10}$$

$$f(x) = \frac{(\xi - x)^{\alpha-1} e^{-(\xi-x)/\beta}}{\beta \cdot \Gamma(\alpha)} \quad \text{Equation 11}$$

If  $\gamma = 0$  then Pearson type 3 follows the Normal distribution:

$$F(x) = \Phi \left( \frac{x - \mu}{\sigma} \right) \quad \text{Equation 12}$$

$$f(x) = \phi \left( \frac{x - \mu}{\sigma} \right) \quad \text{Equation 13}$$

Where  $G$  is the incomplete Gamma function and  $\Phi$  the CDF and  $\phi$  PDF of the Normal distribution.

#### A.2.2.4 Parameter estimation methods

A common statistical procedure for estimating distribution parameters is the use of a maximum likelihood estimator or the method of moments. ECCC uses and recommends the use of the method of moments technique to estimate the parameters for EV1. Golder uses the method of moments to calculate the parameters of the Gumbel distribution. Golder uses L-moments to calculate parameters of the GEV distribution. The following sections describe the method of moments procedure for calculating the parameters of the Gumbel distribution and L-moments method for calculating parameters of the GEV distribution.

##### A.2.2.4.1 Method of Moments

The most popular method for estimating the parameters of the Gumbel distribution is method of moments (Hogg et al. 1989). In the case of the Gumbel distribution, the number of unknown parameters is equal to the mean and standard deviation of the sample mean. The first two moments of the sample data are sufficient to derive the parameters of the Gumbel distribution in Equation 14 and Equation 15. These are defined as:

$$\mu = \frac{1}{N} \sum_{i=1}^N Q_i \quad \text{Equation 14}$$

$$\sigma = \sqrt{\frac{1}{N-1} \sum_{i=1}^N (Q_i - \bar{Q})^2} \quad \text{Equation 15}$$

Where  $\mu$  is the mean,  $\sigma$  the value of standard deviation of the historical data,  $Q_i$  the maximum precipitation data for year  $i$ , and  $\bar{Q}$  the mean of the precipitation data.

##### A.2.2.4.2 L-moments Method

The L-moments (Hosking and Wallis 1997) and maximum likelihood methods are commonly used to estimate the parameters of the GEV distribution and fit to annual maxima series. The L-moments are a modification of the probability-weighted moments (PWMs), as they use the PWMs to calculate parameters that are easier to interpret. The PWMs can be used in the calculation of parameters for statistical distributions (Millington et al. 2011). They provide an advantage, as they are easy to work with, and more reliable as they are less sensitive to outliers. L-moments are based on linear combinations of the order statistics of the annual maximum rainfall amounts (Hosking and Wallis 1997 and Overeem et al. 2007). The PWMs are estimated by:

$$b_0 = n^{-1} \sum_{j=1}^n x_j \quad \text{Equation 16}$$

$$b_1 = n^{-1} \sum_{j=2}^n \frac{j-1}{n-1} x_j \quad \text{Equation 17}$$

$$b_2 = n^{-1} \sum_{j=3}^n \frac{(j-1)(j-2)}{(n-1)(n-2)} x_j \quad \text{Equation 18}$$

Where  $x_j$  is the ordered sample of annual maximum series (AMS) and  $b_i$  are the first PWMs. The sample L-moments can then be obtained as:

$$\ell_1 = b_0 \quad \text{Equation 19}$$

$$\ell_2 = 2b_1 - b_0 \quad \text{Equation 20}$$

$$\ell_3 = 6b_2 - 6b_1 + b_0 \quad \text{Equation 21}$$

#### A.2.2.4.3 L-Moments for the GEV parameters

The GEV parameters: location ( $\mu$ ), scale ( $\alpha$ ) and shape ( $k$ ) are defined (Hosking and Wallis 1997) as:

$$k = 7.8590c + 2.9554c^2 \quad \text{Equation 22}$$

where:

$$c = \frac{2}{3 + \ell_3/\ell_2} - \frac{\ln(2)}{\ln(3)} \quad \text{Equation 23}$$

$$\alpha = \frac{\ell_2 k}{(1 - 2^{-k}) \cdot \Gamma(1 + k)} \quad \text{Equation 24}$$

$$\mu = \ell_1 - \alpha \frac{1 - \Gamma(1 + k)}{k}$$

Where  $\Gamma$  is the gamma function,  $\ell_1$ ,  $\ell_2$  and  $\ell_3$  the L-moments, and  $\mu$  the location,  $\alpha$  the scale and  $k$  the shape parameters of the GEV distribution.

#### A.2.2.4.4 L-Moments for the Pearson Type 3 (PE3) and Log Pearson Type 3 (LP3)

The parameters location ( $\mu$ ), scale ( $\sigma$ ) and shape ( $\gamma$ ) are defined in (Hosking and Wallis 1997) for the Pearson Type 3 distribution are as follows:

$$\gamma = 2\alpha^{-0.5} + \text{sign}(\tau_3) \quad \text{Equation 25}$$

$$\sigma = \frac{\lambda_2 \pi^{0.5} \alpha^{0.5} \Gamma(\alpha)}{\Gamma(\alpha + 0.5)} \quad \text{Equation 26}$$

$$\mu = \lambda_1 \quad \text{Equation 27}$$

To estimate the value of  $\alpha$ :

$$\text{If } 0 < |\tau_3| < \frac{1}{3}, \text{ let } z = \frac{3\pi\tau_3^2}{1 + 0.2960 \cdot z} \text{ and use:} \quad \text{Equation 28}$$

$$\alpha = \frac{z + 0.1880 \cdot z^2 + 0.0442 \cdot z^3}{z + 0.1880 \cdot z^2 + 0.0442 \cdot z^3}$$

$$\text{If } \frac{1}{3} < |\tau_3| < 1, \text{ let } z = 1 - |\tau_3| \text{ and use:}$$

$$\alpha = \frac{0.3636 \cdot z - 0.59567 \cdot z^2 + 0.25361 \cdot z^3}{1 - 2.78861 \cdot z + 2.56096 \cdot z^2 - 0.77045 \cdot z^3} \quad \text{Equation 29}$$

### A.2.2.5 Goodness-of-Fit tests

Goodness of fit tests can be reliably used in climate statistics to assist in selecting the best distribution to fit the given data. These tests are usually applied to reject candidate statistical distributions and provide a sense of how well a given distribution fits the data being tested. These tests describe the differences between the observed data points and the calculated values from the distribution. The performances the three statistical distribution considered are tested by using the following goodness-of-fit tests: Kolmogorov-Smirnov test, Anderson-Darling estimate and Chi-Squared test, described next.

#### A.2.2.5.1 Kolmogorov-Smirnov Test

The Kolmogorov-Smirnov (KS) test it is used to decide whether the sample being tested originates from a specific continuous statistical distribution. The KS statistic ( $D$ ) is based on the largest vertical difference between the theoretical and the empirical CDFs (Cumulative Distribution Function) and is calculate as:

$$D = \max_{1 \leq i \leq n} \left( F(x_i) - \frac{i-1}{n}, \frac{i}{n} - F(x_i) \right) \quad \text{Equation 30}$$

Where, the samples  $x_i$  are assumed to be random, originating from some distribution with CDF of  $F(x_i)$ ,  $n$  the sample size, and  $i$  the  $i$ th sample, calculated when the data is sorted in ascending order. The hypothesis for this distribution (test) is rejected if the test statistic is greater than the critical value at a chosen significance level. For the significance level of  $\alpha=5\%$ , the critical value is selected is based on the sample size and tables are available. The value of the statistics  $D$  is used to rank the distributions.

#### A.2.2.5.2 Anderson-Darling Test

The Anderson-Darling (AD) test compares an observed CDF to an expected CDF. This method gives more weight to the tail of the distribution than KS test, which in turn leads to the AD test being stronger and having more weight than the KS test. The test rejects the hypothesis regarding the distribution level if the statistic obtained is greater than a critical value at a given significance level ( $\alpha$ ). The significance level most commonly used is  $\alpha = 5\%$ , producing a critical value of 2.5018. This number is then compared with the test distributions statistic to determine if it can be rejected or not. The AD test statistic is calculated as:

$$AD = -n - \frac{1}{n} \sum_{i=1}^n (2i-1) [\ln(F(X_i)) + \ln(1 - F(X_{n+1-i}))] \quad \text{Equation 31}$$

Where  $n$  the sample size, and  $i$  the  $i^{th}$  sample, calculated when the data is sorted in ascending order,  $F(x_i)$  the CDF of the distribution being tested, and The samples  $x_i$  are assumed to be random, originating from some distribution with CDF of  $F(x_i)$ . The value of the AD test is used to rank the distributions.

#### A.2.2.5.3 Chi-Square Test

The Chi-Squared test is used to determine if a sample comes from a given distribution. The test is based on binned data, and the number of bins ( $k$ ) is determined by:

$$k = 1 + \log N \text{ with } N \text{ the sample size} \quad \text{Equation 32}$$

The test statistic ( $\chi^2$ ) is calculated as:

$$\chi^2 = \sum_{i=1}^k \frac{(O_i - E_i)^2}{E_i}$$

**Equation 33**

Where  $O_i$  is the observed frequency,  $E_i = F(x_2) - F(x_1)$  with  $x_1$  and  $x_2$  as the limits of the  $i^{th}$  bin.

The statistics  $\chi^2$  is used to assist in ranking the distributions and the significance level,  $\alpha = 0.05$  produced a critical value of 12.592. For values above this threshold the distribution being tested is rejected.

### **A.2.3 Calculation of Baseline Probable Maximum Precipitation (PMP)**

This section describes the method of the calculation of the baseline values of the PMP using the Transposition method following the recommendation by Wood (2019), and corresponds to steps 1 through 5 from Figure A.2. The Transposition method is based on observed historical events and requires careful analysis and identification of major storms from the available records. The stations in the study area are screened for the largest storms in the observational record and are used to construct the DAD curves, which are then maximized by applying maximization and the transposition factors (described in Section A.2.3.2) to the area of study. These steps are described in the following subsections.

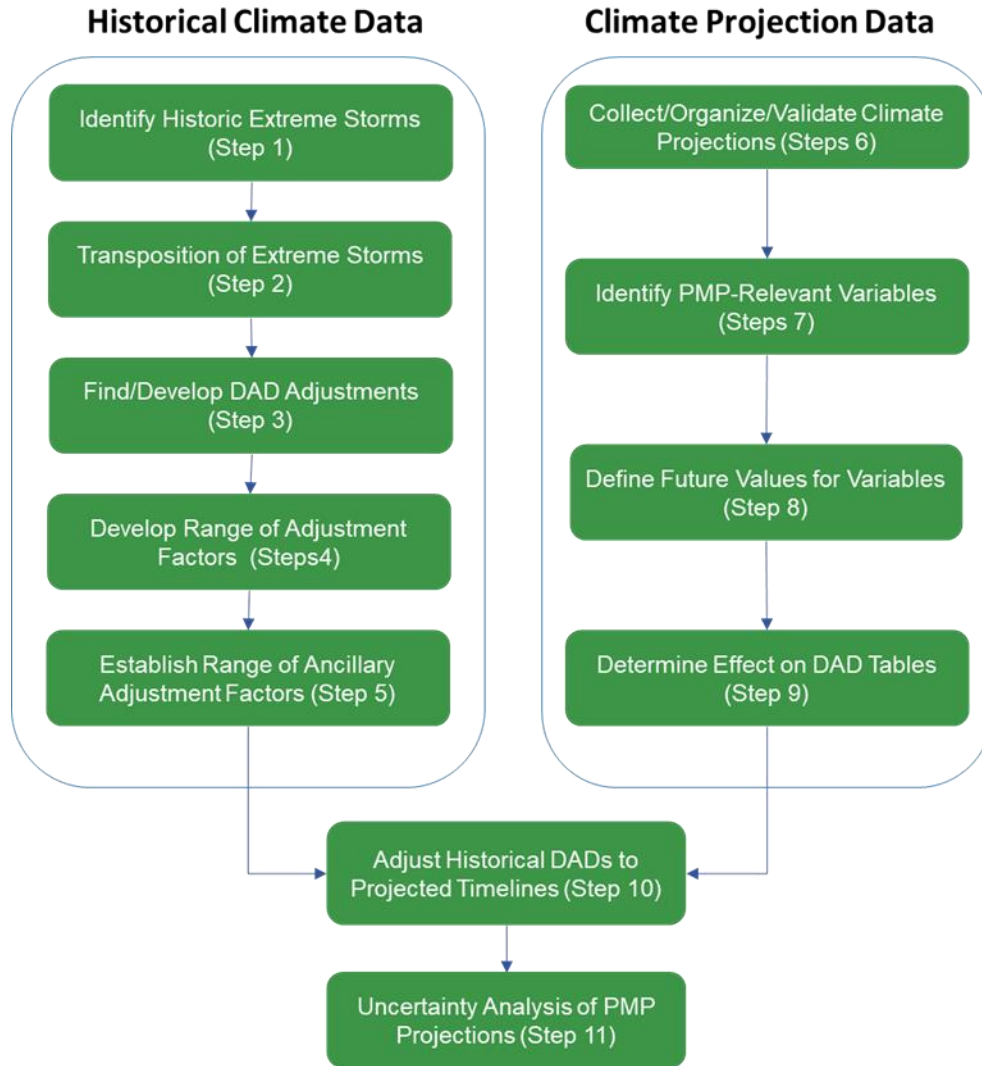


**Figure A.2: Baseline and Future PMP Analyses Flowchart**

### A.2.3.1 Construction of the DAD curves in the Hershfield method

The methodology used in this study is based on the one described by WMO (2009). The precipitation is weighted among stations according to their distance from other stations where the selected storms are recorded using a pairwise comparison. This step is equivalent to an averaged weighting of the precipitation. Averaged weighting is done pairwise with stations that have records for the selected storm, and the centre is defined at the station that recorded the highest precipitation for the selected event with additional meteorological information about the storm. From the centre of the storm, the area is defined using the distance to each station (also in a pairwise approach) defining the set of area/depth points used to develop the DAD curves (as in Section 3.3.3). This approach is a simplification of the methodology using isohyetal maps; however, given the very low density of stations utilized, it is expected to yield similar results to other methods. The depth-area-duration (DAD) curves are then constructed for 1-day, 2-day, and 3-day durations using envelopment (following WMO 2009) of the area/depth points found as described above. The in-place storm maximization and storm transposition play a large role in the final value of the PMP calculated.

The WMO acknowledges that there is significant uncertainty regarding PMP calculations and recommends that a comparison of other method and reported values is conducted. A comparison with previous studies completed for the area and the Hershfield method is conducted to validate the result. The Hershfield method, described in WMO (2009), is a robust statistical method to calculate the PMP values that relies on observations of annual maximum values of daily total precipitation. It is usually recommended for watersheds up to 1,000 km<sup>2</sup> (WMO 2009b). The PMP using the Hershfield method is calculated as follows:

$$PMP = X_n + KS_n \quad \text{Equation 34}$$

Where  $X_n$  and  $S_n$  are the mean and standard deviation (respectively) of the annual maximum 1-day precipitation, and  $K$  is a frequency factor that is a function of  $X_n$  and rainfall intervals. Adjustments needed to be made to  $X_n$  and  $S_n$  to account for the length of record used and the maximum observed rainfall event. Multiplicative factors for  $X_n$  and  $S_n$  were found to be 1.005 and 1.035 respectively when accounting for the length of record used (Figure 4.4 of WMO 2009). Multiplicative factors for  $X_n$  and  $S_n$  were found to be 0.997 and 0.971 respectively when accounting for the maximum observed rainfall event (Figure 4.2 of WMO 2009). The values of  $K$  as a function of rainfall duration and mean of the annual maximum series are given in Figure 4.1 of WMO (2009).

### A.2.3.2 Storm maximization and Transposition method

One of the steps of the calculation of the PMP using DAD curves (Transposition method) is the storm maximization using precipitable water (PWC) content of the rainfall event and the transposition to the study area (WMO 2009). For the storm maximization and transposition, the maximum PWC is estimated using the relationship between dew point temperature and the PWC as shown in Figure A.3. This relationship was determined by OMNR (2006) and is valid for the province of Ontario. The PWC values are based on the 12-hour persistent dewpoint maps (100-year return period with and adjusted statistical distribution as shown in Figure F3.2 from OMNR 2006), and the mean temperature as proxy for the dewpoint temperature, where dewpoint data is not available.

The in-place maximized storms are transposed to the Ignace area by evaluation of the precipitable water transposition factors. Based on the 100-year return period 12-hour persistent dew-point maps (Figure F3.2) from OMNR (2006), the in-place maximization ratio is calculated as follows:

$$r_{storm} = \frac{PWC_{100-year-A}}{PWC_{storm}} \quad \text{Equation 35}$$

Where  $PWC_{100-year-A}$  is the maximum precipitable water for 100-years return period of the 12-hour persistent dew point (using the maps provided by OMNR (2006)) and  $PWC_{storm}$  is the maximum precipitable water for the storm event both at the location of the storm center. The daily mean temperature is used as proxy for the dew point, since information on dew-point is not available, both at the location of the storm center and at the Ignace study area.

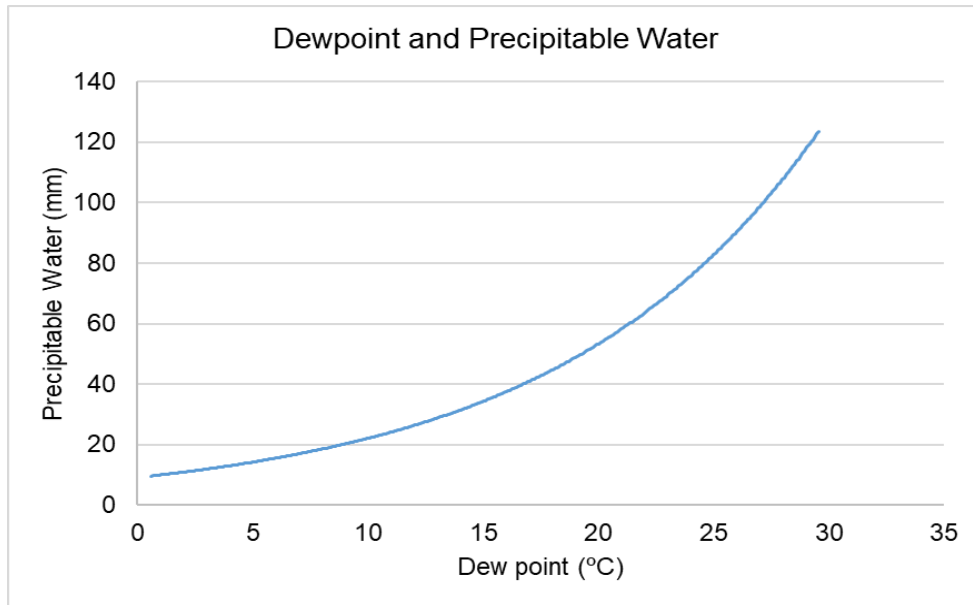


**Figure A.3: Precipitable Water and Dew Point relationship (Adapted from: OMNR 2006).**

The transposition ratio is calculated as follows:

$$r_{transp} = \frac{PWC_{100-year-B}}{PWC_{100-year-A}} \quad \text{Equation 36}$$

Where  $PWC_{100-year-B}$  is the maximum precipitable water for 100-years return period of the 12-hour persist dew point at the transposition location (using the maps provided by OMNR 2006).

The final storm maximization factor is calculated as

$$r = r_{storm} \times r_{transp} \quad \text{Equation 37}$$

The maximization for the 2- and 3-Day PMP is calculated by adding the delta to the 2 and 3-day DAD from the 1-Day PMP maximization result.

This method is used to derive the final storm maximization factor in Section 3.3.3.

#### A.2.3.3 Converting daily PMPs to sub-daily

The hourly precipitation data are not available from ECCC and therefore the sub-daily PMP is estimated using ratio factors calculated from the sub-daily IDF curves defined for the study area. The ratios are estimated by taking the 24-hour duration and 100-year return period as reference, and the other sub-daily durations (5, 10, 15, 30 minutes, 1, 2, 6, 12 hours) are scaled accordingly to calculate the sub-daily PMP values. The 100-year return period is selected since it provides a more realistic and reliable estimate among sub-daily durations than higher return period. It is important to note that this estimate has uncertainties and assumes that the PMP follows the same distribution as the IDF curves for 24-hours durations and 100-year return period.

#### A.2.4 Rain on Snow Procedure

The calculation of the rain on snow follows the methodology adopted by ECCC (Louie and Hogg 1980) to estimate runoff from snowmelt. The methodology uses a degree-day method to separate rainfall and snowfall from precipitation and model the processes of snow accumulation and melt. The following steps are used in the procedure:

- 1) The snowpack accumulation is estimated based on the daily mean temperature and the total rainfall. If temperature is  $> 0^{\circ}\text{C}$ , precipitation falls as rain and no snowpack is accumulated; if temperature is  $< 0^{\circ}\text{C}$ , precipitation falls as snow and is accumulated to the snowpack.
- 2) The snowmelt amount (SM) is estimated based on the model presented in Equation 38 for Eastern Canada Forested Basin (Pysklywec et al. 1968) and is depleted from the snowpack.

$$SM = 0.0397 (Ta - 27.6) \left( \frac{\text{inches}}{\text{day}} \right) \quad \text{Equation 38}$$

Where  $Ta$  is the mean daily air temperature in  $^{\circ}\text{F}$ .

- 3) The calculated snowmelt is added to the rainfall amount, if any (rain + snowmelt).
- 4) The process is repeated for all days in the data series are calculated.
- 5) Finally, the daily maximums of the combined rainfall and snowmelt for each year are calculated and a Gumbel distribution is fitted to estimate the several required return periods.

### A.3 FUTURE CLIMATE PROJECTIONS DEVELOPMENT

Future climate projections are important for understanding how climate is projected to change from the climate baseline. The future climate projections come from publicly available statistical downscaled future climate projections on a daily scale. Recognizing the inherent uncertainty with projections, multiple projections from multiple models and scenarios are included in the analysis. Therefore, the future projections are provided in terms of percentiles.

The following sub-sections describe the methodology to develop future climate change projections and to incorporate these projections to the PMP estimates and IDF curves. The methodology presented in these subsections supports the analyses and results for the future projections for PMP and IDF curves presented in Section 4.

### **A.3.1 Data Sources for Future Climate**

Future climate projections are important for understanding how climate is projected to change from the climate baseline. The Intergovernmental Panel on Climate Change (IPCC) is generally considered to be the definitive source of information related to past and future climate change as well as climate science. In 1988, the IPCC was formed by the World Meteorological Organization (WMO) and the United Nations Environment Program (UNEP) to review international climate change data. The IPCC is generally considered to be the definitive source of information related to past and future climate change as well as climate science. As an international body, the IPCC provides a common source of information relating to emission scenarios, provides third party reviews of models, and recommends approaches to document future climate projections. Periodically, the IPCC issues assessment reports summarizing the most current state of climate science. The Fifth Assessment Report (AR5) (IPCC 2013) represents the most current complete synthesis of information regarding climate change. The Sixth Assessment report (AR6) is due for release in May 2022 and will include updated climate scenarios and projections (IPCC 2020). The updated projections are anticipated to be in line with the AR5 but will include additional emissions scenarios to be assessed.

### **A.3.2 Global Climate Change Projections**

Future climate is typically projected using general circulation models (GCMs; also used interchangeably with global climate models) that involve the mathematical representation of global land, sea and atmosphere interactions over a long period of time. GCMs are one of the tools available that allows us to estimate and understand changes in climatic conditions for future periods. In order to provide global projections of climate, the spatial and temporal resolution of GCMs (hundreds of kilometers and monthly) is coarse compared to meteorological models (kilometers and hourly).

These GCMs have been developed by various government agencies, but they share a number of common elements described by the IPCC. The IPCC does not run the models but acts as a clearinghouse for the distribution and sharing of the model forecasts. Future climate projection data are available from about 30 GCMs. GCMs require extensive inputs to characterize the physical processes and social development paths that could alter climate in the future. In order to represent the wide range of the inputs possible to global climate models, the IPCC has established a series of RCPs that help define the future levels of radiative forcing terms. The IPCC identified four greenhouse gas (GHG) emission scenarios, namely, RCP 2.6, RCP 4.5, RCP 6.0, and RCP 8.5 (business-as-usual). The pathways are named after the radiative forcing projected to occur by 2100.

Beyond 2100, the radiative forcing is described using extensions of the RCPs called Extended Concentration Pathways (ECPs) that help define the trajectory of greenhouse gas concentrations out to the year 2300. It should be noted that the ECPs (i.e., climate change model projections beyond 2100) contain a high degree of uncertainty. These four RCPs and ECPs have been described more fully by van Vuuren et al (2011) in their paper “The representative concentration pathways: an overview” and have been summarized in Table A.1. The IPCC identified four RCPs; however, this report focuses on the three RCPs (RCP 2.6, RCP 4.5, and RCP 8.5) currently available from ClimateData.ca (ClimateData.ca 2019).

### A.3.2.1 Regional climate change projections

GCMs resolution is generally too coarse for direct use as it does not resolve weather and extreme weather patterns or climatology at local scales. Outside of using the GCM output directly, there are different options to analyze climate projections at a regional scale. Most downscaled climate datasets include minimum temperature, maximum temperature and precipitation. The focus is on statistical or dynamically downscaled datasets which have a higher temporal and spatial resolution of the data; however, they may have limited variables available. The availability of daily downscaled data allows for better characterization of climate extremes, especially for precipitation. The availability of high spatial resolution (10 km instead of hundreds of km in global climate models or GCMs) provides better data to represent site-specific information for the study.

**Table A.1: Characterization of Representative Concentration Pathways**

Name	Radiative Forcing in 2100 and 2300	Characterization
RCP 8.5, ECP 8.5	8.5 W/m <sup>2</sup> (2100) 12 W/m <sup>2</sup> (2300)	Increasing greenhouse gas emissions over time, with no stabilization, representative of scenarios leading to high greenhouse gas concentration levels (business-as-usual GHG emissions); and comparable to the SRES A2/A1FI scenarios. Past 2100, greenhouse gas emissions stabilize near 2250 at 12 W/m <sup>2</sup> .
RCP 6.0, ECP 6.0	6.0 W/m <sup>2</sup>	Without additional efforts to constraint emissions (baseline scenarios); and comparable to SRES B2 scenario. Past 2100, greenhouse gas emissions stabilize near 2150 at 6.0 W/m <sup>2</sup> .
RCP 4.5, ECP 4.5	4.5 W/m <sup>2</sup>	Total radiative forcing is stabilized shortly after 2100, without overshoot. This is achieved through a reduction in greenhouse gases over time through climate policy; and comparable to SRES B1 scenario. Past 2100, greenhouse gas emissions stabilize near 2150 at 4.5 W/m <sup>2</sup> .
RCP 2.6, ECP 3PD	2.6 W/m <sup>2</sup>	“Peak and decline” scenario where the radiative forcing first reaches 3.1 W/m <sup>2</sup> by mid-century and returns to 2.6 W/m <sup>2</sup> by 2100. This is achieved through a substantial reduction in greenhouse gases over time through stringent climate policy. Past 2100, greenhouse gases remain constant at concentrations in 2100.

Note: Summarized from van Vuuren et al. (2011); W/m<sup>2</sup> = watt per square metre.

The climate change impact assessment for this study considers 136 bias-corrected climate projections from two distinct data sources:

- BCCAQ v2: Pacific Climate Impact Consortium (ClimateData.ca) data using Bias Correction/Constructed Analogues with Quantile mapping reordering (BCCAQ) version 2– (ClimateData 2019)
- GDO-DCP LOCA: Bias Correct models using Localized Constructed Analogs (LOCA, Pierce et al. 2014 and Reclamation 2013)

The BCCAQv2 data consists of 24 models (72 projections), using RCP 2.6, RCP4.5, and RCP8.5, and the LOCA data consists of 32 models for RCP 4.5 and RCP 8.5 only (64 projections), for a total of 136 projections for the dataset (hereinafter referred as the ensemble). The GCMs that were incorporated into each downscaling method are shown in Table A.2. Additional information on each model including the associated institution and resolution and methods used for each model component are provided in Appendix A of Flato et al. (2013). The downscaled projections are available for two different horizontal resolutions: 1/8 degree or approximately 12 km (BCCAQv2) and 1/16 degrees or approximately 6 km (LOCA). Both datasets provide downscaled climate model results from 1950 to 2100 for daily total precipitation, minimum temperature, and maximum temperature.

**Table A.2: Global Climate Models used in BCCAQv2 and LOCA Downscaling Methods**

Dataset Characteristic	ClimateData.ca (BCCAQv2) <sup>(1)</sup>	GDO-DCP Archive (LOCA) <sup>(2)</sup>
<b>Climate Models</b>		
ACCESS1-0	—	X
ACCESS1-3	—	X
bcc-csm1-1	X	X
bcc-csm1-1-m	X	X
BNU-ESM	X	—
CanESM2	X	X
CCSM4	X	X
CESM1-BGC	—	X
CESM1-CAM5	X	X
CMCC-CM	—	X
CMCC-CMS	—	X
CNRM-CM5	X	X
CSIRO-Mk3-6-0	X	X
EC-EARTH	—	X
FGOALS-g2	X	X
GFDL-CM3	X	X
GFDL-ESM2G	X	X
GFDL-ESM2M	X	X
GISS-E2-H	—	X
GISS-E2-R	—	X
HadGEM2-AO	X	X
HADGEM2-CC	—	X
HadGEM2-ES	X	X
INMCM4	—	X
IPSL-CM5A-LR	X	X

Dataset Characteristic	ClimateData.ca (BCCAQv2) <sup>(1)</sup>	GDO-DCP Archive (LOCA) <sup>(2)</sup>
IPSL-CM5A-MR	X	X
MIROC5	X	X
MIROC-ESM	X	X
MIROC-ESM-CHEM	X	X
MPI-ESM-LR	X	X
MPI-ESM-MR	X	X
MRI-CGCM3	X	X
NorESM1-M	X	X
NorESM1-ME	X	—
<b>Spatial Resolution</b>		
6 km	—	X
12 km	X	—
<b>Years Available</b>		
1950 - 2100	X	X
<b>Climate Variables</b>		
Minimum Temperature	X	X
Maximum Temperature	X	X
Mean Temperature	X	X
Total Precipitation	X	X

Both data sources provide spatially downscaled data; however, the BCCAQv2 approach has some drawbacks that makes it difficult to find good analog days for the entire domain as the domain size increases. It is also more likely that the model can miss days with precipitation and localized extreme precipitation events that are important to capture. These drawbacks are discussed in detail in *Downscaled CMIP3 and CMIP5 Climate Projections* by Bracken (2016). The LOCA approach was developed to address these issues of BCCAQv2 and was therefore used in this analysis.

The ClimateData.ca portal provides statistically downscaled daily Canada-wide climate scenarios, at a gridded resolution of 300 arc-seconds (or roughly 10 km) for the simulated period of 1950-2100 (ClimateData.ca 2019). The climate variables available from ClimateData.ca data include minimum temperature, maximum temperature and precipitation. The selection of data for this project is based on the available temporal and spatial resolution of the data. The availability of daily downscaled data allows for better characterization of the climate extremes, especially for precipitation. The availability of high spatial resolution (10 km instead of hundreds of km in GCMs) provides better representation for site-specific studies like this project.

The LOCA data is retrieved from the GDO-DCP archive, which provides fine spatial resolution translations of climate projections using three downscaling techniques including daily LOCA for the United States. The archive uses global climate projections from the World Climate Research Programme's (WCRP) CMIP3 and CMIP5 multi-model dataset that was used for the IPCC fifth assessment report (GDO-DCP 2019).

GCM projections are downscaled to a finer resolution using the Bias Correction/Constructed Analogues with Quantile mapping reordering version 2 (BCCAQv2) developed by the Pacific Climate Impacts Consortium (PCIC) (ClimateData.ca 2019). This downscaling method is a statistical algorithm that disaggregates the GCM outputs to a finer spatial and temporal resolution; in other words, they take the gridded data and calculate values that reflect the local conditions that cannot be simulated by the GCM. The Bias Correction/Constructed Analogues with Quantile mapping reordering interpolates spatially to a finer scale on a daily basis. More detailed description and model performance can be found in Werner and Cannon (2016).

Since no one model or climate scenario can be viewed as completely accurate, the IPCC recommends that climate change assessments use as many models and climate scenarios as possible, or a "multi-model ensemble". For this reason, the multi-model ensemble approach is used in this study to delineate the probable range of results and better capture the actual outcome (an inherent unknown). Best practices recommend using all plausible futures for greenhouse gases that includes to best- and worst-case scenarios (RCP 2.6, 4.5, 6.0, and 8.5) when considering long timescales to address uncertainty. In addition, a multi-model ensemble is also recommended since the mean of an ensemble is generally closer to the observed values for past climate than any given individual model or scenario (Charron 2016).

Before beginning the future climate projections, the 136 potential members of the multi-model ensemble are reviewed to observe whether the general temperature and precipitation ranges reasonably match the observed ranges of climate for the region. Monthly averages are used to capture the known seasonality of the region. From this evaluation, all scenarios from the ensemble demonstrated typical behaviour within the current climate normal for the region and within the monthly averages.

The downscaled data has a daily temporal resolution (GCMs typically have monthly temporal resolution) which allows for the characterization of future climate extremes. In addition, the improved horizontal resolution of 10 km in the downscaled data could better improve the representation of the study area, given the complex terrain in study area.

#### **A.3.2.2 Uncertainty of climate change downscaling methods**

To address the inherent uncertainty associated with climate change projections, multiple projections from multiple models and scenarios are used in this study. ECCC (2016) recommends that multiple climate models and emission scenarios should be used to overcome the range of natural climate variability and uncertainties regarding future greenhouse gas emissions pathways and climate response. Instead of selecting one single projection, projections from all available model runs are used to describe the probable range of results. The future projections are provided in terms of percentiles of the range of future climate projections.

### A.3.3 Projecting Future Rainfall Statistics (IDF Curves)

This subsection describes the methodology to estimate IDF curves using modelled data from the ensemble and the methodology to assess changes to future rainfall (i.e., 2050s and 2080s), when compared to model baseline from the ensemble. This section, specifically, describes in detail Golder's IDF curve updating methods, including the Quantile Delta Method (QDM) and the Ratio Method (RM). This section supports the results and analysis presented in Section 4.2 of the main report.

The ensemble approach is used to obtain daily precipitation (1950 to 2100) to develop IDF curves representative of the model baseline (ideally same period as the current climate baseline) and the desired future periods, following the methods described in Section A.2.2. Specifically, IDF curves are developed for multi-day precipitation (methodology described in Section A.2.2.2.) and for sub-daily and daily observations applied only at stations with sub-daily observation records (methodology described in section A.2.2.1). Statistical distributions (A.2.2.3) and goodness-of fit tests (A.2.2.5) are completed for each IDF developed under this task.

Once the IDF curves are developed for each climatic projection (model baseline and desired future periods), each model within the ensemble (approximately 136 models sourced from ClimateData.ca and LOCA) and each duration (e.g., multi-day precipitation or sub-daily and daily precipitation), future IDF curves are then compared to model baseline IDF curves. The QDM and RM methods are selected to produce a statistical range for the percentage change in absolute values.

The difference in IDF estimates between the QDM and RM models, across the entire ensemble is used to present the changes from the model baseline over a range of percentiles for selected return periods and duration of storm. Percent changes in precipitation associated with the 50<sup>th</sup> percentile are presented in Section 4.2. Detailed percentile differences across the dataset are presented Appendix B.

The projected change in the IDF curves can be applied to the observed estimates in order to obtain absolute values adjusted for climate change. This is represented by the equation given below:

$$IDF_{future} = IDF_{observed} \cdot (1 + IDF_{change}) \quad \text{Equation 39}$$

Where the absolute value for the future IDF estimate ( $IDF_{future}$ ) is obtained using the observed IDF estimate ( $IDF_{observed}$ ) and the percentage change ( $IDF_{change}$ ) projected under the selected future conditions. All changes should be applied for the same return periods and durations between the future percentage changes and the observed IDF estimates. For example, if the observed IDF estimate ( $IDF_{observed}$ ) is 109.8 mm for the 1-day 100-year return period and the projected percentage change at the 50<sup>th</sup> percentile ( $IDF_{change}$ ) is 14.3% for the 1-day 100-year return period, the estimated future IDF absolute value ( $IDF_{future}$ ) is  $109.8 \text{ mm} \cdot (1 + 0.143) = 125.5 \text{ mm}$ .

### A.3.3.1 Quantile Delta Mapping (QDM)

This method is based on the Equidistant Quantile Matching (EQM) algorithm (Li et al. 2010, Piani et al. 2010, Hassanzadeh et al., 2014, Srivastav et al., 2014, Cannon et al. 2015 and Schardong et al. 2018). First, the current climate baseline (based on observations), model baseline, and modelled future annual maximum rainfall datasets are fitted with statistical distributions. This method is generic to any of the four potential statistical distribution to be tested. Next, the current climate baseline annual maximum rainfall and model baseline annual maximum rainfall are equated using a functional relationship. This relationship establishes a mathematical connection between daily modelled and sub-daily observed annual maximum precipitation. Projected changes in climate ( $\Delta_m$ ) are calculated between the quantiles of the model baseline ( $IDF_{baseline}$ ) and future ( $IDF_{future}$ ) distributions corresponding to selected return periods of the IDF curve. This is done using the following equation for a given sub-daily duration  $i$ ,

$$\Delta_{m_i} = \frac{IDF_{future_i}}{IDF_{baseline_i}} - 1 \quad \text{Equation 40}$$

The projected future sub-daily IDF ( $IDF_{projected}$ ) is then calculated using the functional relationship ( $f$ ) established previously, along with the projected changes in climate ( $\Delta_m$ ) for each sub-daily duration.

$$IDF_{projected_i} = f(IDF_{baseline_i}) \cdot \Delta_{m_i} \quad \text{Equation 41}$$

After the distribution of the future sub-daily IDF has been obtained, extreme values are then extracted using the inverse cumulative distribution function with the probability of the selected return periods.

Downscaled climate projections from the data portals used here are limited to daily temporal resolutions. Therefore, sub-daily rainfall projections are not available, and it is assumed here that the projected changes in the 1-day modelled IDFs is uniform across the sub-daily durations. This allows for  $\Delta_m$  to be constant for each sub-daily rainfall duration. Applying changes in daily to sub-daily precipitation extremes has been done in the past; however, it should be noted that changes in atmospheric processes governing rainfall production will unlikely be uniform for short to long time durations (e.g., convective scale processes at shorter durations versus large scale synoptic systems at longer durations) (CSA 2012). Therefore, the projected changes in sub-daily extremes should be interpreted with caution, and values used for design purposes should select a higher percentile to account for uncertainty related to the projected changes in sub-daily precipitation extremes.

The QDM, as well as the EQM, follows the steps presented in the flowchart of Figure A.4.

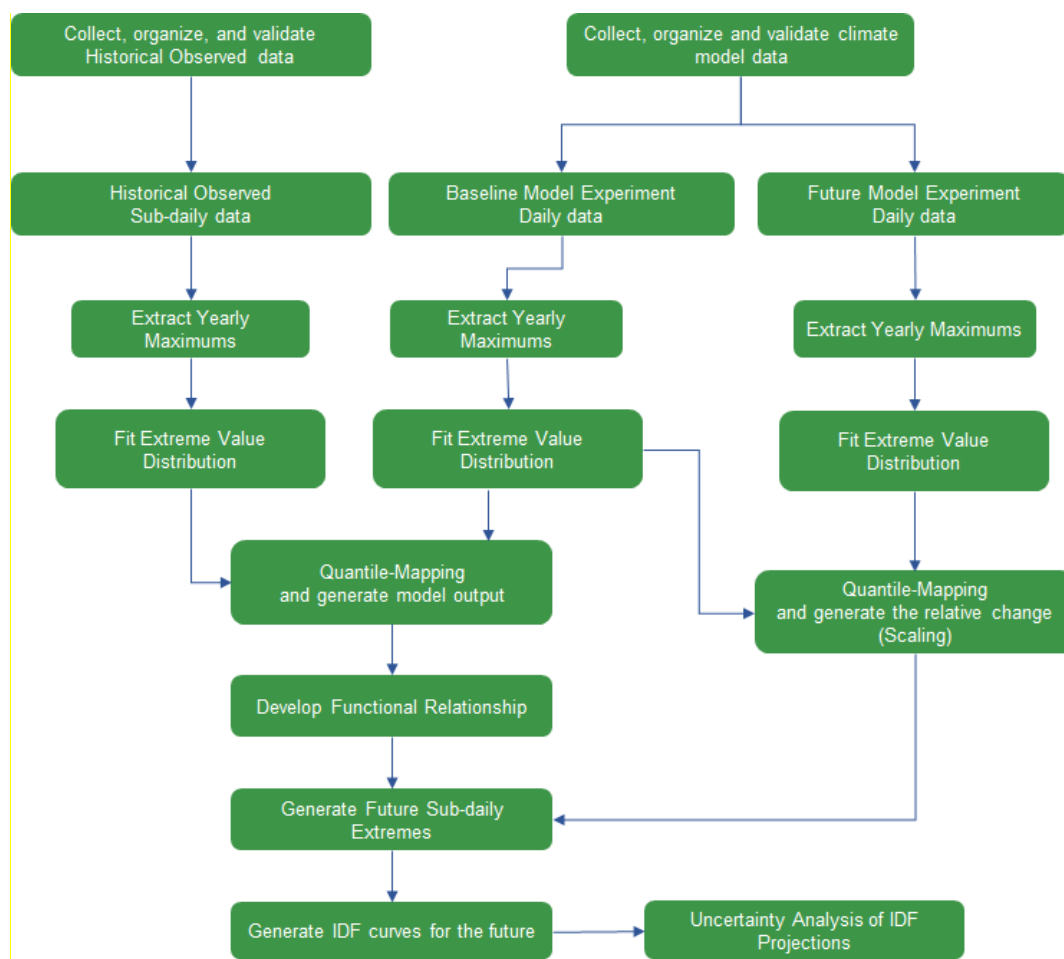


**Figure A.4: QDM Method Flowchart (Adopted from Schardong and Simonovic 2019)**

### A.3.3.2 Ratio Method (RM)

The Ratio Method (RM) (Olsson et al. 2009) is generic for any statistical distribution selected and allows for analysis of any return period, including the 500-year return period. Details on how RM has been used in this work are shown in Figure A.5. Ratios are calculated between the model baseline and future projected IDF curves which signify the projected changes due to climate change. Since this method uses only the daily GCM results to estimate a percentage change between baseline and future conditions, the smallest timestep for which a percent change is generated is one-day. The 1-day changes are then applied uniformly to each sub-daily duration. The inclusion of the RM method in addition to the QDM method captures an additional source of uncertainty pertaining to the method used for updating the IDF curves for climate change, as the results of both methods are used when generating percentile levels from the multi-model ensemble.

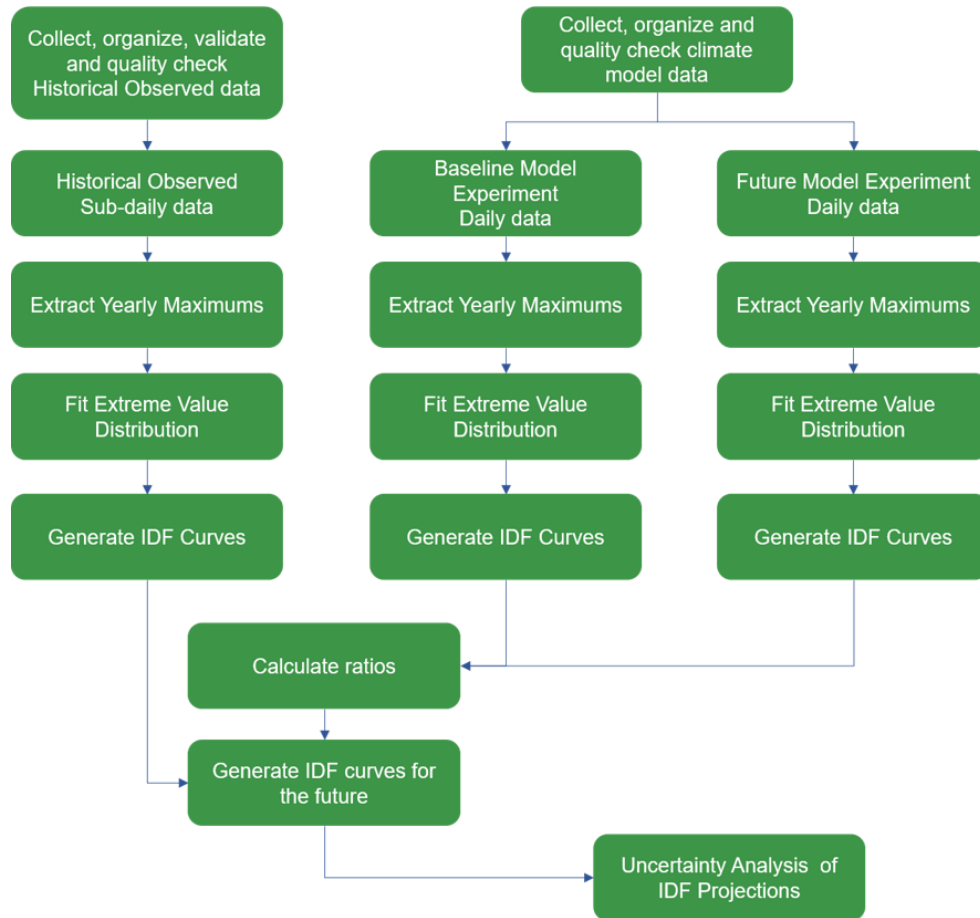


**Figure A.5: Ratio Method Flowchart**

### A.3.4 Projecting Future Changes in PMPs

Future climate projections follow the steps outlined in Figure A.2. First, downscaled daily climate projections are obtained (Step 6). Next, variables relevant to the estimation of PMP using the Moisture Maximization and Hershfield methods are extracted which include daily total precipitation and daily minimum temperature (Step 7). The results for the future time periods using these methods are calculated (Step 8). Percentiles are calculated across the results of both methods used for all members of the multi-model ensemble. The percentage changes for each percentile are then applied to the DAD tables for current climate presented in Section 3.3.3 (Steps 9 and 10). All percentiles for the DAD tables are given in Appendix B, which provide an indication of the level of uncertainty associated with the climate projections on the DAD tables (Step 11).

The change in PMP for the future are presented as percent changes between the model baseline period (1950- 1993) and the selected future periods (2050s and 2080s) across all models within the ensemble. The Hershfield method follows the same approach used to develop PMP estimates for current climate (see Section A.2.3).

The Moisture Maximization method requires the moisture content and other variables, which are not readily available from the modelled climate datasets. In order to calculate the moisture content for the model result datasets that do not provide this variable, the daily minimum temperature projections from the multi-model ensemble are used as a proxy for the dew point temperature, which is used to estimate saturation vapor pressure. The saturation vapor is then used as a proxy for the precipitable water. No additional proxies are required to be used to describe other variables. Uncertainty regarding the projected changes in PMP from the multi-model ensemble is shown using percentiles which demonstrate how the PMP projections are distributed. The minimum and maximum projections were calculated, along with those corresponding to the 5<sup>th</sup>, 25<sup>th</sup>, 50<sup>th</sup>, 75<sup>th</sup>, and 95<sup>th</sup> percentiles.

The projected change in the PMP values can be applied to the observed estimates in order to obtain absolute values adjusted for climate change. This is represented by the equation given below:

$$PMP_{future} = PMP_{observed} \cdot (1 + PMP_{change}) \quad \text{Equation 42}$$

Where the future value for the PMP estimate ( $PMP_{future}$ ) is obtained using the observed PMP estimate ( $PMP_{observed}$ ) by the percentage change ( $PMP_{change}$ ) in the value for the PMP.

### A.3.5 Projecting Future Changes in Rain on Snow and Snowpack

The method for projecting changes in rain on snow and snowpack follows the method applied to the baseline climate described in Section A.2.4. Daily snowpack and snowmelt is estimated for each of the models in the ensemble methodology adopted by ECCC (Louie and Hogg 1980), and snowmelt is added to assumed rainfall to estimate rain on snow. The method uses a degree-day method, which assumes that in the case of sub-zero temperatures, precipitation falls as snow, which can accumulate to form snowpack. For temperatures above zero, precipitation falls as rain and accumulated snow begins to melt. The resulting annual maximum series for rainfall and snowmelt for each model and baseline/future period is then fitted to a Gumbel distribution to estimate the return period, and the resulting return values are then compared within each model to estimate a percentage change between the baseline and the future periods.

## **APPENDIX B: FUTURE RAINFALL STATISTICS**

Additional future rainfall statistics tables are provided in the companion spreadsheet for this report. This format was selected in order to allow for the results to be more readily accessible and improve the readability of the report. The minimum, maximum, mean, standard deviation, and percentiles ranging from 5% to 99% provide information on the distribution of the projected changes in climate from the multi-model ensemble. These statistics are provided for daily, and multi-day IDF curves, as well as PMP, combined rainfall and snowmelt, and peak snowpack accumulation for the multi-model ensemble climate projections. Projections for both the 2050s and 2080s time periods for all of the additional statistics are included.

## REFERENCES

- Bracken, C. 2016. Downscaled CMIP3 and CMIP5 Climate Projections – Addendum, Release of Downscaled CMIP5 Climate Projections (LOCA) and Comparison with Preceding Information. Bureau of Reclamation. Retrieved from [https://gdo-dcp.ucllnl.org/downscaled\\_cmip\\_projections/techmemo/Downscaled\\_Climate\\_Projections\\_Addendum\\_Sept2016.pdf](https://gdo-dcp.ucllnl.org/downscaled_cmip_projections/techmemo/Downscaled_Climate_Projections_Addendum_Sept2016.pdf).
- Canadian Standards Association (CSA). 2012. Draft Standard Plus 4013-12 Technical Guide Development, interpretation and use of rainfall intensity-duration-frequency (IDF) information: Guideline for Canadian water resources practitioners.
- Cannon, A.J., S.R. Sobie, and T.Q. Murdock. 2015. Bias Correction of GCM Precipitation by Quantile Mapping: How Well Do Methods Preserve Changes in Quantiles and Extremes? *Journal of Climate*, 28(17), 6938-6959. DOI: 10.1175/JCLI-D-14-00754.1.
- Charron, I. 2016. A Guidebook on Climate Scenarios: Using Climate Information to Guide Adaptation Research and Decisions, 2016 Edition. Ouranos, 94 pages.
- Cunnane, C. 1989. Statistical Distributions for Flood Frequency Analysis. Operational Hydrology Report no. 33, World Meteorological Organization.
- Environment and Climate Change Canada (ECCC). 2016. Climate Data and Scenarios for Canada: Synthesis of Recent Observation and Modelling Results. Environment and Climate Change Canada. Available at: <https://www.canada.ca/en/environment-climate-change/services/climate-change/publications/data-scenarios-synthesis-recent-observation.html>.
- Environment and Climate Change Canada (ECCC). 2019a. Engineering Climate Datasets. Available at [https://climate.weather.gc.ca/prods\\_servs/engineering\\_e.html](https://climate.weather.gc.ca/prods_servs/engineering_e.html). Accessed June 15, 2019.
- Environment and Climate Change Canada (ECCC). 2019b. Historical Climate Data. Available at: [http://climate.weather.gc.ca/historical\\_data/search\\_historic\\_data\\_e.html](http://climate.weather.gc.ca/historical_data/search_historic_data_e.html). Accessed June 15, 2019.
- Flato, G., J. Marotzke, B. Abiodun, P. Braconnot, S.C. Chou, W. Collins, P. Cox, F. Driouech, S. Emori, V. Eyring, C. Forest, P. Gleckler, E. Guilyardi, C. Jakob, V. Kattsov, C. Reason and M. Rummukainen. 2013: Evaluation of Climate Models. In: *Climate Change 2013: The Physical Science Basis. Contribution of Working Group I to the Fifth Assessment Report of the Intergovernmental Panel on Climate Change* [Stocker, T.F., D. Qin, G.-K. Plattner, M. Tignor, S.K. Allen, J. Boschung, A. Nauels, Y. Xia, V. Bex and P.M. Midgley (eds.)]. Cambridge University Press, Cambridge, United Kingdom and New York, NY, USA.
- GDO-DCP. Downscaled CMIP3 and CMIP5 Climate and Hydrology Projections. Accessed 2019. Retrieved from [https://gdo-dcp.ucllnl.org/downscaled\\_cmip\\_projections/#Welcome](https://gdo-dcp.ucllnl.org/downscaled_cmip_projections/#Welcome).
- Guo, J.C.Y, B. Urbonas, and K. Stewart. 2001. Rain Catch under Wind and Vegetal Cover Effects. *Journal of Hydrologic Engineering*, Vol. 6, Issue 1. [https://doi.org/10.1061/\(ASCE\)1084-0699\(2001\)6:1\(29\)](https://doi.org/10.1061/(ASCE)1084-0699(2001)6:1(29)).
- Hassanzadeh, E., A. Nazemi, and A. Elshorbagy. 2014. Quantile-Based Downscaling of Precipitation using Genetic Programming: Application to IDF Curves in the City of Saskatoon. *J. Hydrology. Eng.*, 19(5), 943-955.

- Hogg, W. D., D. A. Carr, and B. Routledge. 1989. Rainfall Intensity–Duration–Frequency Values for Canadian Locations. Ottawa: Environment Canada, Atmospheric Environment Service.
- Hosking, J.R.M. and J.R. Wallis. 1997. Regional Frequency Analysis. Cambridge University Press, Cambridge, U.K.
- Intergovernmental Panel on Climate Change (IPCC). 2013. Climate Change 2013: The Physical Science Basis. Contribution of Working Group I to the Fifth Assessment Report of the Intergovernmental Panel on Climate Change. Retrieved on March 15, 2017 from <https://www.ipcc.ch/report/ar5/wg1/>.
- Intergovernmental Panel on Climate Change (IPCC). 2020. The IPCC and the Sixth Assessment Cycle. Retrieved on May 8<sup>th</sup>, 2020 from [https://www.ipcc.ch/site/assets/uploads/2020/05/2020-AC6\\_en.pdf](https://www.ipcc.ch/site/assets/uploads/2020/05/2020-AC6_en.pdf).
- Li, H., J. Sheffield, and E.F. Wood. 2010. Bias Correction of Monthly Precipitation and Temperature Fields from Intergovernmental Panel on Climate Change AR4 Models Using Equidistant Quantile Matching. *Journal of Geophysical Research*, 115(D10), D10101.
- Louie, P. Y. T. and W. D. Hogg. 1980. Extreme Value Estimates of Snowmelt. *Proceedings of Canadian Hydrology Symposium 80* (Toronto, ON: 64-78 National Research Council Canada).
- Mekis, É. and L.A. Vincent. 2011. An Overview of the Second Generation Adjusted Daily Precipitation Dataset for Trend Analysis in Canada. *Atmosphere-Ocean* 49, 163–177. <https://doi.org/doi: 10.1080/07055900.2011.583910>.
- Millington, N., S. Das, and S.P. Simonovic. 2011. The Comparison of GEV, Log-Pearson Type 3 and Gumbel Distributions in the Upper Thames River Watershed under Global Climate Models. *Water Resources Research Report no. 077*, Facility for Intelligent Decision Support, Department of Civil and Environmental Engineering, London, Ontario, Canada, 53 pages. ISBN: (print) 978-0-7714-2898-2; (online) 978-0-7714-2905-7.
- National Aeronautics and Space Administration (NASA). 2019. Modern-Era Retrospective analysis for Research and Applications, Version 2. Retrieved from <https://gmao.gsfc.nasa.gov/reanalysis/MERRA-2/>.
- Olsson, J., K. Berggren, M. Olofsson, and M. Viklander. 2009. Applying Climate Model Precipitation Scenarios for Urban Hydrological Assessment: A Case Study in Kalmar City, Sweden. *Atmos. Res.*, 92:364–375, doi:10.1016/j.atmosres.2009.01.015.
- Ontario Ministry of Natural Resources (OMNR). 2006. PMP for Ontario. Prepared by IBI Group. December 2006.
- Overeem, A., A. Buishand, and I. Holleman. 2007. Rainfall Depth-Duration-Frequency Curves and Their Uncertainties. *Journal of Hydrology*. 348(1-2), 124-134. DOI:10.1016/j.jhydrol.2007.09.044.
- Piani, C., G.P. Weedon, M. Best, S.M. Gomes, P. Viterbo, S. Hagemann, and J.O. Haerter. 2010. Statistical Bias Correction of Global Simulated Daily Precipitation and Temperature for the Application of Hydrological Models. *Journal of Hydrology*, 395(3-4), 199–215.
- Pierce, D. W., D. R. Cayan, and B. L. Thrasher. 2014. Statistical Downscaling Using Localized Constructed Analogs (LOCA), *Journal of Hydrometeorology*, 15(6), 2558-2585, 2014; and Pierce, D. W., D. R. Cayan, E. P. Maurer, J. T. Abatzoglou, and K. C. Hegewisch, 2015: Improved bias correction techniques for hydrological simulations of climate change. *J. Hydrometeorology*, v. 16, 2421-2442. DOI: <http://dx.doi.org/10.1175/JHM-D-14-0236.1>.

- Pysklywec, D.W., K.S. Davar and D.I. Bray. 1968. Snowmelt at an Index Plot, Water Resource, 4(5), 937-946.
- Reclamation, 2013. Downscaled CMIP3 and CMIP5 Climate Projections: Release of Downscaled CMIP5 Climate Projections, Comparison with Preceding Information, and Summary of User Needs. U.S. Department of the Interior, Bureau of Reclamation, Technical Service Center, Denver, Colorado, 116 p. Available at: [http://gdo-dcp.ucllnl.org/downscaled\\_cmip\\_projections/techmemo/downscaled\\_climate.pdf](http://gdo-dcp.ucllnl.org/downscaled_cmip_projections/techmemo/downscaled_climate.pdf).
- Schardong A., A. Gaur, S.P. Simonovic and D. Sandink. 2018. Computerized Tool for the Development of Intensity-Duration-Frequency Curves under a Changing Climate: Technical Manual v.3. Water Resources Research Report no. 103, Facility for Intelligent Decision Support, Department of Civil and Environmental Engineering, London, Ontario, Canada, 67 pages. ISBN: 978-0-7714-3107-4.
- Schardong, A. and S.P. Simonovic. 2019. Application of Regional Climate Models for Updating Intensity-duration-frequency Curves under Climate Change. International Journal of Climate Change. 9(5): 311-330. DOI: 10.9734/ijecc/2019/v9i530117.
- Srivastav, R.K., A. Schardong, and S. P. Simonovic. 2014. Equidistance Quantile Matching Method for Updating IDF Curves under Climate Change, Water Resources Management, 28(9): 2539-2562.
- van Vuuren, D.P., Edmonds, J., Kainuma, M. et al. 2011. The Representative Concentration Pathways: An Overview. Climatic Change 109, 5. <https://link.springer.com/article/10.1007/s10584-011-0148-z>.
- Werner, A.T. and A.J. Cannon. 2016. Hydrologic Extremes – An Intercomparison of Multiple Gridded Statistical Downscaling Methods. Hydrol. Earth Syst. Sci., 20: 1483-1508. doi: 10.5194/hess-20-1483-2016.
- Wood. 2019. Climate Change Impacts Review and Method Development. Nuclear Waste Management Report NWMO-TR-2019-05. Toronto, Canada. Available at: <http://rms.nwmo.ca/Sites/APM/Reports/NWMO-TR-2019-05.pdf>.
- World Meteorological Organization (WMO). 2009. Manual on Estimation of Probable Maximum Precipitation (PMP). World Meteorological Organization (WMO). WMO-No. 1045.